COMPUTER SIMULATION OF THE LAMINAR UPFLOW OF AIR IN HEATED VERTICAL TUBES

by

Jorman Albert Koski, B.S. in Eng. Phys., M.S. in M.E.

A DISSERATION

IN

MECHANICAL ENGINEERING

Submitted to the Graduate Faculty
of Texas Tech University in
Partial Fulfillment of
the Requirements for
the Degree of

DOCTOR OF PHILOSOPHY

Approved

August, 1970

HC
801
T3
1970
No.11
cop.2

ACKNOWLEDGEMENTS

Appreciation is gratefully acknowledged to Professor Monty E. Davenport for his direction of this dissertation. I also wish to thank Professors Duane P. Jordan and L. J. Powers for their help as members of my committee.

TABLE OF CONTENTS

	Page
ACKNOWLEDGEMENTS	ii
LIST OF TABLES	vi
LIST OF FIGURES	vii
LIST OF SYMBOLS	ix
ABSTRACT	xiii
I. INTRODUCTION	1
1.1 Initial Remarks	1
1.2 Problem Geometry	2
1.3 Previous Investigations	4
1.4 Parallel Investigations	9
1.5 General Approach to the Solution	9
1.6 Objectives of the Analysis	10
II. GOVERNING EQUATIONS	12
2.1 Introduction	12
2.2 General Assumptions	12
2.3 Pertinent Physical Laws	13
2.4 Control Volume	14
2.5 Continuity Equation	15
2.6 Axial Momentum Equation	17
2.7 Radial Momentum Equation	20

TABLE OF CONTENTS (cont)

		Page
2.8	Energy Equation	23
2.9	Boundary Conditions	27
2.10	Additional Relations	29
2.11	Dimensionless Parameters	31
2.12	Dimensionless Equations	31
2.13	State Relations	36
III.	METHODS OF NUMERICAL SOLUTION	39
3.1	Introduction	39
3.2	Control Volumes	39
3.3	General Observations About the Governing Equations	42
3.4	Approximations Used with the Continuity Equation	43
3.5	Approximations Used with the Axial Momentum Equation and Energy Equation	50
3.6	Approximations Used with the Radial Momentum Equation	53
3.7	The Gauss-Seidel Method of Solving Linear Algebraic Equations	53
3.8	General Notes on the Numerical Solution	62
3.9	Methods of Solving Governing Equations	65
3.10	Flow Chart of Computer Solution	70
3.11	Methods Utilized to Check Validity of Solution	73

TABLE OF CONTENTS (cont)

		Page
IV.	PRESENTATION AND ANALYSIS OF RESULTS	80
	4.1 Restatement of Objectives	80
	4.2 Strategy of Computer Simulation	80
	4.3 Analysis of the Flow Field	83
	4.4 Comparison with Other Analyses	92
	4.5 Correlations for Friction Factor and Nusselt Number	101
V.	CONCLUSIONS AND RECOMMENDATIONS	104
	5.1 Summary of Results	104
	5.2 A Critique of Solution Approach	105
	5.3 Recommendations for Further Study	106
LIST OF REFERENCES		109
APPENDIX		112
	A. Data Summary	112
	B. Comparison of Correlations to Numerical and Experimental Results	125
	C. Definition of Bulk Parameters	138

LIST OF TABLES

Table		Page
2-1	Entrance Conditions	28
2-2	Boundary Conditions	28
2-3	Dimensionless Variables	32
3-1	Approximations Used with the Axial Momentum Equation and Energy Equation	54
3-2	Derivative Approximations for Differential Equation for Differential Equation Forms of Axial Momentum Equation and Energy Equation	57
3-3	Approximations Used with the Radial Momentum Equation	58
3-4	Full Stream Control Volume Equation Checks for Run 390	75
4-1	Summary of Input Data for Computer Simulations	84

LIST OF FIGURES

Figure		Page
1-1	Tube geometry	3
2-1	Typical control volume	15
2-2	Control volume for continuity equation	16
2-3	Control volumes for axial momentum equation	18
2-4	Control volumes for radial momentum equation	20
2-5	Control volume for energy equation	25
3-1	Grid network for numerical solution	40
3-2	Typical control volumes related to grid network	41
3-3	Plane depicted in grid Diagrams of Figure 3-2	41
3-4	Grid networks for differential equation approximations	48
3-5	Computer solution flow chart	71
3-6	Comparison of constant properties solution with Graetz solution	78
4-1	Variation of axial velocity profiles with free convection (Run 392)	85
4-2	Variation of radial velocity profiles with free convection (Run 392)	86
4-3	Temperature profile development (Run 391)	88
4-4	Variation of friction factor with free convection (Run 392)	89
4-5	Variation of Nusselt number with free convection (Run 392)	90

LIST OF FIGURES (cont)

Figure		Page
4-6	Comparison of computer solution axial velocity profiles to experimental values (Run 391)	93
4-7	Comparison of computer solution radial velocity profiles to values deduced from experimental data (Run 391) . . .	95
4-8	Comparison of computer solution friction factor values to experimental values (Run 386)	96
4-9	Comparison of computer solution Nusselt number to experimental values (Run 386)	97
4-10	Axial velocity comparison of Run 392-8 to Table 51 in Wilkins [26]	99
4-11	Temperature comparison of Run 392-8 to Table 51 in Wilkins [26]	100

LIST OF SYMBOLS

Roman Alphabet

A	area, ft^2
a	exponent for viscosity variation, $\mu = \mu_{ref} (T/T_{ref})^a$
b	exponent for thermal conductivity variation, $k = k_{ref} (T/T_{ref})^b$
c	exponent for specific heat variation, $c_p = c_{p,ref} (T/T_{ref})^c$
c_p	specific heat at constant pressure, $Btu/lb_m - {}^oR$
c_v	specific heat at constant volume, $Btu/lb_m - {}^oR$
D	tube diameter, ft
f	friction factor, $\frac{2 \tau_w \rho_b \pi^2 r_w^4}{\dot{m}}$
g	gravitational constant, $32.2 \frac{lb_m - ft}{lb_f - sec^2}$
h	specific enthalpy, Btu/lb_m
$\bar{h}$	convective heat transfer coefficient, $Btu/ft^2 - hr - {}^oR$
k	thermal conductivity, $Btu/hr - ft - {}^oR$
$\dot{m}$	mass flow rate, lb_m / sec

LIST OF SYMBOLS (cont)

N^{*}_{Gr}	modified Grashof number, $\frac{\rho_b^2 \, g \, D^3}{\mu_b^2}$
N_{Nu}	Nusselt number, $\frac{\bar{h} \, D}{k_b}$
N_{Fr}	Froude number, $\frac{u_b^2}{D \, g}$
N^{*}_{Gz}	modified Graetz number, $\frac{x}{r_w \, N_{Re} \, N_{Pr}}$
M	Mach number, $\frac{u_b}{\sqrt{\gamma \, RT_b}}$
N_{Pr}	Prandtl number, $\frac{\mu \, c_p}{k}$
N_{Re}	Reynolds number, $\frac{\rho_b \, u_b \, D}{\mu_b}$
p	pressure, lb_f/ft^2
q''	heat flux, Btu/ft^2 - hr
r	radial coordinate, ft
T	temperature, ^{o}R
u	axial velocity, ft/sec
v	radial velocity, ft/sec
V	volume, ft^3
x	axial coordinate, ft

LIST OF SYMBOLS (cont)

Greek Alphabet

γ	ratio of specific heats, c_p/c_v
θ	angular coordinate, radians
μ	viscosity, $lb_m/ft\text{-}sec$
ρ	density, lb_m/ft^3
σ	stress tensor component, lb_f/ft^2
τ	shear stress, lb_f/ft^2

Subscripts

b	denotes bulk parameter (See Appendix C for definitions of bulk parameters)
cp	denotes variable evaluated using constant properties assumptions
e	denotes variable evaluated at end of control volume used for radial momentum
i	denotes variable evaluated at inner face of control volume
in	denotes variable evaluated at inlet conditions
l	denotes variable evaluated at left face of control volume
o	denotes variable evaluated at outer face of control volume
pf	denotes variable evaluated at pure forced convection conditions

LIST OF SYMBOLS (cont)

r denotes variable evaluated at right face of control volume

ref denotes variable evaluated at specified reference conditions

w denotes variable evaluated at wall conditions

Superscripts

+ denotes dimensionless variable

Miscellaneous Symbols

$\simeq$ denotes approximate equality

$\triangleq$ denotes definition

ABSTRACT

A computer oriented numerical model based on integral equations is used to simulate the laminar upflow of air in a heated vertical tube. The simulations are based on boundary conditions encountered by Gerald S. Kirby and James L. Chance of Texas Tech University while conducting an experimental analysis of the problem. The computer results are compared to the experimental results both in the flow fields produced and in the friction factors and Nusselt numbers determined.

In addition, the computer model is used to study the effect of free convection on the flow field. The data derived are then used to develop friction factor and Nusselt number correlations which account for the free convection effects present.

CHAPTER I

INTRODUCTION

1.1 Initial Remarks

For nearly a century researches have been presenting analyses intended to predict the laminar flow behavior of fluids in heated tubes. Early analyses have been refined and new approaches presented by many ingenious investigators, but to this date no really general solution for all fluids and boundary conditions has been produced, and perhaps such a solution will never be found.

The previous solutions for the tubular fluid flow geometry more often than not employ physically unrealistic boundary conditions such as step changes in the tube wall temperature. Only very simplified cases have been handled with physically meaningful boundary conditions. In addition, no one has presented a direct theoretical versus experimental verification of the flow field velocity and temperature profiles predicted by the analyses for conditions involving moderate to high heating rates. This comparison has not been made because the appropriate experimental data were not available until recently when Kirby [17][1] and Chance [3] presented their experimental profiles.

The elimination of all the solution deficiencies for all fluids

---

[1]Numbers in brackets refer to similarly numbered references in the List of References.

and conditions is an extremely formidable problem. Some insight may be obtained, however, by limiting the study to a specific class of problems. This is the approach taken in this investigation, where the laminar upflow of air in heated circular tubes is considered. An earnest effort is made to remove the flaws of previous solutions already mentioned. A numerical computer oriented approach is employed, and the results of the analysis have been extensively compared with the data of Kirby and Chance. The comparison is further facilitated by careful simulation of the experimental boundary conditions in the computer analysis.

The numerical computer model is also used to generate data showing the effects of free convection on the flow scheme. This type of analysis is difficult experimentally because many differently sized test configurations must be constructed. These data have been used to establish correlations for friction factor and Nusselt number under conditions of varying free convection.

The solution approach taken in the investigation is somewhat different from the usual differential equation method of solving fluid flow problems. Instead, integral equations have been used as a starting point for the discrete numerical approximations usable in computer simulations.

1.2 Problem Geometry

The problem geometry is shown in Figure 1-1. Gas enters a circular tube and flows upward through an unheated entry section where

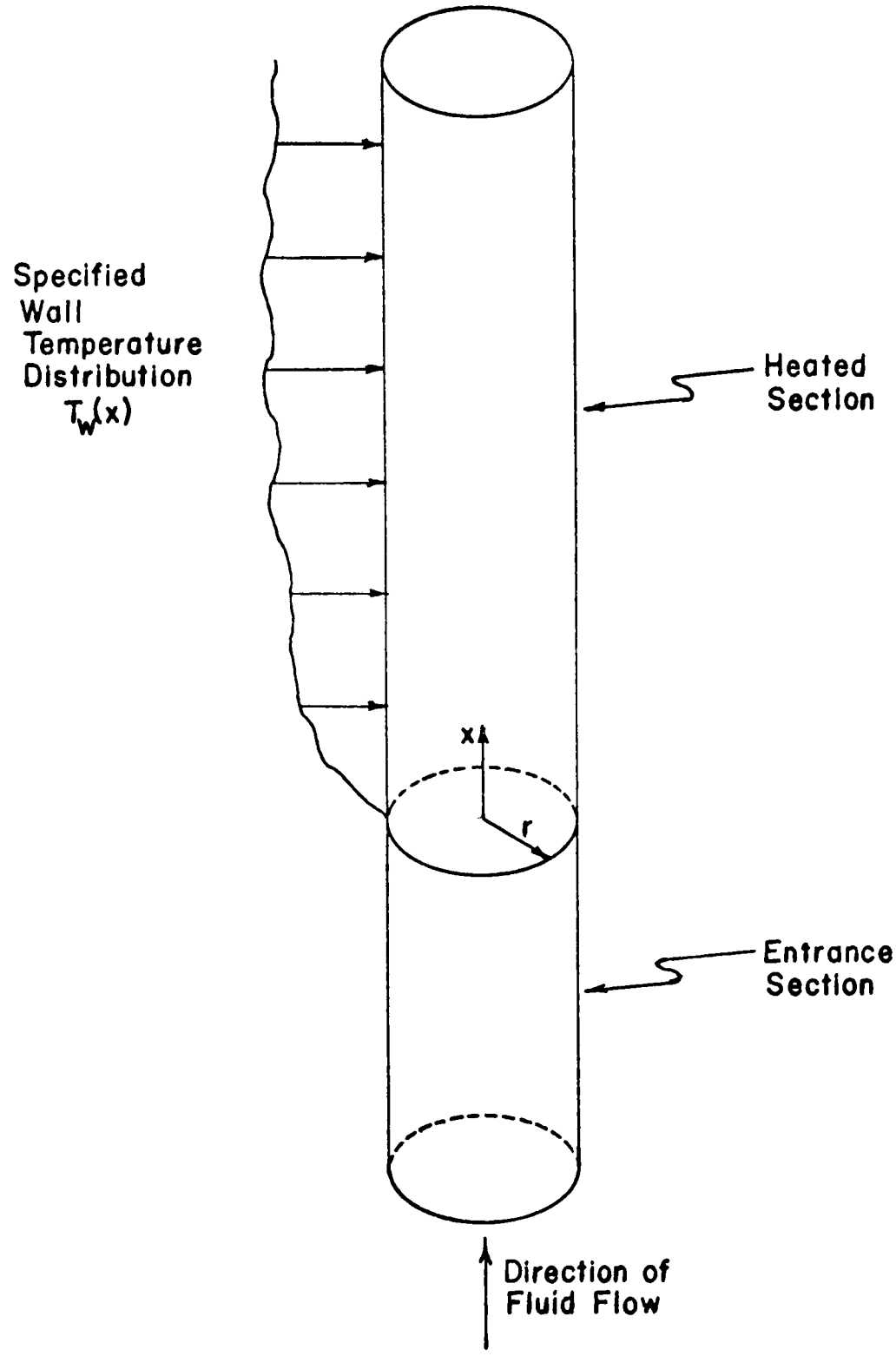

Fig. 1-1.--Tube geometry

the laminar gas flow becomes fully developed hydrodynamically. After passing through the entry section, the gas enters a heated section where the wall temperature varies in a prescribed manner. As the gas is heated, it becomes buoyant, and a flow regime involving combined free and forced convection develops.

1.3 Previous Investigations

Historically Graetz [9] in 1885 was the first to present a solution for the problem of laminar flow in a heated tube. Using a separation of variables technique, he achieved a solution of the partial differential equation describing energy flow. His analysis required the assumption of constant fluid properties; that is density, viscosity, thermal conductivity, and specific heat were considered as constants. This has the effect of limiting the validity of the solution to problems involving small temperature differences. Various modifications and extensions of the solution abound in the literature [2, 16, 22, 23].

In 1951 Deissler [6] put forth a theoretical solution for the problem in which property variations were included. Although his analysis indicated proper trends in friction factors, it did not correlate well with experimental results, and further work in the area was indicated. With respect to heat transfer, Deissler's work indicated the Nusselt number should slightly decrease as the temperature difference increased.

Five years later Hallman [10] presented a theoretical solution

in which only density was allowed to vary. He considered internal heat generation and demonstrated that free convection should cause an increase in Nusselt number over those values found for pure forced convection. He also showed that velocity profiles should flatten as free convection effects increase.

Koppel and Smith [19] in 1961 presented a numerical solution for the difficult problem of flow of carbon dioxide close to its critical point, a region where fluid property values are very sensitive to small changes of the state variables. However, their analysis contains an error in the energy equation in which specific heat at constant pressure is factored from a derivative expression and then allowed to vary significantly. Their analysis also neglects the presence of a radial velocity in the tube.

The same year, Davenport [4] presented a combined experimental-theoretical analysis which indicated the radial velocity of the fluid, which until that time had been considered negligible, could substantially affect results. He backed up his experiment with a theoretical model in which he assumed some possible shapes a radial velocity distribution could take and then showed that, although the magnitudes of the assumed terms were small, they could have a significant influence on friction factors.

To correlate his experimental results, Davenport used an equation of the form

$$\frac{f}{f_{cp}} = \left(\frac{T_w}{T_b}\right)^a \qquad (1.3.1)$$

in which f is the experimentally determined friction factor; f_{cp} is the

friction factor which would exist for fully developed flow but evaluated using local bulk conditions; T_w is the wall temperature at the axial position of interest; T_b is the local bulk temperature; and a is an experimentally chosen exponent which correlates the data. In his experiment he found a to be about 1.35.

Davenport also reported that experimentally determined Nusselt numbers were essentially the same as those determined from constant properties solutions, when local bulk values were used in the constant property expressions. It should be noted that the diameter (1/8") of the tube employed in the experiment minimized the effects of free convection.

One of the most significant of the recent theoretical analyses is that of Worsøe-Schmidt [27], who further validated Davenport's research by providing a finite difference solution to the governing differential equations. His analysis considered radial velocity, but included the usual boundary layer assumptions such as assuming constant pressure across the flow stream and neglecting the second derivatives along the tube axis.

Worsøe-Schmidt's boundary conditions involve step changes in wall temperature and heat flux. This leads him to ignore the obviously erroneous solutions obtained in the region of the physically unrealistic step. Unfortunately these values affect the values found downstream, thus raising serious doubts as to the correctness of the axial tube lengths actually required to develop the profiles he presents.

Like Koppel and Smith, Worsøe-Schmidt moves specific heat through

derivatives as if it were constant, and then allows it to vary. However, in this case, the results are probably not strongly affected since Worsøe-Schmidt considers gases whose specific heats are not a strong function of temperature.

His solution demonstrates the effect of buoyancy on the friction factor but does not analyze the issue in detail. Quantitatively, his friction factor results are different from Davenport's. He finds the exponent of a of equation (1.3.1) to be 1.0, as opposed to Davenport's value of 1.35. He attributes this discrepancy to experimental uncertainty in Davenport's analysis. However, close examination reveals that the two researchers reported different definitions of friction factor, making a direct comparison invalid.

Worsøe-Schmidt also demonstrates that increased free convection causes increases in Nusselt number values.

Another recent important work is that of Wilkins [26] who explores a wider variety of fluids than Worsøe-Schmidt. Although his basic equations and solution approach are similar to that of Worsøe-Schmidt, he reports his data in a different manner, relying on a graphical and tabular format rather than a correlation equation for summarizing results. To correlate his data, Wilkins utilizes a free convection parameter based on a modified definition of the Grashof number, the Reynolds number, and a defined viscosity ratio. Further analysis and comparison of Wilkins' work is considered in Chapter IV.

Also recently Deissler and Presler [7] have presented a numerical solution which allows property variation, but includes the boundary

layer assumptions. Their solution does not consider free convection, which restricts their domain of validity to situations where free convection effects are small.

The numerical solutions of Hornbeck [13], and McMordie and Emery [20], for laminar flow in heated tubes have concentrated on simultaneously developing temperature and velocity fields. Both of these papers assume constant fluid properties, and are thus not applicable to gases at high heating rates. Hornbeck does include radial velocity in his solution, while McMordie and Emery include axial conduction in theirs.

On the experimental side of the problem, three works stand out. These are the works of Kays and Nicoll [15], Dalle-Donne and Bowditch [5], and the previously mentioned work of Davenport [4].

Kays and Nicoll investigate the behavior of the Nusselt number for variations of tubular geometry. They consider both heated and cooled internal flow of air in a tube as well as external crossflow. Their results demonstrate that for moderate heating, constant property thermal entry length solutions are valid, if the properties involved are evaluated at local bulk conditions.

As reported earlier Davenport demonstrated that friction factors were considerably higher than early theoretical analyses predicted. Again, it is important to point out that his experimental results were based on an electrically heated one-eighth inch inside diameter tube.

Dalle-Donne and Bowditch obtain exponents on the order of 1.67 for use in the friction factor expression (1.3.1). It should be noted

that their experimental apparatus employed comparatively large one-fourth inch and one-half inch inside diameter tubes. Considering all other factors approximately the same, this means that their apparatus should be more affected by free convection effects than Davenport's apparatus. Since it has already been demonstrated by Hallman that increased free convection should increase friction factors, this could partially reconcile the differences between the two independent experiments.

1.4 Parallel Investigations

Concurrent to this theoretical investigation, G. S. Kirby [17] and J. L. Chance [3] investigated the same geometry with an experimental apparatus constructed to allow precise measurement of local temperature and velocity fields within the tube. This has permitted a degree of cross-coordination and cross-checking of numerical and experimental results never before attained for this type of experiment. By directly applying the experimental boundary conditions obtained by Kirby and Chance to the theoretical model, a point by point comparison of velocity and temperature fields is facilitated, resulting in a rigorous check on the analytical computer solution. As a further check, bulk parameters such as friction factors and Nusselt numbers have also been compared for given sets of boundary conditions. Further explanation and comments concerning this comparison are found in Chapter IV.

1.5 General Approach to the Solution

Previous analyses of this problem have included boundary layer

assumptions such as neglecting certain elements of the stress tensor and assuming constant fluid pressure across the flow stream in order to make the axial momentum equation more amenable to solution. Although this is common practice, it is difficult to verify that for conditions of high heating rates these assumptions are valid. Much after-the-fact discussion and justification has followed the earlier analyses, but, as pointed out by Hancock [11], a particular solution might not demonstrate an effect to be important when the effect is already assumed negligible at the outset of the analysis. Keeping this in mind, the analysis presented here has avoided, wherever possible, the commonly made simplifying assumptions. This approach should point out any fallacies in the application of common assumptions to situations involving large departures from equilibrium.

1.6 Objectives of the Analysis

In this section the analysis objectives are listed so that they may provide an aid to understanding the problem development and also provide a point of future reference as the various objectives are fulfilled.

The first major objective of the analysis is the derivation of a computer solvable mathematical model of the tubular flow geometry. The approach taken differs from the usual approach in two ways. First, integral rather than differential equations are used as a point of departure in deriving the mathematical model. Secondly, many of the commonly used boundary layer assumptions are omitted from the derivation,

making the model more complete than models used in previous analyses.

Once the mathematical model is complete, it may be put to several uses. In this investigation the model is applied to three major areas of study. First, data are developed to allow graphical plotting of the flow field. Secondly, the data obtained are extensively compared to the experimental data of Kirby [17] and Chance [3] and the analytical data of Wilkins [26]. The experimental comparison is greatly aided by the ability to simulate directly the experimental boundary conditions and then compare the results in a point-by-point manner. Finally, the flow data are used as a basis for creating dimensionless correlations for Nusselt number and friction factor which include the effects of free convection on these parameters.

CHAPTER II

GOVERNING EQUATIONS

2.1 Introduction

In this chapter the equations necessary for the problem solution are presented and put into a dimensionless form to generalize the results obtained from their solution. For completeness, additional information necessary for solution, such as boundary conditions and thermodynamic state relations, is also included in the chapter.

As mentioned in the first chapter, a scheme different from the usual differential equation approach is used in the analysis. Although the equations considered have their roots in the same physical laws, they are expressed in integral equation form which requires in the numerical approximation scheme the use of integral approximations such as Simpson's rule as well as the more commonly employed multipoint difference approximations for derivatives. The exact approximations used are stated later in Chapter III.

2.2 General Assumptions

Assumptions listed in this section apply to the overall approach to the problem. Assumptions which have limited application to a specific equation will be given with the affected equation.

The general assumptions are the following:

1. The fluid is Newtonian.

2. Laminar flow exists throughout the tube.
3. Steady flow exists.
4. The fluid flows in an upward direction.
5. Viscosity, thermal conductivity, and specific heat are functions of temperature only.
6. The fluid obeys the perfect gas law.

The first assumption excludes a few cases like rarefied gases from the formulation; however, in a large majority of situations this assumption is valid. The second and third assumptions further formulate the problem, allowing the appropriate equations to be selected and derived. The terminology "steady flow" essentially means that no variations with time occur in the flow. The fourth assumption, when combined with symmetrical boundary conditions, sets up a condition of angular symmetry around the longitudinal tube axis. This removes the angle coordinate from the equations, reducing the problem from a three dimensional problem to a two dimensional case. The last two assumptions are based on experimental data and are common practice in engineering heat transfer solutions dealing with a wide range of gases.

2.3 Pertinent Physical Laws

Mathematically, the number of unknown variables in a problem must usually be matched by the number of applicable independent equations before a definite solution can be extracted. Thus for the problem at hand, it is necessary to enumerate the important variables and the number of governing physical laws which may be successfully applied.

The variables to be found in the solution are velocity in the axial direction designated by the variable u, radial velocity v, the fluid temperature T, the pressure p, and density ρ. All the variables including pressure may vary continuously in both the axial and radial directions.

Since five dependent variables have been enumerated, it is necessary to utilize five independent governing relations among the variables. The five to be used are the continuity equation based on conservation of mass, axial momentum and radial momentum equations based on Newton's Second Law of Motion, the energy equation based on the First Law of Thermodynamics, and the Perfect Gas Law, the equation of state assumed for the particular substance to be studied in this investigation. Further development will show that this set of equations along with some additional state relations and boundary conditions yields a set of equations which are solvable by numerical methods.

2.4 Control Volume

The finite control volume used in the derivation of the governing equations is a circular ring element centered on the tube's longitudinal axis as shown in Figure 2-1. For convenience in the derivation, flow is visualized as being from left to right with the tube represented in a horizontal rather than its true vertical orientation.

The only governing equation which does not utilize this type of control volume is the radial momentum equation which will be considered as a separate case. In the diagram, A_i is the inner area of the ring,

A_o is the outer area, A_l is the left (upstream) face, and A_r is the right (downstream) face. This subscripting system is used consistently throughout all of the equation derivations and is used whenever any variable must be associated with a particular face of the fluid element.

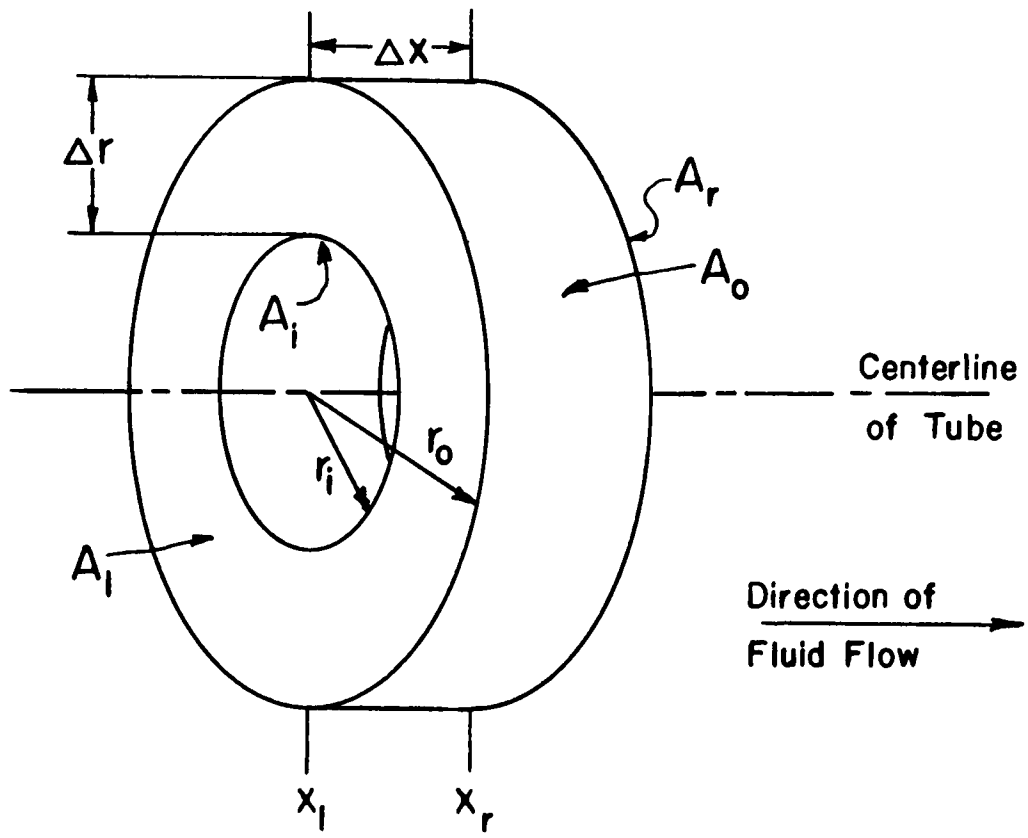

Fig. 2-1.--Typical control volume

2.5 Continuity Equation

The first equation to be derived, the continuity equation, is based on the principle of conservation of mass. Symbolically the principle may be written in terms of the "Rate of Creation" operator[1]

---

[1]See Kays [16] for further details of the uses of this operator.

as

$$\text{ROC (mass)} = 0 \tag{2.5.1}$$

where

$$\text{ROC (}\quad\text{)} \triangleq \text{outflow - inflow + rate of increase of storage} \tag{2.5.2}$$

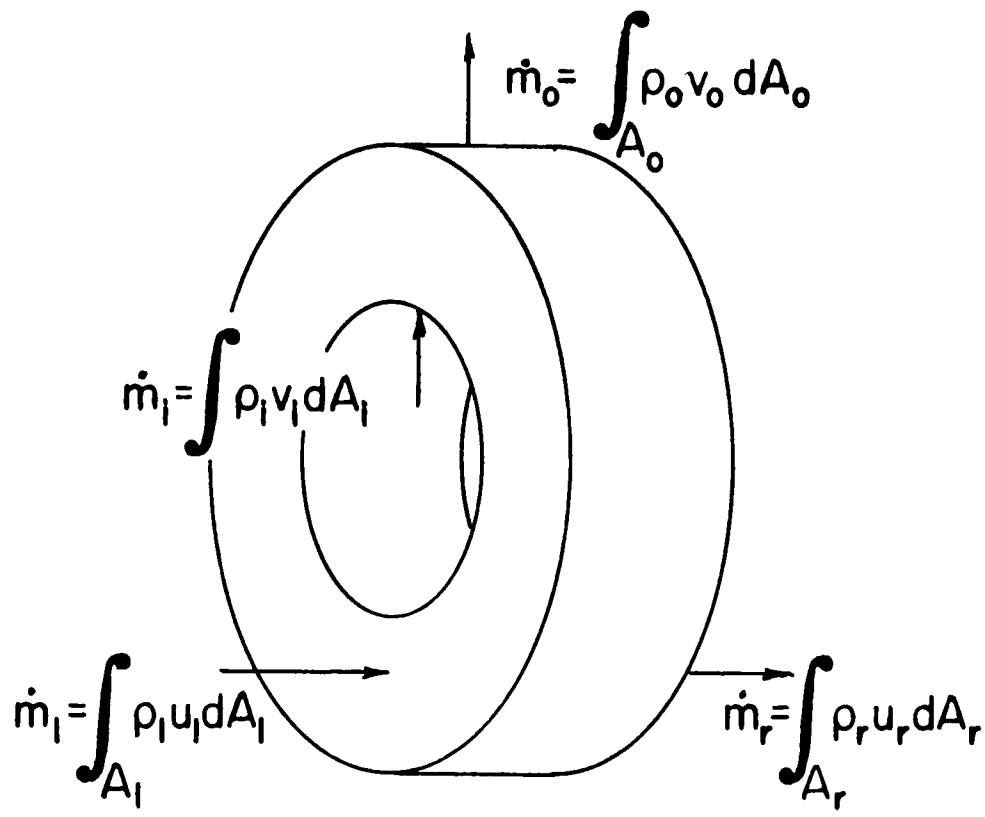

Fig. 2-2.--Control volume for continuity equation

Consider the control volume shown in Figure 2-2. The mass flows may be broken down according to the ROC operator as follows:

Mass outflows:

$$\dot{m}_o + \dot{m}_r = \int_{A_o} \rho_o v_o dA_o + \int_{A_r} \rho_r u_r dA_r$$

Mass inflows:

$$\dot{m}_i + \dot{m}_l = \int_{A_i} \rho_i v_i dA_i + \int_{A_l} \rho_l u_l dA_l$$

Change in mass storage:

0 (By the steady flow assumption)

Applying the operator of equation (2.5.1), the continuity equation is found to be

$$\int_{r_i}^{r_o} \rho_r u_r r dr - \int_{r_i}^{r_o} \rho_l u_l r dr + \int_{x_l}^{x_r} \rho_o v_o r_o dx - \int_{x_l}^{x_r} \rho_i v_i r_i dx = 0 \qquad (2.5.3)$$

Here the areas have been expressed in terms of the geometric coordinates, x and r, and a factor of 2π has been removed from all terms of the equation.

2.6 Axial Momentum Equation

The axial momentum equation is based on Newton's Second Law which may be expressed in terms of the previously used "Rate of Creation" operator as

$$ROC\ (M_x) = \Sigma F_x \qquad (2.6.1)$$

The expression ROC (M_x) represents the net momentum flux from the fluid element in the axial direction while ΣF_x represents the summation of the forces acting on the element in the axial direction. The fluxes and forces involved are shown in Figure 2-3.

Application of the ROC operator gives the following results

Integrated momentum flux outflows:

$$M_r + M_o = \int_{A_r} \rho_r u_r^2 dA_r + \int_{A_o} \rho_o u_o v_o dA_o$$

Integrated momentum flux inflows:

$$M_l + M_i = \int_{A_l} \rho_l u_l^2 dA_l + \int_{A_i} \rho_i u_i v_i dA_i$$

Change in momentum storage:

0 (By the steady flow assumption)

Summation of axial forces:

$$\Sigma F_x = \int_{A_r} \sigma_{xx,r} dA_r - \int_{A_l} \sigma_{xx,l} dA_l + \int_{A_o} \sigma_{xr,o} dA_o - \int_{A_i} \sigma_{xr,i} dA_i - \int_{v} \rho g dV$$

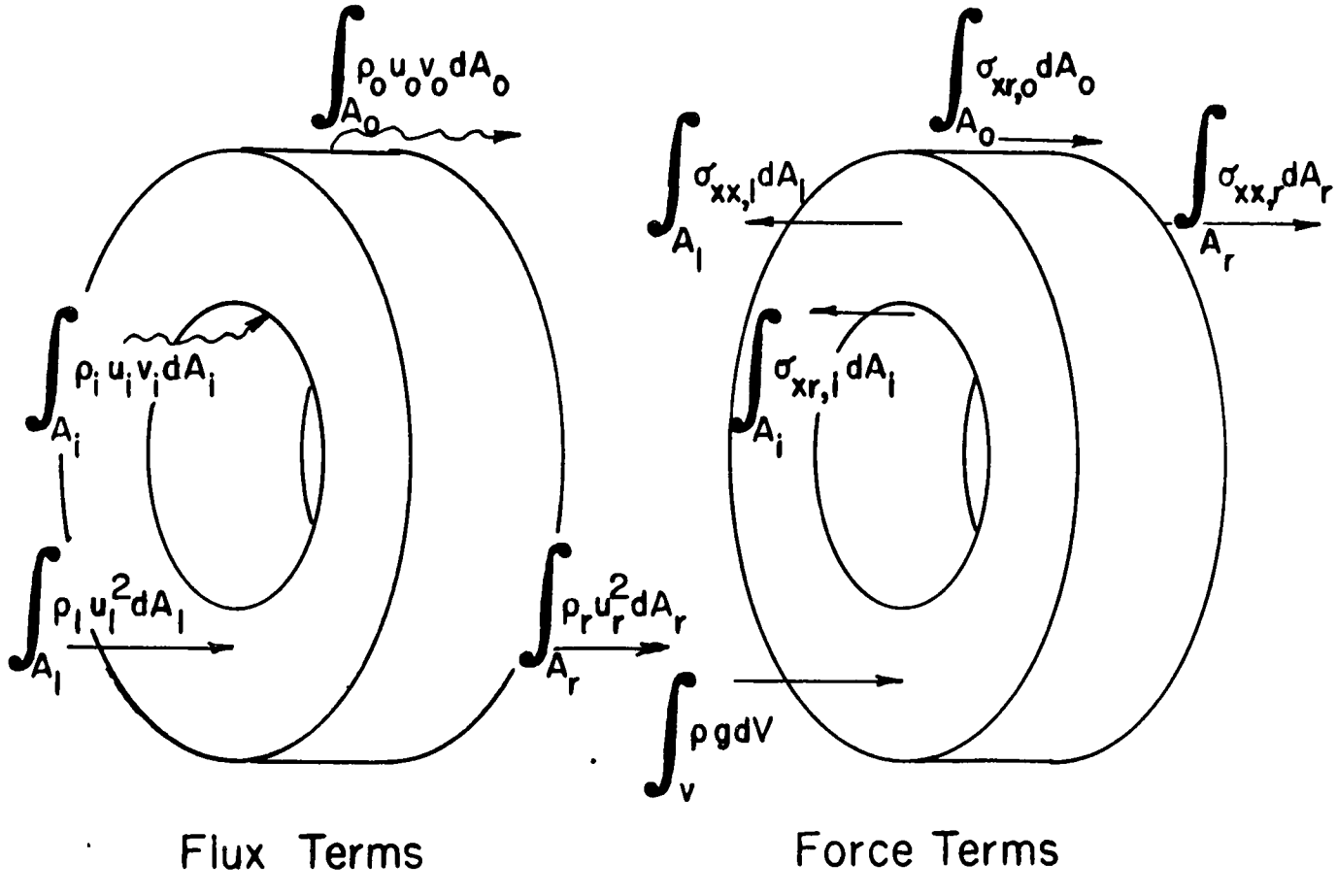

Fig. 2-3.--Control volumes for axial momentum

In the summation of forces, the last term is the buoyancy force exerted on the entire volume element by gravity, and the terms involving σ represent the stresses exerted on the various control volume faces. A summary of the stress tensor terms for a Newtonian fluid may be found in Schlichting [21] and Hughes and Gaylord [14]. These stress tensor elements in terms of variables already defined are

$$\sigma_{xx} = -p + 2\mu \frac{\partial u}{\partial x} - \frac{2}{3}\left[\frac{1}{r}\frac{\partial}{\partial r}(rv) + \frac{\partial u}{\partial x}\right] \tag{2.6.2}$$

$$\sigma_{xr} = \mu\left(\frac{\partial v}{\partial x} + \frac{\partial u}{\partial r}\right) \tag{2.6.3}$$

Now combining all the terms involved in the order required by the ROC operator of equation (2.5.2) the axial momentum equation may be formed.

$$\int_{r_i}^{r_o} \rho_r u_r r dr - \int_{r_i}^{r_o} \rho_1 u_1 r dr + \int_{x_1}^{x_r} \rho_o u_o v_o r_o dx - \int_{x_1}^{x_r} \rho_i u_i v_i r_i dx$$

$$= \int_{r_i}^{r_o} \left[-p_r + 2\mu_r \frac{\partial u_r}{\partial r} - \frac{2}{3}\mu_r\left(\frac{1}{r}\frac{\partial}{\partial r}(rv_r) + \frac{\partial u_r}{\partial x}\right)\right] r dr$$

$$- \int_{r_i}^{r_o} \left[-p_1 + 2\mu_1 \frac{\partial u_1}{\partial r} - \frac{2}{3}\mu_1\left(\frac{1}{r}\frac{\partial}{\partial r}(rv_r) + \frac{\partial u_r}{\partial x}\right)\right] r dr$$

$$+ \int_{x_1}^{x_r} \mu_o\left(\frac{\partial v_o}{\partial x} + \frac{\partial u_o}{\partial r}\right) r_o dx - \int_{x_1}^{x_r} \mu_i\left(\frac{\partial v_i}{\partial x} + \frac{\partial u_i}{\partial r}\right) r_i \, dx$$

$$- \int_{x_1}^{x_r} \int_{r_i}^{r_o} \rho g \, r dr dx \tag{2.6.4}$$

Again the areas in the equation have been expressed in terms of the geometric coordinates, and a factor of 2π has been removed from each term.

2.7 Radial Momentum Equation

An independent governing relation involving radial momenta and forces may be obtained by analyzing the control volume shown in Figure 2-4. Here rectangular Cartesian coordinates have been imposed on a control volume which is one half of the control volume used for the previous derivations. Because of symmetry around the centerline of the tube, the actual radial orientation of the y and z axes is immaterial. To enable equation formulation, the momenta and forces in the y direction have been arbitrarily selected for analysis.

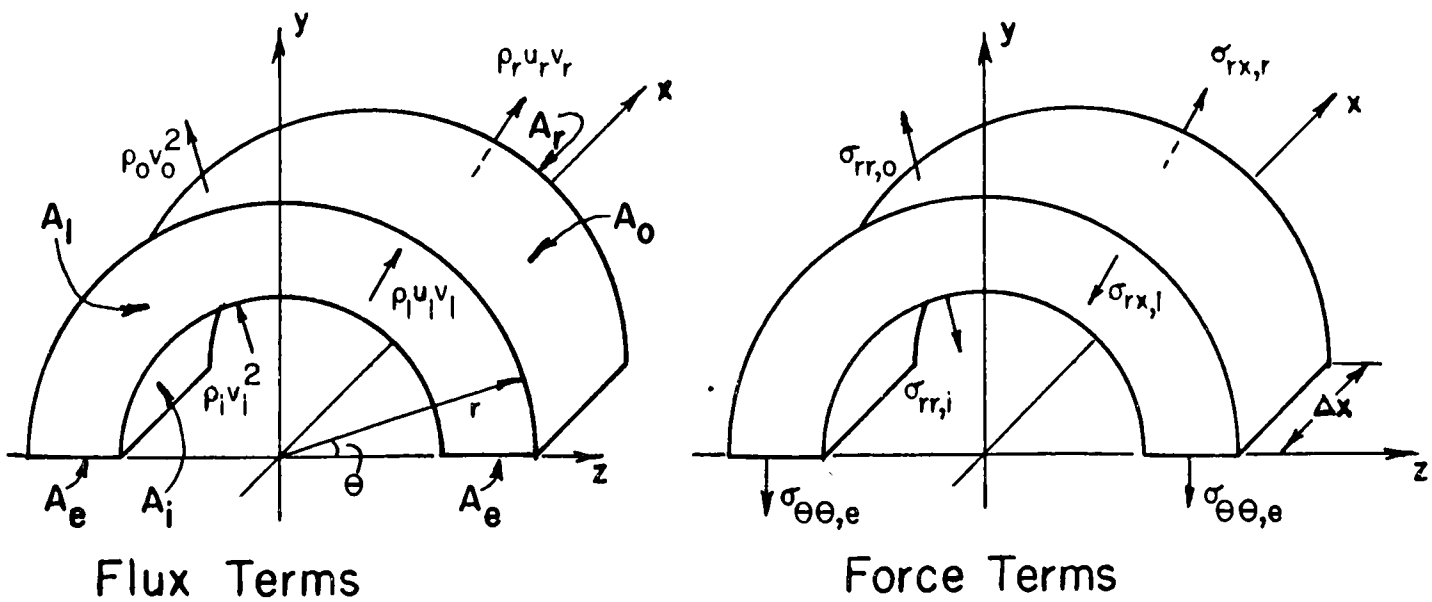

Fig. 2-4.--Control volume for radial momentum equation

As an example of how the equation terms are derived, consider that the y-component of the momentum flux through the outer face may be written as $\rho_o v_o^2 \sin\theta$. Then to obtain the total integrated momentum flux over the outer surface of the control volume, the following integral may be generated:

$$M_o = \int_0^{\pi} \int_{x_1}^{x_r} \rho_o v_o \sin\theta \; r_o dx \, d\theta \tag{2.7.1}$$

Carrying out the angular integration yields

$$M_o = 2 \int_{x_1}^{x_r} \rho_o v_o^2 dx \tag{2.7.2}$$

Similar analyses may be applied to the inner, left, and right faces of the control volume. The rectangular ends of the control volume must be treated differently. In this case a typical term appears as

$$F_e = \int_{x_1}^{x_r} \int_{r_i}^{r_o} \sigma_{\theta\theta,e} dr dx \tag{2.7.3}$$

where the subscript e denotes a variable evaluated at the end of the control volume. Since the velocity in the θ direction is zero by problem symmetry, no momentum flux is found through the ends of the control volume and only force terms must be evaluated.

After performing the angular integration, the forces and fluxes through the various control volume faces may be summarized as follows:

Integrated momentum flux outflows:

$$M_o + M_r = 2\int_{x_1}^{x_r} \rho_o v_o^2 r_o dx + 2\int_{r_i}^{r_o} \rho_r u_r v_r r dr$$

Integrated momentum flux inflows:

$$M_i + M_1 = 2\int_{x_1}^{x_r} \rho_i v_i^2 r_i dx + 2\int_{r_i}^{r_o} \rho_1 u_1 v_1 r dr$$

Change in momentum storage:

0 (By the steady flow assumption)

Summation of forces in y-direction:

$$F_y = 2\int_{x_1}^{x_r} \sigma_{rr,o} r_o dx - 2\int_{x_1}^{x_r} \sigma_{rr,i} r_i dx$$

$$+ 2\int_{r_i}^{r_o} \sigma_{xr,r} r dr - 2\int_{r_i}^{r_o} \sigma_{xr,1} r dr$$

$$- 2\int_{r_i}^{r_o}\int_{x_1}^{x_r} \sigma_{\theta\theta,e} dr dx$$

In the force terms the stress tensor elements for a Newtonian fluid are [14]

$$\sigma_{rr} = -p + 2\mu \frac{\partial v}{\partial r} - \frac{2}{3}\mu \left[\frac{1}{r}\frac{\partial}{\partial r}(rv) + \frac{\partial u}{\partial x}\right] \qquad (2.7.5)$$

$$\sigma_{\theta\theta} = -p + 2\mu \left(\frac{v}{r}\right) - \frac{2}{3}\mu \left[\frac{1}{r}\frac{\partial}{\partial r}(rv) + \frac{\partial u}{\partial x}\right] \qquad (2.7.6)$$

$$\sigma_{rx} = \mu \left(\frac{\partial v}{\partial x} + \frac{\partial u}{\partial r}\right) \qquad (2.7.7)$$

Application of the force-momentum principle in the form

$$\text{ROC}\,(M_y) = \Sigma F_y$$

to the listed forces and fluxes gives the sought after relation.

$$\int_{x_1}^{x_r} \rho_o v_o r_o dx - \int_{x_1}^{x_r} \rho_i v_i r_i dx + \int_{r_i}^{r_o} \rho_r u_r v_r r dr - \int_{r_i}^{r_o} \rho_1 u_1 v_1 r dr$$

$$= \int_{x_1}^{x_r} \left[-p_o + 2\mu_o \frac{\partial v_o}{\partial r} - \frac{2}{3}\mu_o\left(\frac{1}{r}\frac{\partial}{\partial r}(rv_o) + \frac{\partial u_o}{\partial x}\right)\right] r_o dx$$

$$- \int_{x_1}^{x_r} \left[-p_i + 2\mu_i \frac{\partial v_i}{\partial r} - \frac{2}{3}\mu \left(\frac{1}{r}\frac{\partial}{\partial r}(rv_i) + \frac{\partial u_i}{\partial x}\right)\right] r_i dx$$

$$+ \int_{r_i}^{r_o} \mu_r\left(\frac{\partial v_r}{\partial x} + \frac{\partial u_r}{\partial r}\right) r dr - \int_{r_i}^{r_o} \mu_1\left(\frac{\partial v_1}{\partial x} + \frac{\partial u_1}{\partial r}\right) r dr$$

$$- \int_{x_1}^{x_r} \int_{r_i}^{r_o} \left[-p_e + 2\mu_e\left(\frac{v_e}{r}\right) - \frac{2}{3}\mu_e\left(\frac{1}{r}\frac{\partial}{\partial r}(rv_e) + \frac{\partial u_e}{\partial x}\right)\right] dr dx \qquad (2.7.8)$$

2.8 Energy Equation

The energy equation is based upon the First Law of Thermodynamics. In terms of the ROC operator of equation (2.5.2), it may be expressed as

$$\text{ROC (energy)} = 0 \qquad (2.8.1)$$

In order to make the equation more tractable, the following simplifying

assumptions are made.

1. Neglect viscous dissipation of energy.

2. Neglect kinetic energy of the gas flow.

The first assumption is common engineering practice and, as pointed out by Kays [16], is valid for conditions of low Mach number flow of low Prandtl number fluids. In this investigation both of these conditions are satisfied since the Mach number is usually on the order of 0.004 and the Prandtl number is about 0.7.

The second assumption is also common practice where low velocity flows of comparatively light fluids are encountered. In this investigation the kinetic energy terms constructed for spot checking this assumption were always at least one or two orders of magnitude smaller than the next smallest term in the equation.

The inclusion of the viscous dissipation term and kinetic energy term in the energy equation presents no barrier to obtaining a computer solution. However, upon analysis, the slightly increased accuracy obtained by including the terms is more than offset by the increased programming complexity introduced by their inclusion. For further investigation into other fluid flow regimes, the inclusion of these terms into the existing computer code would involve only moderate revisions.

The principal energy flow terms are the axial and radial convection terms and the radial and axial conduction terms. In preparation for application of the ROC operator, the terms may be broken down as is shown in Figure 2-5.

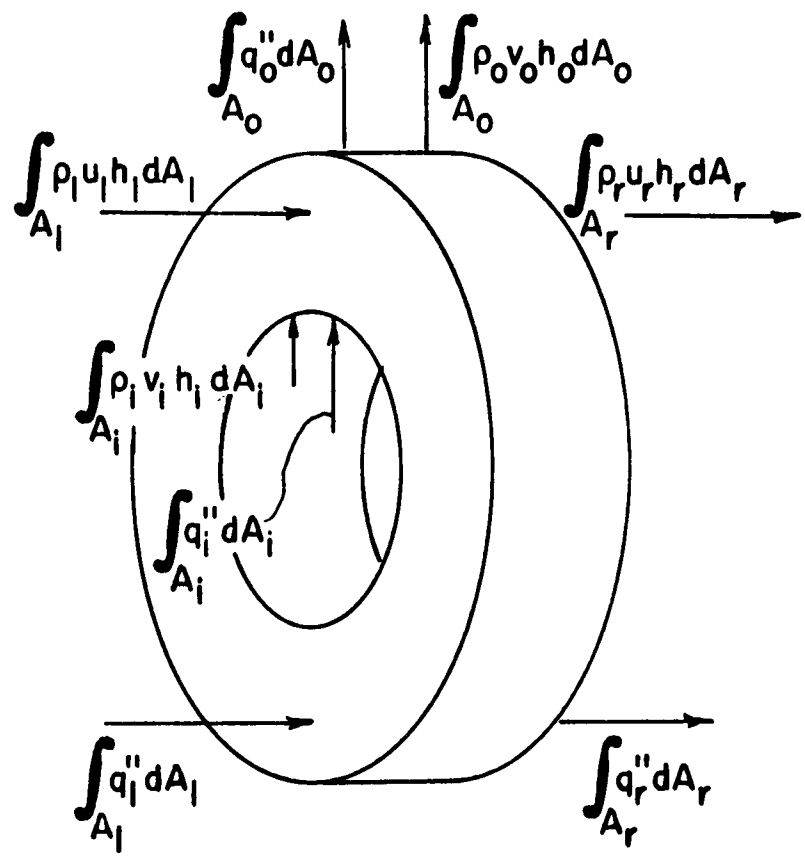

Fig. 2-5.--Control volume for energy equation

Grouping of the terms into inflow terms and outflow terms gives

Energy outflows:

$$E_o + E_r = \int_{A_o} \rho_o v_o h_o dA_o + \int_{A_r} \rho_r u_r h_r dA_r$$

$$+ \int_{A_o} q_o'' \, dA_o + \int_{A_r} q_r'' \, dA_r$$

Energy inflows:

$$E_i + E_l = \int_{A_i} \rho_i v_i h_i dA_i + \int_{A_l} \rho_l u_l h_l dA_l$$

$$+ \int_{A_i} q''_i \, dA_i + \int_{A_l} q''_l \, dA_l$$

Change in energy storage:

0 (By the steady flow assumption)

Now, substituting Fourier's heat conduction rate equations,

$$q''_{axial} = -k \frac{\partial T}{\partial x} \quad \text{(axial direction)} \qquad (2.8.2)$$

$$q''_{radial} = -k \frac{\partial T}{\partial r} \quad \text{(radial direction)} \qquad (2.8.3)$$

into the conduction terms and collecting the terms according to the ROC operator yields the energy equation.

$$\int_{r_i}^{r_o} \rho_r u_r h_r r dr - \int_{r_i}^{r_o} \rho_l u_l h_l r dr + \int_{x_l}^{x_r} \rho_o v_o h_o r_o dx - \int_{x_l}^{x_r} \rho_i v_i h_i r_i dx$$

$$- \int_{r_i}^{r_o} k_r \frac{\partial T_r}{\partial x} r dr + \int_{r_i}^{r_o} k_l \frac{\partial T_l}{\partial x} r dr$$

$$- \int_{x_l}^{x_r} k_o \frac{\partial T_o}{\partial r} r_o dx + \int_{x_l}^{x_r} k_i \frac{\partial T_i}{\partial r} r_i dx = 0 \qquad (2.8.4)$$

Here again, the area terms have been expressed in cylindrical coordinates, and a factor of 2π has been removed from all terms. In the equation, the enthalpy h at a given temperature T_a may be expressed for a perfect gas as

$$h_a = h_{ref} + \int_{T_{ref}}^{T_a} c_p dT \qquad (2.8.5)$$

where the subscript "ref" refers to an arbitrarily established reference condition, and c_p is taken to be a function of temperature.

2.9 Boundary Conditions

Further formulation of the mathematical model involves the statement of the boundary and entrance conditions to be applied to the problem solution. To clarify, the term "entrance condition" as used here refers to conditions existing at the cross-section of the tube where heating begins, while boundary conditions refer to conditions along the tube wall and at the tube centerline. Some of the conditions are specified as part of the process of defining the problem, while others are a result of physical laws governing the flow. A statement of the entrance conditions in which the variables are expressed as functions of the coordinates x and r is shown in Table 2-1. Similarly the boundary conditions are shown in Table 2-2. In both tables the subscript w denotes a condition evaluated at the wall, the variable with the subscript label "in" denotes an entrance condition, and the subscript b denotes a bulk parameter defined according to a rule given in Appendix C.

TABLE 2-1

ENTRANCE CONDITIONS

1. $u(0,r) = 2u_{b,in}\left[1 - (\frac{r}{r_w})^2\right]$ 2. $v(0,r) = 0$ 3. $p(0,r) = p_{in}$ = constant 4. $T(0,r) = T_{in}$ = constant	All entrance conditions specified as part of problem definition

TABLE 2-2

BOUNDARY CONDITIONS

Condition	Source of Condition
1. $u(x,r_w) = 0$	No slip at tube wall
2. $v(x,r_w) = 0$	Solid boundary
3. $T(x,r_w) = T_w(x)$	Chosen to fit experimental data; tabulated in Chapter IV
4. $\frac{\partial u}{\partial r}(x,r \to 0) = 0$	By problem symmetry, no momentum flux across centerline of tube
5. $\frac{\partial T}{\partial r}(x,r \to 0) = 0$	By problem symmetry, no conductive heat transfer at centerline of tube
6. $v(v,r \to 0) = 0$	By problem symmetry, no mass flow across centerline of tube

The fourth and fifth boundary conditions are derived by taking the appropriate rate equations, in this case the shear force expression for a Newtonian fluid, $\tau = \mu \frac{\partial u}{\partial r}$, and Fourier's conduction law, $q'' = -k \frac{\partial T}{\partial r}$, and evaluating these laws at the centerline of the tube. The symmetry imposed on the problem by upflow and symmetrical boundary conditions at the wall of the tube forces the derivatives in these expressions to zero.

2.10 Additional Relations

In addition to the integral equations used as a basis for the solution in the main portion of the stream, additional differential equations will be used in the region of the centerline, where the integral equations sometimes fail to yield suitable relations. The main problem with integral equations is that at the centerline many integrals contain the radius r, which is, of course, zero at this point. This does not create the case of indeterminant forms encountered in differential equations, but it effectively establishes that no matter what bounded value a variable at the centerline takes on, it will not affect the value of the integral. Looking at this from the point of view of equation solution, an integral containing the radius r simply does not contain the information necessary to fix the value of a variable at the centerline. The equations in which this problem occurs are the continuity, axial momentum, and energy equations. To circumvent the problem and allow determination of centerline variables such as axial velocity and temperature, differential equations are employed near the centerline and extrapolated to it. As mentioned this is complicated by

the differnetial equations becoming indeterminant at the centerline. Terms involving zero over zero become common requiring L'Hospital's rule to be invoked to give determinant relationships. The equations used will now be stated with their associated specialized centerline forms.

Continuity:

General form:

$$\frac{\partial}{\partial x}(\rho u) + \frac{1}{r}\frac{\partial}{\partial r}(\rho v r) = 0 \qquad (2.10.1)$$

Centerline form:

$$\frac{\partial}{\partial x}(\rho u) + 2\rho\frac{\partial v}{\partial r} = 0 \qquad (2.10.2)$$

Axial momentum:

General form:

$$\rho u\frac{\partial u}{\partial x} + \rho v\frac{\partial v}{\partial r}$$

$$= -\frac{\partial p}{\partial x} - \rho g + \frac{\partial}{\partial x}\left[2\mu\frac{\partial u}{\partial x} - \frac{2}{3}\mu\left(\frac{\partial u}{\partial x} + \frac{1}{r}\frac{\partial v}{\partial r}\right)\right]$$

$$+ \frac{1}{r}\frac{\partial}{\partial r}\left[\mu r\left(\frac{\partial v}{\partial x} + \frac{\partial u}{\partial r}\right)\right] \qquad (2.10.3)$$

Centerline form:

$$\rho u\frac{\partial u}{\partial x} = -\frac{\partial p}{\partial x} - \rho g + \frac{4}{3}\mu\frac{\partial^2 u}{\partial x^2} + 2\mu\frac{\partial^2 u}{\partial r^2}$$

$$+ \frac{2}{3}\mu\frac{\partial^2 v}{\partial x \partial r} + \frac{4}{3}\mu\frac{\partial \mu}{\partial x}\frac{\partial u}{\partial x} - \frac{4}{3}\frac{\partial u}{\partial x}\frac{\partial v}{\partial r} \qquad (2.10.4)$$

Energy equation:

General form:

$$\frac{\partial}{\partial x}(\rho u h) + \frac{1}{r}\frac{\partial}{\partial r}(\rho v r h)$$

$$= \frac{\partial}{\partial x}\left(k\frac{\partial T}{\partial x}\right) + \frac{1}{r}\frac{\partial}{\partial r}\left(kr\frac{\partial T}{\partial r}\right) \qquad (2.10.5)$$

Centerline form:

$$\rho u \frac{\partial h}{\partial x} = k \frac{\partial^2 T}{\partial x^2} + \frac{\partial T}{\partial x} \frac{\partial k}{\partial x} + 2k \frac{\partial^2 T}{\partial r^2} \qquad (2.10.6)$$

In the case of the energy equation, the approximation $h_a = h_{ref} + c_p (T_a - T_{ref})$ is useful for enthalpy with c_p assumed to be a constant. However, this happens only at the centerline where the temperature changes comparatively slowly, making the approximation more valid than if used across the entire flow stream.

In the case of the continuity equation and the axial momentum equation employment of differential equations at the tube wall also became necessary. In the latter case the equation was used to generate an independent equation necessary to fill out a set of equations. The equations used are as follows:

Continuity at wall:

$$\frac{\partial v}{\partial r} = 0 \qquad (2.10.7)$$

Axial momentum at wall:

$$\frac{\partial p}{\partial x} = \rho g - \mu \frac{\partial^2 u}{\partial r^2} - \frac{\partial u}{\partial r} \frac{\partial \mu}{\partial r} - \mu \frac{\partial u}{\partial r} \qquad (2.10.8)$$

The general form of these equations has already been stated.

2.11 Dimensionless Parameters

In order to make the problem solution as general as possible, dimensionless parameters have been selected for substitution into the governing equations. These dimensionless parameters are denoted by a superscript + sign and are tabulated in Table 2-3.

2.12 Dimensionless Equations

Substitution of the dimensionless variables defined in the

TABLE 2-3

DIMENSIONLESS VARIABLES

$$u^+ = \frac{u}{u_{b,in}} \qquad \rho^+ = \frac{\rho}{\rho_{in}}$$

$$v^+ = \frac{v}{u_{b,in}} \qquad \mu^+ = \frac{\mu}{\mu_{in}}$$

$$T^+ = \frac{T}{T_{b,in}} \qquad k^+ = \frac{k}{k_{in}}$$

$$p^+ = \frac{p_{in} - p}{\rho_{in}\, u_{b,in}^2} \qquad c_p^+ = \frac{c_p}{c_{p,in}}$$

$$x^+ = \frac{x}{r_w} \qquad h^+ = \frac{h}{c_{p,in}\, T_{in}}$$

$$r^+ = \frac{r}{r_w}$$

previous section into the governing equations results in a set of dimensionless equations. In the process of arriving at these dimensionless equations, certain groupings of constants may be factored and manipulated into commonly recognized forms such as the Reynolds number and the Prandtl number. The following equations are used as a basis for the discrete numerical model.

Continuity equation:

$$\int_{r_i}^{r_o} \rho_r^+ u_r^+ r^+ dr^+ - \int_{r_i}^{r_o} \rho_l^+ u_l^+ r^+ dr^+ + \int_{x_l}^{x_r} \rho_o^+ v_o^+ r_o^+ dx^+ - \int_{x_l}^{x_r} \rho_i^+ v_i^+ r_i^+ dx^+ = 0 \qquad (2.12.1)$$

Axial momentum equation:

$$\frac{N_{Re,in}}{2}\left[\int_{r_i^+}^{r_o^+}\rho_r^+u_r^{+2}r^+dr^+ - \int_{r_i^+}^{r_o^+}\rho_l^+u_l^{+2}r^+dr^+ + \int_{x_l^+}^{x_r^+}\rho_o^+u_o^+v_o^+r_o^+dx^+ - \int_{x_l^+}^{x_r^+}\rho_i^+u_i^+v_i^+r_i^+dx^+\right]$$

$$= \frac{N_{Re,in}}{2}\left[\int_{r_i^+}^{r_i^+}p_r^+r^+dr^+ - \int_{r_i^+}^{r_o^+}p_l^+r^+dr^+\right]$$

$$+ \frac{N^*_{Gr,in}}{4\,N_{Re,in}}\int_{x_l^+}^{x_r^+}\int_{r_i^+}^{r_o^+}\rho^+r^+dr^+dx^+ + 2\int_{r_i^+}^{r_o^+}\mu_r^+\frac{\partial u_r^+}{\partial x^+}r^+dr^+$$

$$- 2\int_{r_i^+}^{r_o^+}\mu_l^+\frac{\partial u_l^+}{\partial x^+}r^+dr^+$$

$$- \frac{2}{3}\int_{r_i^+}^{r_o^+}\mu_r^+\frac{\partial}{\partial r^+}(r^+v_r^+)\,dr^+ + \frac{2}{3}\int_{r_i^+}^{r_o^+}\mu_l^+\frac{\partial}{\partial r^+}(r^+v_l^+)\,dr^+$$

$$- \frac{2}{3}\int_{r_i^+}^{r_o^+}\mu_r^+\frac{\partial u_r}{\partial x^+}r^+dr^+ + \frac{2}{3}\int_{r_i^+}^{r_o^+}\mu_l^+\frac{\partial u_l}{\partial x^+}r^+dr^+$$

$$+ \int_{x_l^+}^{x_r^+}\mu_o^+\frac{\partial v_o^+}{\partial x^+}r_o^+dx^+ - \int_{x_l^+}^{x_r^+}\mu_i^+\frac{\partial v_i^+}{\partial x^+}r_i^+dx^+$$

$$+ \int_{x_l^+}^{x_r^+}\mu_o^+\frac{\partial u_o^+}{\partial r^+}r_o^+dx^+ - \int_{x_l^+}^{x_r^+}\mu_i^+\frac{\partial u_i^+}{\partial r^+}r_i^+dx^+ \qquad (2.12.2)$$

Radial momentum equation:

$$\frac{N_{Re,in}}{2}\left[\int_{x_l^+}^{x_r^+}\rho_o^+ v_o^{+2} r_o^+ dx^+ - \int_{x_l^+}^{x_r^+}\rho_i^+ v_i^{+2} r_i^+ dx^+ + \int_{r_i^+}^{r_o^+}\rho_r^+ v_r^+ u_r^+ r^+ dr^+ + \int_{r_i^+}^{r_o^+}\rho_l^+ v_l^+ u_l^+ r^+ dr^+\right]$$

$$= \frac{N_{Re,in}}{2}\left[\int_{x_l^+}^{x_r^+} p_o^+ r_o^+ dx^+ - \int_{x_l^+}^{x_r^+} p_i^+ r_i^+ dx^+ - \int_{x_l^+}^{x_r^+}\int_{r_i^+}^{r_o^+} p_e^+ dr^+ dx^+\right]$$

$$+ 2\int_{x_l^+}^{x_r^+}\mu_o^+ \frac{\partial v_o^+}{\partial r^+} r_o^+ dx^+ - \int_{x_l^+}^{x_r^+}\mu_i^+ \frac{\partial v_i^+}{\partial r^+} r_i^+ dx^+$$

$$- \frac{2}{3}\int_{x_l^+}^{x_r^+}\mu_o^+ \frac{\partial}{\partial r^+}(r^+ v_o^+)\, dx^+ + \frac{2}{3}\int_{x_l^+}^{x_r^+}\mu_i^+ \frac{\partial}{\partial r^+}(r^+ v_i^+)\, dx^+$$

$$- \frac{2}{3}\int_{x_l^+}^{x_r^+}\mu_o^+ \frac{\partial u_o^+}{\partial x^+} r_o^+ dx^+ + \frac{2}{3}\int_{x_l^+}^{x_r^+}\mu_i^+ \frac{\partial u_i^+}{\partial x^+} r_i^+ dx^+$$

$$+ \int_{r_i^+}^{r_o^+}\mu_r^+ \left(\frac{\partial v_r^+}{\partial x^+} + \frac{\partial u_r^+}{\partial r^+}\right) r^+ dr^+ - \int_{r_i^+}^{r_o^+}\mu_l^+ \left(\frac{\partial v_l^+}{\partial x^+} + \frac{\partial u_l^+}{\partial r^+}\right) r^+ dr^+$$

$$- \int_{x_l^+}^{x_r^+}\int_{r_i^+}^{r_o^+}\left[2\mu_e^+ \left(\frac{v_e^+}{r^+}\right) - \frac{2}{3}\left(\frac{1}{r^+}\frac{\partial}{\partial r^+}(r^+ v_e^+) + \frac{\partial u_e^+}{\partial x^+}\right)\right] dr^+ dx^+ \qquad (2.12.3)$$

Energy equation:

$$\frac{N_{Re,in}}{2}\left[\int_{r_i^+}^{r_o^+}\rho_r^+u_r^+h_r^+r^+dr^+ - \int_{r_i^+}^{r_o^+}\rho_1^+u_1^+h_1^+r^+dr^+ + \int_{x_1^+}^{x_r^+}\rho_o^+v_o^+h_o^+r_o^+dx^+ - \int_{x_1^+}^{x_r^+}\rho_i^+v_i^+h_i^+r_i^+dx^+\right]$$

$$+\frac{1}{N_{Pr,in}}\left[\int_{r_i^+}^{r_o^+}k_1^+\frac{\partial T_1^+}{\partial x^+}r^+dr^+ - \int_{r_i^+}^{r_o^+}k_r^+\frac{\partial T_r^+}{\partial x^+}r^+dr^+ - \int_{x_1^+}^{x_r^+}k_o^+\frac{\partial T_o^+}{\partial r^+}r_o^+dx^+ + \int_{x_1^+}^{x_r^+}k_i^+\frac{\partial T_i^+}{\partial r^+}r_i^+dx^+\right] = 0 \qquad (2.12.4)$$

where the dimensionless numbers used in the equations are defined as follows:

$$N_{Re,in} = \frac{2\rho_{in}\,u_{b,in}\,r_w}{\mu_{in}} \qquad (2.12.5)$$

$$N_{Pr,in} = \frac{\mu_{in}\,c_{p,in}}{k_{in}} \qquad (2.12.6)$$

$$N^*_{Gr,in} = \frac{8\rho_{in}^2\,r_w^3\,g}{\mu_{in}^2}\,. \qquad (2.12.7)$$

The dimensionless form of the specialized differential equations stated earlier are

Centerline continuity equation:

$$\frac{\partial}{\partial x^+}(\rho^+u^+) + 2\rho^+\frac{\partial v^+}{\partial r^+} = 0 \qquad (2.12.8)$$

Centerline axial momentum equation:

$$\frac{N_{Re,in}}{2}\rho^+u^+\frac{\partial u^+}{\partial x^+} = \frac{N_{Re,in}}{2}\frac{\partial p^+}{\partial x^+} - \frac{N^*_{Gr,in}}{4\,N_{Re,in}}\rho^+ + \frac{4}{3}\mu^+\frac{\partial^2 u^+}{\partial x^{+2}} + 2\mu^+\frac{\partial^2 u^+}{\partial r^{+2}} + \frac{2}{3}\mu^+\frac{\partial^2 v^+}{\partial x^+\partial r^+} + \frac{4}{3}\frac{\partial \mu^+}{\partial x^+}\frac{\partial u^+}{\partial r^+} - \frac{4}{3}\frac{\partial \mu^+}{\partial x^+}\frac{\partial v^+}{\partial r^+} \qquad (2.12.9)$$

Centerline energy equation:

$$\frac{N_{Re,in}}{2}\rho^+u^+\frac{\partial h^+}{\partial x^+} = \frac{1}{N_{Pr,in}}\left[k^+\frac{\partial^2 T^+}{\partial x^{+2}} + \frac{\partial k^+}{\partial x^+}\frac{\partial T^+}{\partial r^+} + 2k^+\frac{\partial^2 T^+}{\partial r^{+2}}\right] \qquad (2.12.10)$$

Wall continuity equation:

$$\frac{\partial v^+}{\partial r^+} = 0 \qquad (2.12.11)$$

Wall axial momentum equation:

$$\frac{N_{Re,in}}{2}\frac{\partial p^+}{\partial x^+} = \frac{N_{Gr,in}}{4\,N_{Re,in}}\rho^+ - \mu^+\frac{\partial^2 u^+}{\partial r^{+2}} - \frac{\partial u^+}{\partial r^+}\frac{\partial \mu^+}{\partial r^+} - \mu^+\frac{\partial u^+}{\partial r^+} \qquad (2.12.12)$$

2.13 State Relations

Besides the equations based on physical law, state relations which relate physical properties such as thermal conductivity and viscosity to other physical properties are required in the analysis. The

sources of these relations are experimental or statistical mechanical in nature and vary from fluid to fluid. For this report air is chosen as being an important, typical compressible fluid. The thermodynamic state relations chosen to represent air are

Viscosity:

$$\mu = \mu_{ref} \, (T/T_{ref})^{a} \tag{2.13.1}$$

Thermal conductivity:

$$k = k_{ref} \, (T/T_{ref})^{b} \tag{2.13.2}$$

Specific heat:

$$c_p = c_{p,ref} \, (T/T_{ref})^{c} \tag{2.13.3}$$

Perfect Gas Equation of State:

$$p = \rho RT$$

The appropriateness of these relations has been discussed by Worsøe-Schmidt [27]. For the present analysis, the exponents $a = 0.67$, $b = 0.71$, and $c = 0.12$ have been used. These are the same exponents justified by Worsøe-Schmidt for his analysis of air. By using $T_{ref} = T_{in}$ in the relations and substituting other dimensionless variables into equations (2.13.1), (2.13.2) and (2.13.3) dimensionless relations for use with the dimensionless governing equations may be found as follows:

Viscosity:

$$\mu^{+} = T^{+a} \tag{2.13.4}$$

Thermal conductivity:

$$k^{+} = T^{+b} \tag{2.13.5}$$

Specific heat:

$$c_p^+ = T^{+c} \tag{2.13.6}$$

In the case of the equation of state for a perfect gas, introduction of dimensionless variables gives

$$\rho^+ = \frac{1}{T^+} - \frac{\gamma M_{in}^2 p^+}{T^+} \tag{2.13.7}$$

Here, γ is the ratio of specific heats c_p/c_v, and M_{in} is the Mach number at the entrance to the heated section.

CHAPTER III

METHODS OF NUMERICAL SOLUTION

3.1 Introduction

The approach to be utilized in obtaining a solution to the equations is that of the conversion of the integral and differential equations into what mathematicians involved in numerical analysis call "discrete approximations" to these equations. This type of approximation, in which a grid network of variables defined at points replaces the continuous variables such as temperature and velocity, lends itself well to computer solution. Once the grid network is established, then difference formulas and approximate integration formulas may be used to approximate the derivatives and integrals. By this process the problem is converted from that of solving formidable non-linear integral and differential equations to that of solving a large set of less formidable algebraic equations. When constructing these discrete approximations, however, it is necessary to give careful consideration to equation stability in the numerical analysis sense of the word. More will be said on this subject as the formulation progresses.

3.2 Control Volumes

The basis for construction of the governing equations of Chapter II is the control volume. It is now necessary to relate the control

volumes used in Chapter II to the grid network used for numerical solution of the equations. Although a single grid network as shown in Figure 3-1 is used throughout the problem solution, the relationship of the control volumes to the grid varies somewhat from equation to equation. To permit the derivation of the discrete approximations to proceed, typical sections of the large grid have been isolated as shown in Figure 3-2. These sections may be visualized as planes passing through the control volume of interest as shown in Figure 3-3.

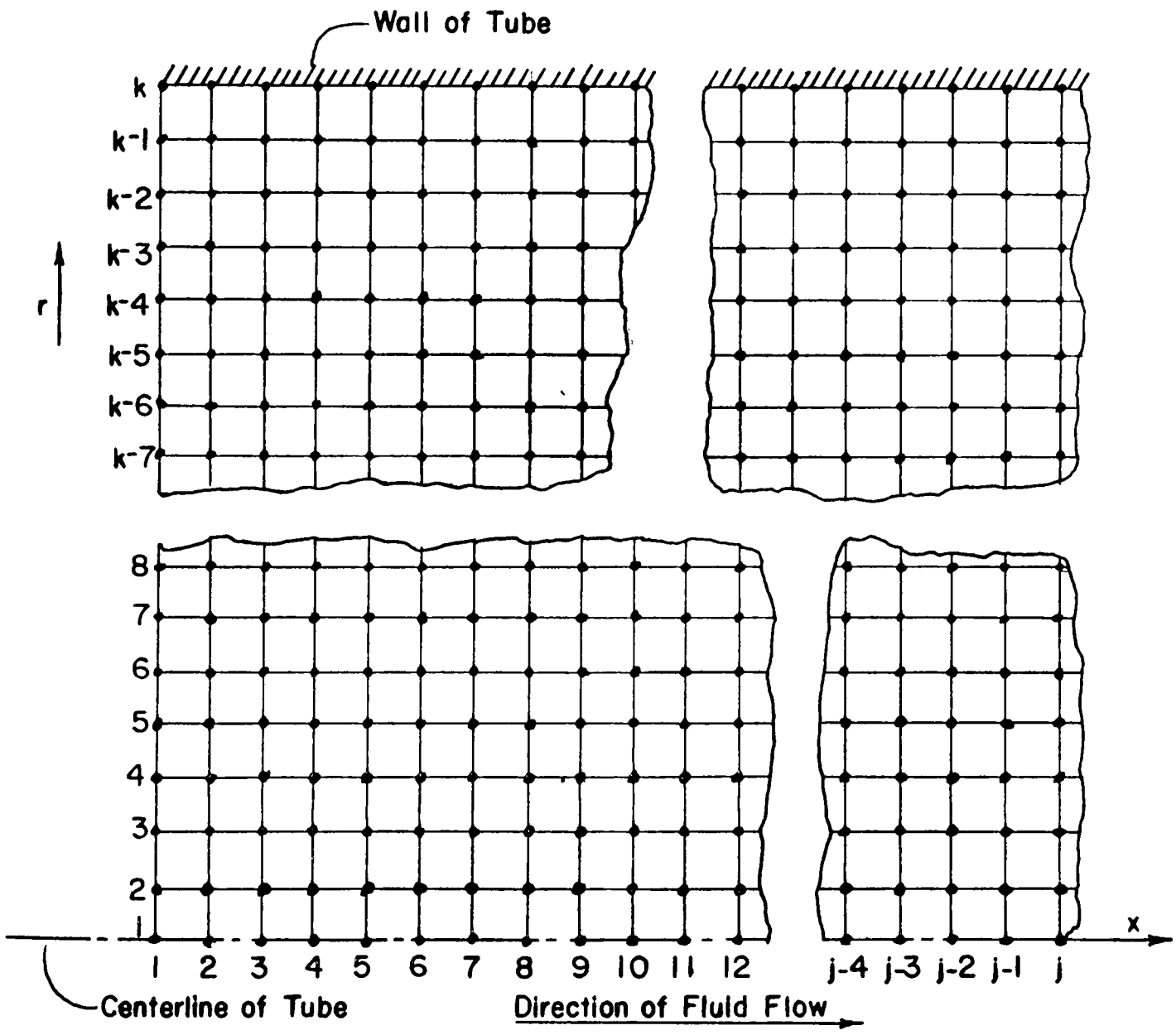

Fig. 3-1.--Grid network for numerical solution

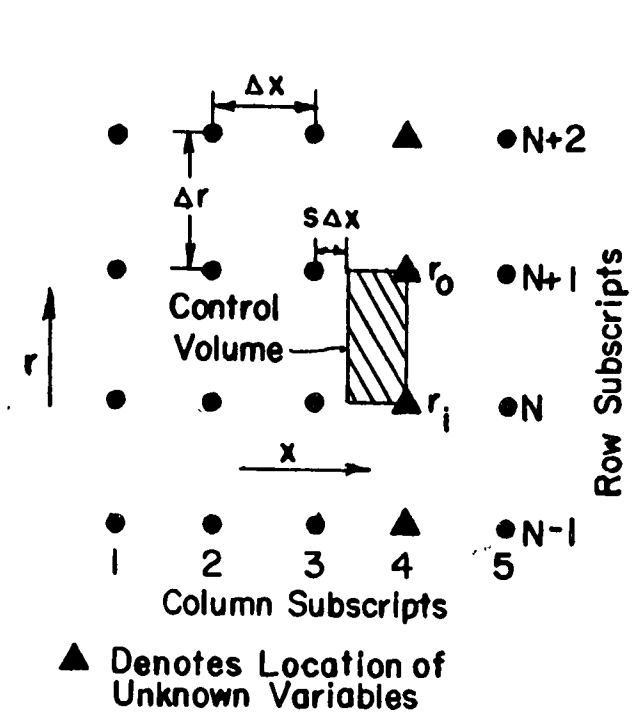

(a)

Typical control volume used for continuity and radial momentum equation.

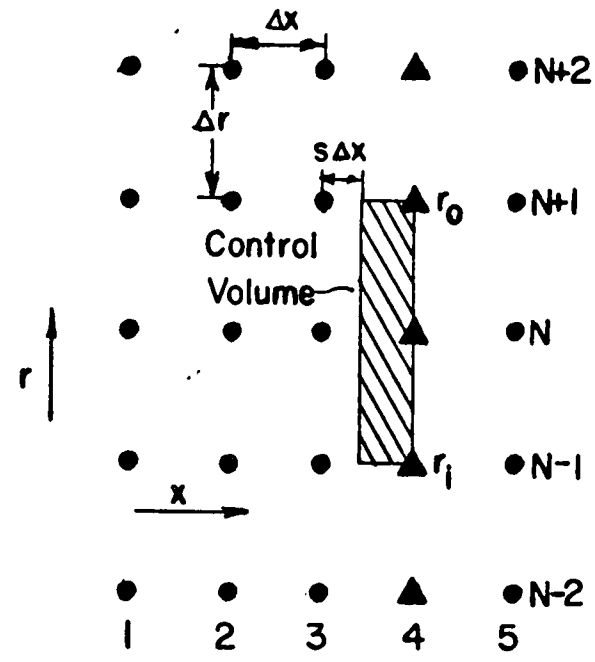

(b)

Typical control volume used for axial momentum and energy equation.

Fig. 3-2.--Typical control volumes related to grid network

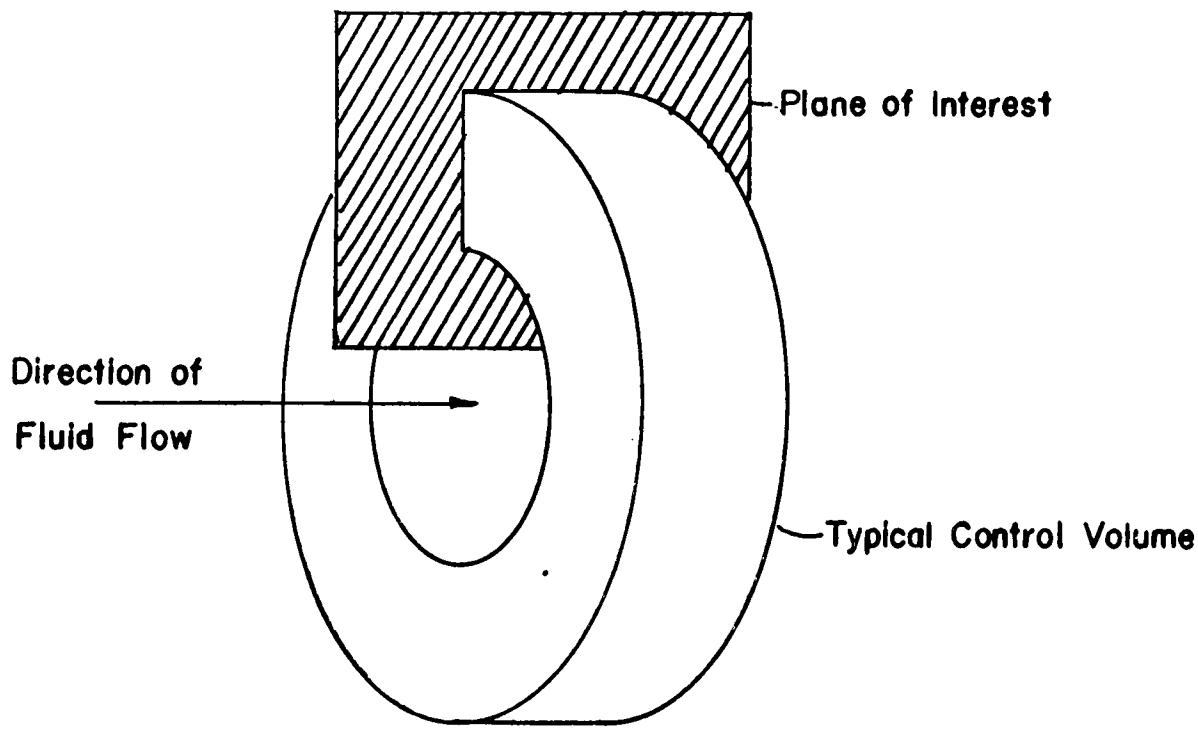

Fig. 3-3.--Plane depicted in grid diagrams of Figure 3-2

The continuous variables of the equations of Chapter II are replaced in this chapter by variables defined only at grid points. The position of these discrete variables in the tube is located by a subscripting system related to Figure 3-1. For the typical variable, $U_{n,m}$, the first subscript represents the number of the row of grid points found by starting at the centerline and counting toward the wall, while the second subscript represents the number of the column of grid points found by counting from left to right starting at the beginning of heating.

It should be noted that the use of the numbers one through five as column labels in Figure 3-2 is for convenience of derivation only. The typical points of Figure 3-2 may be sequentially overlaid at successive axial positions shown in Figure 3-1 to permit solution of the entire problem domain.

3.3 General Observations About the Governing Equations

Before becoming deeply involved in the mechanics of the discrete approximations to the governing equations, the equations may be examined for features which simplify the approximation process. The principle feature of this nature is that like terms appear on opposite faces of the control volume; that is, if a particular integral must be evaluated on the left face, it must also be evaluated (with opposite signs) on the right face of the control volume. By grouping these paired terms together and approximating them as a unit, some simplifications of the approximation process is attained. The same is true of integrals evaluated at the inner and outer faces of the control volume, although

the results are somewhat different.

In approximate numerical methods small errors may creep into the solution from several sources. Examples of such error sources are the discretization[1] error, the error inherent in the approximation method itself, and round-off error, caused by the fact that all numerical calculations must be rounded off to a fixed number of decimal (or binary) places. If these errors continue to accumulate and grow, the error may possibly mask the problem solution and thus reduce the answers obtained to so much random noise. Mathematicians designate as stable a numerical scheme in which errors do not grow or accumulate appreciably. Over the years rules have been developed which allow checking a discrete model to ascertain its stability without actually performing numerical experiments on the model chosen. Unfortunately for the nonlinear problem considered here, the methods developed to insure stability deal mostly with linear boundary value problems. However, by observing the precautions taken with the linear problems, they may be applied without complete guarantee of their success, to nonlinear problems.

3.4 Approximations Used with the Continuity Equation

Of the equations encountered in the analysis, the continuity equation is the most tractable. For this reason it serves as a good example for demonstrating the method of obtaining the discrete approximations.

---

[1]The term "discretization," while not found in dictionaries is used in the literature by Henrici [12] and others.

To begin the derivation, consider that an approximation for an example pair of integrals

$$\int_{x_l}^{x_r} f_o\,(x,r_o)\,dx - \int_{x_l}^{x_r} f_i\,(x,r_i)\,dx \qquad (3.4.1)$$

is to be found, where f is some function of interest. Examination of the control volume in Figure 3-2 shows that the inner and outer faces do not extend the full distance between the column of grid points labeled "4" and the column labeled "3". Trapezoid Rule[1] integration of the general form

$$\int_{x_l}^{x_r} f\,(x)\,dx \simeq \frac{x_r - x_l}{2}\left[f\,(x_l) + f\,(x_r)\right] \qquad (3.4.2)$$

may be used, but the left hand points at which the function must be evaluated do not coincide with any of the grid points. To find the value of the function at this left side of the control volume, linear interpolation is employed. Thus, the function f evaluated at the left face may be written in terms of the function evaluated at the columns labeled "3" and "4" as

$$f\,(x_l)\big|_m \simeq (1-s)\,f\,(x_{m,3}) + s f\,(x_{m,4}) \qquad (3.4.3)$$

where $s\Delta x$ is the distance from column three to the left face of the control volume and m is the radial grid location where the function is

---

[1]Further information regarding the Trapezoid Rule and other integration formulas may be found in the NBS Handbook of Mathematical Functions [1].

evaluated. Applying the results of equations (3.4.2) and (3.4.3) to the original expression (3.4.1) gives

$$\int_{x_l}^{x_r} f_o\,(x,r_o)\,dx - \int_{x_l}^{x_r} f_i\,(x,r_i)\,dx$$

$$\approx (1+s)\,\frac{\Delta x'}{2}\left[f_{N+1,4} - f_{N,4}\right]$$

$$+ (1-s)\,\frac{\Delta x'}{2}\left[f_{N+1,3} - f_{N,3}\right] \qquad (3.4.4)$$

where the subscripts refer to the functions evaluated at the like numbered grid points of the Figure 3-2, and

$$\Delta x' = (1-s)\,\Delta x \qquad (3.4.5)$$

The reason for taking this approach to the approximation may now be discussed. By varying the value of s, some control is gained over the relative importance to the solution of the grid columns marked "3" and "4" on Figure 3-2. Examination of the expression (3.4.4) shows that the larger s is made, the larger the effect the column labeled "4" has on the value of the integral approximation. For the computer program the variable s is varied to help insure the stability of the numerical solution. This weighting method is somewhat analogous to the techniques known as implicit methods which are used in the numerical approximation of differential equations.

The effect of the variable s on the solution accuracy is open to further analytical study. Notice that both the Trapezoid Rule and linear interpolation are based on straight line approximations to the function of interest. In fact, the expression (3.4.4) may be derived in

a direct manner without using linear interpolation by using a Trapezoid Rule type formula based on the condition that one of the known points lies outside the integration interval. This indicates that the error terms involved in the approximation formula should be second order terms based on both the width of the integration interval and the distance between the known function points.

Several computer runs were made for a selected set of input data (Run 385) and the value of s was varied over the range 0.3 to 0.6. It was found that, although solution times varied, the answers obtained for the first few solution steps did not vary significantly, the largest variation occuring in the fourth decimal place. Upon experimentation a determination was made that a value for s of about 0.6 yielded the fastest accurate results. Substitution of the solution values obtained using a value of s of 0.6 also gives good results when substituted into control volumes where full trapezoid integration between grid points has been utilized.

The approximation of integrals involving the r-coordinate follows in a similar manner giving the result

$$\int_{r_i}^{r_o} g\,(x_r,r)\,dr - \int_{r_i}^{r_o} g\,(x_l,r)\,dr$$

$$\simeq (1-s)\,\frac{\Delta r}{2}\left[g_{N,4} + g_{N+1,4}\right] - (1-s)\,\frac{\Delta r}{2}\left[g_{N,3} + g_{N+1,3}\right] \qquad (3.4.6)$$

Again in the expression linear interpolation has been used to evaluate

the values at the left hand face of the control volume.

Using the expressions (3.4.4) and (3.4.6) the integral continuity equation

$$\int_{r_i}^{r_o} \rho_r u_r r dr - \int_{r_i}^{r_o} \rho_1 u_1 r dr + \int_{x_1}^{x_r} \rho_o v_o r_o dx - \int_{x_1}^{x_r} \rho_i v_i r_i dx = 0 \qquad (3.4.7)$$

may be approximated by the expression

$$\begin{aligned} &(1-s_c)\,\frac{\Delta r}{2}\left[\rho_{N,4} u_{N,4} r_i + \rho_{N+1,4} u_{N+1,4} r_o\right] \\ &- (1-s_c)\,\frac{\Delta r}{2}\left[\rho_{N,3} u_{N,3\ i} r_i + \rho_{N+1,3} u_{N+1,3} r_o\right] \\ &+ (1+s_c)\,\frac{\Delta x'}{2}\left[\rho_{N+1,4} v_{N+1,4} r_o - \rho_{N,4} v_{N,4} r_i\right] \\ &- (1-s_c)\,\frac{\Delta x'}{2}\left[\rho_{N+1,3} v_{N+1,3} r_o - \rho_{N,3} v_{N,3} r_i\right] = 0 \qquad (3.4.8) \end{aligned}$$

where s_c is the specific value of s in the expressions (3.3.4) and (3.3.6) which is used in the continuity equation. This equation will be factored and solved for radial velocity in a manner described later in this chapter.

Recall that in Chapter II, two forms of the differential continuity equation are listed. These are the following:

Continuity at the tube wall:

$$\frac{\partial v}{\partial r} = 0 \qquad (3.4.9)$$

Continuity at the tube centerline:

$$\frac{\partial \rho u}{\partial x} + 2\rho \frac{\partial v}{\partial r} = 0 \qquad (3.4.10)$$

These expressions are also approximated and utilized in the analysis at the points where they apply.

To obtain a discrete approximation for equation (3.4.9), consider the grid shown in Figure 3-4a.

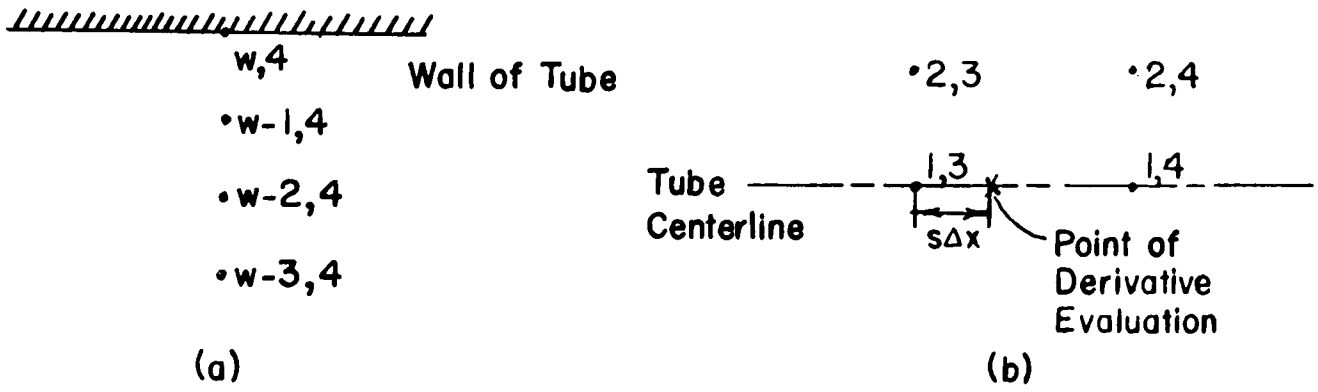

Fig. 3-4.--Grid networks for differential equation approximations

From page 914 of the NBS Handbook of Mathematical Functions [1] an approximation to $\frac{\partial v}{\partial r}$ may be written as

$$\left.\frac{\partial v}{\partial r}\right|_w \simeq \frac{3v_{w,4} - 4v_{w-1,4} + v_{w-2,4}}{2\Delta r} \qquad (3.4.11)$$

However, from the second boundary condition listed in Table 2-2, the velocity at the wall is zero, and the approximation to equation (3.4.9) becomes

$$\frac{-4v_{w-1,4} + v_{w-2,4}}{2\Delta r} = 0 \qquad (3.4.12)$$

which can be rewritten to

$$v_{w-1,4} = \frac{v_{w-2,4}}{4} \qquad (3.4.13)$$

This expression is used to insert the condition of zero radial velocity at the wall into the continuity equation solution.

In the previous chapter it was stated that integral equations are unaffected by changes of the values of variables at the centerline. For this reason the integral approximation of equation (3.4.8) does not project changes of the centerline axial velocity into changes in the radial velocity near the centerline. To avoid this problem the differential equation (3.4.10) is approximated and extrapolated to the centerline to find the value of radial velocity near the centerline. The approximation used for equation (3.4.10) is implicit in nature, that is, the derivative is not evaluated directly at one of the grid points, but rather it is evaluated between points as indicated on Figure 3-4b. This evaluation may be accomplished by the linear interpolation scheme already described, or by expanding the functions in Taylor series and then truncating the series and grouping the results appropriately. In either case, the results are identical. The approximations used are

$$\left.\frac{\partial f}{\partial x}\right|_{s\Delta x} \simeq \frac{f_{1,4}-f_{1,3}}{\Delta x} \tag{3.4.13}$$

$$\left.\frac{\partial g}{\partial r}\right|_{s\Delta x} \simeq s\,\frac{g_{2,4}-g_{1,4}}{\Delta r} + (1-s)\,\frac{g_{2,3}-g_{1,3}}{\Delta r} \tag{3.4.14}$$

Applying these approximations to equation (3.4.10) gives

$$\frac{\rho_{1,4}u_{1,4}-\rho_{1,3}u_{1,3}}{\Delta x} + 2\left[(1-s)\,\rho_{1,3} + s\rho_{1,4}\right]\left[s\,\frac{v_{2,4}-v_{1,4}}{\Delta r} + (1-s)\,\frac{v_{2,3}-v_{1,3}}{\Delta r}\right] = 0 \tag{3.4.15}$$

but, since

$$v_{1,3} = v_{1,4} = 0$$

the equation (3.4.15) becomes

$$\frac{\rho_{1,4}u_{1,4}-\rho_{1,3}u_{1,3}}{\Delta x} + \frac{2}{\Delta r}\left[(1-s)\,\rho_{1,3} + s\rho_{1,4}\right]\left[sv_{2,4} + (1-s)\,v_{2,3}\right] = 0 \quad (3.4.16)$$

which may be solved for $v_{2,4}$ provided all other variables are assumed to be known.

3.5 Approximations Used with the Axial Momentum Equation and Energy Equation

The discrete approximations for the axial momentum equation and energy equation are obtained in a manner similar to that used for the continuity equation; however, because of the increased complexity of the equations, some additional approximation techniques must be applied. In order to explain the methods to be used, let us consider the approximation for typical terms in the axial momentum equation.

The terms to be used in the illustration are

$$\int_{x_l}^{x_r} \mu_o \frac{\partial u_o}{\partial r}\, r_o dx - \int_{x_l}^{x_r} \mu_i \frac{\partial u_i}{\partial r}\, r_i dx \quad (3.5.1)$$

Notice that these terms involve derivatives as well as integrals. The choice of the approximation for the derivatives is relatively open, but from stability considerations some choices are better than others. A list of some of the available approximations is found on page 914 of the Handbook of Mathematical Functions [1]. The approximations chosen to be used in this example are the following:

$$\frac{\partial u_o}{\partial r} \simeq \frac{u_{N-1,m}-6u_{N,m}+3u_{N+1,m}+2u_{N+2,m}}{6\Delta r} \quad (3.5.2)$$

$$\frac{\partial u_i}{\partial r} \simeq \frac{-2u_{N-2,m}-3u_{N-1,m}+6u_{N,m}-u_{N+1,m}}{6\Delta r} \qquad (3.5.3)$$

The subscripts refer to like numbered grid points of Figure 3-2b with m = 3 or m = 4 as required by the integration formula.

For these terms the integration formula to be used is the same as that used for the continuity equation except that because of the control volume configuration, N must be replaced with N-1. Thus, the integral approximation becomes

$$\int_{x_1}^{x_r} f_o\,(x,r_o)\,dx - \int_{x_1}^{x_r} f_i\,(x,r_i)\,dx$$
$$\simeq (1+s)\,\frac{\Delta x'}{2}\left[f_{N+1,4} - f_{N-1,4}\right]$$
$$+ (1-s)\,\frac{\Delta x'}{2}\left[f_{N+1,3} - f_{N-1,3}\right] \qquad (3.5.4)$$

Substitution of the derivative approximations (3.5.2) and (3.5.3) into the integral approximation (3.5.4) gives the approximation of the expression (3.5.1)

$$\int_{x_1}^{x_r} \mu_o \frac{\partial u_o}{\partial r} r_o\,dx - \int_{x_1}^{x_r} \mu_i \frac{\partial u_i}{\partial r} r_i\,dx$$
$$\simeq (1+s_x)\,\frac{\Delta x'}{2}\left[\mu_{N+1,4}\left(\frac{u_{N-1,4}-6u_{N,4}+3u_{N+1,4}+2u_{N+2,4}}{6\Delta r}\right)\right.$$
$$\left. - \mu_{N-1,4}\left(\frac{-2u_{N-2,4}-3u_{N-1,4}+6u_{N,4}-u_{N+1,4}}{6\Delta r}\right)\right]$$
$$+ (1-s_x)\,\frac{\Delta x'}{2}\left[\mu_{N+1,3}\left(\frac{u_{N-1,3}-6u_{N,3}+3u_{N+1,3}+2u_{N+2,3}}{6\Delta r}\right)\right.$$
$$\left. - \mu_{N-1,3}\left(\frac{-2u_{N-2,3}-3u_{N-1,3}+6u_{N,3}-u_{N+1,3}}{6\Delta r}\right)\right] \qquad (3.5.5)$$

where s_x is the value of s used in the integration formula for axial momentum. As before, $\Delta x' = (1-s_x)\,\Delta x$.

The example just presented shows integration with respect to x; for integration with respect to r, a different scheme using Simpson's rule is employed. Simpson's integration formula may be written as

$$\int_{r_i}^{r_o} f\,(x,r)\,dr \simeq \frac{\Delta r}{3}\left[f_{N+1,m}+4f_{N,m}+f_{N-1,m}\right] \qquad (3.5.6)$$

where the subscripts refer to like numbered grid points in Figure 3-2b with m = 3 or m = 4. Using linear interpolation, a pair of integrals evaluated at the right and left faces of the control volume shown in Figure 3-2b may be expressed as

$$\int_{r_i}^{r_o} f\,(x_r,r)\,dr - \int_{r_i}^{r_o} f\,(x_l,r)\,dr$$

$$\simeq (1-s)\,\frac{\Delta r}{3}\left[f_{N+1,4}+4f_{N,4}+f_{N-1,4}\right]$$

$$-\,(1-s)\,\frac{\Delta r}{3}\left[f_{N+1,3}+4f_{N,3}+f_{N-1,3}\right] \qquad (3.5.7)$$

Here again, if derivatives exist in the term being approximated, they must be substituted into the integration formula. A complete summary of the approximations used with the axial momentum equation and energy equation shown in Table 3-1. For clarity the term "march" used in the table refers to the orderly progression of the computer solution in the downstream direction. Further clarification of this marching procedure

is discussed when the solution is flow-charted and discussed later in the chapter.

The approximations used in obtaining discrete versions of the differential equations employed in the solution varies depending on whether the equation is used at the wall or the centerline of the tube. In both cases the point where the derivatives are to be evaluated are not grid points. This type of situation has already been shown in Figure 3-4b and discussed in Section 3.4. The equations approximated are equations (2.12.9), (2.12.10), and (2.12.12). The approximations used are shown in Table 3-2.

3.6 Approximations Used with the Radial Momentum Equation

As shown in Figure 3-2 at the start of the chapter, the relationship of the fluid control volume to the overall grid network differs for the axial and radial momentum equations. Because of this difference, the approximations used with the radial momentum equation differ from the approximations already listed for axial momentum. In either case, the approach is the same: term by term substitution of the approximations into the integral equation. The approximations utilized with radial momentum are shown in Table 3-3. All of the integral approximations are based on the Trapezoid Rule and the use of linear interpolation of values.

3.7 The Gauss-Seidel Method of Solving Linear Algebraic Equations

Let us digress somewhat from the development in order to discuss

TABLE 3-1

APPROXIMATIONS USED WITH THE AXIAL MOMENTUM EQUATION AND ENERGY EQUATION

Integral Approximations

r - Integrals (Simpson's Rule)

$$\int_{r_i}^{r_o} f(x_r, r)\, dr - \int_{r_i}^{r_o} f(x_l, r)\, dr$$

$$\simeq (1-s)\frac{\Delta r}{3}\left[f_{N+1,4}+4f_{N,4}+f_{N-1,4}\right] - (1-s)\frac{\Delta r}{3}\left[f_{N+1,3}+4f_{N,3}+f_{N-1,3}\right]$$

x - Integrals (Trapezoid Rule)

$$\int_{x_l}^{x_r} f(x,r_o)\, dx - \int_{x_l}^{x_r} f(x,r_i)\, dx$$

$$\simeq (1+s)\frac{\Delta x'}{2}\left[f_{N+1,4}-f_{N-1,4}\right] + (1-s)\frac{\Delta x'}{2}\left[f_{N+1,3}-f_{N-1,3}\right]$$

where $\Delta x' = (1-s)\,\Delta x$

Derivative Approximations for Axial Velocity and Temperature

General Form

r - Derivatives

Inner Face

$$\frac{\partial g}{\partial r} \simeq \frac{-2g_{N-2,m}-3g_{N-1,m}+6g_{N,m}-g_{N+1,m}}{6\Delta r} \qquad m = 3 \text{ or } 4$$

TABLE 3-1--Continued

Outer Face

$$\frac{\partial g}{\partial r} \simeq \frac{g_{N-1,m}-6g_{N,m}+3g_{N+1,m}+2g_{N+2,m}}{6\Delta r}$$

x - Derivatives

Right Face

First March - Neglected

Successive Marches

$$\frac{\partial g}{\partial x} \simeq \frac{g_{m,5}-g_{m,4}}{\Delta x} \qquad m = N - 1, N, \text{ or } N + 1$$

Left Face

First March - Neglected

Successive Marches

$$\frac{\partial g}{\partial x} \simeq \frac{g_{m,4}-g_{m,2}}{\Delta x} \qquad m = N - 1, N, \text{ or } N + 1$$

Control Volume at Wall

r - Derivatives

Inner Face - Same as General Form

Outer Face

$$\frac{\partial g}{\partial r} \simeq \frac{11g_{N+1,m}-18g_{N,m}+9g_{N-1,m}-2g_{N-2,m}}{6\Delta r} \qquad m = 3 \text{ or } 4$$

x - Derivatives - Same as General Form

TABLE 3-1--Continued

Derivative Approximations for other Dependent Variables (Axial Momentum Equation Only)

General Form

r - Derivatives

Inner Face

$$\frac{\partial f}{\partial r} \simeq \frac{f_{N,m}-f_{N-2,m}}{2\Delta r} \qquad m = 3 \text{ or } 4$$

Outer Face

$$\frac{\partial f}{\partial r} \simeq \frac{f_{N+2,m}-f_{N,m}}{2\Delta r} \qquad m = 3 \text{ or } 4$$

x - Derivatives

Right Face

First March

$$\frac{\partial f}{\partial x} \simeq \frac{f_{m,4}-f_{m,3}}{\Delta x} \qquad m = N-1, N, \text{ or } N+1$$

Successive Marches

$$\frac{\partial f}{\partial x} \simeq \frac{f_{m,5}-f_{m,3}}{2\Delta x} \qquad m = N-1, N, \text{ or } N+1$$

Left Face (all marches)

$$\frac{\partial f}{\partial x} \simeq \frac{f_{m,4}-f_{m,2}}{2\Delta x}. \qquad m = N-1, N, \text{ or } N+1$$

TABLE 3-2

DERIVATIVE APPROXIMATIONS FOR DIFFERENTIAL EQUATION FORMS OF AXIAL MOMENTUM EQUATION AND ENERGY EQUATION

Centerline Approximation

$$\frac{\partial f}{\partial x} \simeq \frac{f_{1,4}-f_{1,3}}{\Delta x}$$

$$\frac{\partial f}{\partial r} \simeq (1-s)\,\frac{-3f_{1,3}+4f_{2,3}-f_{3,3}}{2\Delta r} + s\,\frac{-3f_{1,4}+4f_{2,4}-f_{3,4}}{2\Delta r}$$

$$\frac{\partial^2 f}{\partial x^2} \simeq (1-s)\,\frac{f_{1,2}-2f_{1,3}+f_{1,4}}{\Delta x^2} + s\,\frac{f_{1,3}-2f_{1,4}+f_{1,5}}{\Delta x^2}$$ (Neglected for first march)

$$\frac{\partial^2 f}{\partial r^2} \simeq (1-s)\,\frac{2f_{2,3}-2f_{1,3}}{\Delta r^2} + s\,\frac{2f_{2,4}-2f_{1,4}}{\Delta r^2}$$

$$\frac{\partial^2 f}{\partial x \partial r} \simeq \frac{-3f_{1,4}+4f_{2,4}-f_{3,4}}{2\Delta x \Delta r} - \frac{-3f_{1,3}+4f_{2,3}-f_{3,3}}{2\Delta x \Delta r}$$

Wall Approximation (Axial Momentum Equation Only)

$$\frac{\partial f}{\partial x} \simeq \frac{f_{w,4}-f_{w-1,4}}{\Delta x}$$

$$\frac{\partial f}{\partial r} \simeq (1-s)\,\frac{3f_{w,3}-4f_{w-1,3}+f_{w-2,3}}{2\Delta r} + s\,\frac{3f_{w,4}-4f_{w-1,4}+f_{w-2,4}}{2\Delta r}$$

$$\frac{\partial^2 f}{\partial r^2} \simeq (1-s)\,\frac{f_{w,3}-2f_{w-1,3}+f_{w-2,3}}{2\Delta r^2} + s\,\frac{f_{w,4}-2f_{w-1,4}+f_{w-2,4}}{2\Delta r^2}$$

$$\frac{\partial^2 f}{\partial x \partial r} \simeq \frac{3f_{w,4}-4f_{w-1,4}+f_{w-2,4}}{2\Delta x \Delta r} - \frac{3f_{w,3}-4f_{w-1,3}+f_{w-2,3}}{2\Delta x \Delta r}$$

TABLE 3-3

APPROXIMATIONS USED WITH THE RADIAL MOMENTUM EQUATION

Integral Approximations

r - Integrals

$$\int_{r_i}^{r_o} f_r r dr - \int_{r_i}^{r_o} f_1 r dr$$

$$\simeq \frac{\Delta r}{2}(1+s_x)\left[r_o f_{N+1,4} + r_i f_{N,4}\right] - \frac{\Delta r}{2}(1-s_x)\left[r_o f_{N+1,3} + r_i f_{N,3}\right]$$

x - Integrals

$$\int_{x_1}^{x_r} f_o r_o dx - \int_{x_1}^{x_r} f_i r_i dx \simeq \frac{\Delta x'}{2} r_o \left[(1+s_x) f_{N+1,4} + (1-s_x) f_{N+1,3}\right]$$

$$- \frac{\Delta x'}{2} r_i \left[(1+s_x) f_{N,4} + (1-s_x) f_{N,3}\right]$$

where $\Delta x' = (1-s_x)\Delta x$

End Area Integrals

$$\int_{x_1}^{x_r}\int_{r_i}^{r_o} f\, dr dx \simeq \frac{\Delta r \Delta x'}{4}\left[(1+s_x) f_{N+1,4} + (1-s_x) f_{N+1,3}\right.$$

$$\left. + \quad (1+s_x) f_{N,4} + (1-s_x) f_{N,3}\right]$$

Derivative Approximations

General Form

r - Derivatives

$$\frac{\partial f}{\partial r} \simeq \frac{f_{N+1,m} - f_{N-1,m}}{2\Delta r} \qquad m = 3 \text{ or } 4$$

TABLE 3-3--Continued

x - Derivatives

Right Face

First March

$$\frac{\partial f}{\partial x} \simeq \frac{f_{m,4}-f_{m,3}}{\Delta x} \qquad m = N + 1 \text{ or } N$$

Successive Marches

$$\frac{\partial f}{\partial x} \simeq \frac{f_{m,5}-f_{m,3}}{2\Delta x} \qquad m = N + 1 \text{ or } N$$

Left Face

$$\frac{\partial f}{\partial x} \simeq \frac{f_{m,4}-f_{m,2}}{2\Delta x} \qquad m = N + 1 \text{ or } N$$

a method of solving linear algebraic equations. The method will later be modified to obtain a solution of the non-linear equations encountered in this investigation. The procedure to be used is known as the Gauss-Seidel iterative method and is described by Varga [25], Fadeeva [8] and others.

To begin the description of the method, consider a typical set of algebraic equations written as

$$\begin{aligned} a_{11}x_1 + a_{12}x_2 + \ldots + a_{1n}x_n &= c_1 \\ a_{21}x_1 + a_{22}x_2 + \ldots + a_{2n}x_n &= c_2 \\ \vdots \quad\quad \vdots \quad\quad & \quad\quad \vdots \quad \vdots \\ a_{n1}x_1 + a_{n2}x_2 + \ldots + a_{nn}x_n &= c_n \end{aligned} \qquad (3.7.1)$$

where the a_{ii} and c_i are real constants and the x_i are the unknowns.

The Gauss-Seidel method of obtaining a solution to a set of equations involves first solving each of the equations for the unknown associated with the diagonal element, while assuming the other variables known. For example, the first two equations might then be written

$$x_1 = \frac{c_1}{a_{11}} - \frac{a_{12}}{a_{11}} x_2 - \frac{a_{13}}{a_{11}} x_3 - \ldots - \frac{a_{1n}}{a_{11}} x_n \qquad (3.7.2)$$

$$x_2 = \frac{c_2}{a_{22}} - \frac{a_{21}}{a_{22}} x_1 - \frac{a_{23}}{a_{22}} x_3 - \ldots - \frac{a_{2n}}{a_{22}} x_n \qquad (3.7.3)$$

Once this is done with all equations, approximate values or guesses at the values of the x_i are chosen and the equations are solved sequentially, one at a time, using the first guess to fill in for x_i yet to be found by solving an equation. The new values of x_i are once again substituted into the equations and the process repeated. The sequential solution of the equations continues until the answers obtained from

successive solutions match to a specified accuracy. At this point a solution to the set of equations has been found.

The success of the Gauss-Seidel method can be assured if a condition known as diagonal dominance is inherent in the equations to be solved. To define this condition, first consider that the equations (3.7.1) may be written in the matrix form

$$A\ x = c \tag{3.7.4}$$

where A is the coefficient matrix made up of the coefficients a_{ii} of the original equation set, x is a column matrix representing the unknown x_i, and c is a column matrix representing the known constants c_i. For a matrix to be diagonally dominant, the following condition must hold for each row:

$$|a_{ii}| \geq \sum_{\substack{j=1 \\ i \neq j}}^{n} |a_{ij}| \tag{3.7.5}$$

Stated verbally, the sum of the magnitudes of the off-diagonal elements must be less than or equal to the magnitude of the diagonal element. For proofs involving the relationship of diagonal dominance to stability of the solution, see Varga [25]. Note at this point that the choice of derivative and integral approximations presented earlier in the chapter was heavily influenced by the need to assure a condition similar to diagonal dominance in the matrices encountered in this investigation.

While considering the Gauss-Seidel scheme, let us also consider some useful matrix properties which, if they exist, greatly speed the solution. If a large number of the matrix coefficients a_{ii} of equation (3.7.4) are zero, the matrix A is said to be sparse. Furthermore, if

the non-zero elements occur in regular groupings around the matrix diagonal, the matrices may be further designated according to the number of non-zero elements.

For example, a matrix is designated tri-diagonal if three non-zero elements are found on each row clustered around the matrix diagonal. An example of a tri-diagonal matrix is the following:

$$\begin{bmatrix} 6 & 5 & 0 & 0 & 0 \\ 1 & -2 & 1 & 0 & 0 \\ 0 & -4 & 8 & 3 & 0 \\ 0 & 0 & 1 & 7 & -2 \\ 0 & 0 & 0 & -2 & 3 \end{bmatrix}$$

Notice that a single non-zero element lies to the right and left of the matrix diagonal. This particular matrix is also diagonally dominant. If two non-zero elements were situated on both sides of the diagonal (making five elements per row), the matrix would be called qui-diagonal. The approximation approach used for the axial momentum and energy equation produce coefficient matrices of the qui-diagonal type, while the approximations for the continuity and radial momentum equations produce a bi-diagonal form of two non-zero elements per row which lends itself to a direct back substitution solution method. By arranging the Gauss-Seidel approach to entirely ignore the known zero coefficients, a substantial increase in solution rapidity is effected.

3.8 General Notes on the Numerical Solution

Substitution of approximations presented earlier into the

governing equations produces a rather lengthy set of algebraic equations, all non-linear in nature. These algebraic equations must be organized into a form suitable for solution. The matrix form into which the equations are placed is closely linked to the Gauss-Seidel numerical solution techniques just discussed.

For an explanation of the solution approach, consider the typical grid network of Figure 3-2. Let us assume that the values of the variables u, v, T, p, and ρ are known at the points located using one, two, three and five as second subscripts. All dependent variables subscripted with four are taken as unknowns to be found. It should be recalled that the one through five subscripting system is flexible and may be overlaid at any axial location shown in Figure 3-1.

When all the variables subscripted with four are isolated to the left of the equations involved and all the other known variables are placed to the right of the equal sign, a non-linear set of algebraic equations is produced for the control volume. Then variation of the integer N, the first subscript, produces a set of equations for all control volumes. Since there are four different governing equations associated with each control volume approximately $4N_{max}$ equations are produced by this procedure, where N_{max} is the largest value of the subscript N. Inclusion of the equation of state reduces the number of unknown variables from about $5N_{max}$ to about $4N_{max}$. The word "about" is used because boundary conditions sometimes fix values of one variable, say u, while requiring the solution of another, say p, at the same boundary point. Algebraically speaking to find the values of u, v, T, p,

and ρ subscripted with four, a set of non-linear equations numbering about $4N_{max}$ must be solved. If N_{max} is 80, then about 320 simultaneous equations must be solved for the same number of unknowns. If this is accomplished, then the solution may be moved one axial step downstream and the procedure repeated until the desired region of solution is mapped. For purposes of this investigation, this step by step movement downstream is referred to as "marching."

The variables subscripted with one, two and three can be found from previous solutions or specified as entrance conditions; however, those variables subscripted with five, which involve downstream information, are not known when the solution is begun. Since, for the cases considered, this downstream information does not have as strong an effect on the solution as boundary and upstream conditions, the terms involved are neglected or replaced with a poorer approximation during the first march down the tube. By successively remarching the solution using the better approximations afforded by the solution found on the previous march, this downstream information is then included in the solution.

At first it appears that the remarching technique just described is not usable because the length of the tube is not defined as part of the problem. In most physical cases, however, the region where the downstream information affects the solution lies at the start of heating where the axial temperature gradients are the strongest. In this situation a march through the region of strong influence into a region where downstream conditions have small influence on the solution is

possible. If the solution is stopped in this region, little error is introduced, making it possible to then start a remarch through the region of strong influence without significantly affecting the accuracy of the results. Remarching through the central region of strong influence is continued until no appreciable change occurs in the solution, indicating that downstream information has been successfully included.

3.9 Methods of Solving Governing Equations

The mathematics encountered in this investigation are greatly complicated by the fact that products and powers of unknowns often appear in the equations to be solved. Methods exist for dealing with these situations, and among these are the following:

1. Solution of the non-linear equations by methods specifically designed for such non-linearities, such as the Newton-Raphson scheme described by Henrici [12] and others
2. Linearization of the equations, followed by a reinsertion of the non-linear effects during solution by iteration techniques

In some situations a combination of methods may give best results. The Newton-Raphson method mentioned above has the disadvantage that a rather large set of additional equations involving partial derivatives of the entire set of algebraic equations must be generated and stored in the computer memory. The second method has the disadvantage that if the wrong choice is made in the linearization approach, iteration may not

produce a convergent solution scheme. Based on experience and examination of the available literature, the second method was chosen for this investigation as being most likely to produce answers with a reasonable amount of programming effort.

The grouping and linearization of the governing equations for computer solution is algebraically a four part process. The first step is the isolation to the right of the equation equal sign all terms that remain constant for the particular axial location under consideration. These terms are all those which contain one, two, three and five as second subscripts, since it is desired to solve for those variables subscripted with four. Once this isolation is accomplished the equations must be studied to determine which dependent variable (velocity, temperature, etc.) has the coefficients dominant over the other variables in that particular equation. For example, the coefficients of axial velocity in the axial momentum equation are proportionately much larger in magnitude than the coefficients of temperature or radial velocity. Once this second step has been accomplished, the variables which are not dominant in each equation are also moved to the right hand side of the equation and treated as temporary constants. Finally, as the fourth step, the coefficients of the dominant variable of each equation are linearized by a factoring process.

To illustrate how this linearization is accomplished, let us follow a sample term through the procedure. Suppose the coefficients of $u_{N,4}$ are arranged in an equation as

$$a\,u_{N,4}^{2} + b\,u_{N,4} + \ldots = \text{constant} \qquad (3.9.1)$$

where a and b are known constants.

By separating the non-linear term $u_{N,4}^{2}$ into $u_{N,4}u_{N,4}$ the relation (3.9.1) may be rewritten

$$(a\,u_{N,4} + b)\,u_{N,4} + \ldots = \text{constant} \qquad (3.9.2)$$

For approximation purposes the term in parentheses is then considered to be a constant.

Using equation (3.9.2) the way the linearization scheme ties into Gauss-Seidel solution method may be shown. Recall that one of the characteristics of the Gauss-Seidel method is that an assumed solution is used as a starting point for iteration. For our purposes, let us use this initial guess at $u_{N,4}$ also for the $u_{N,4}$ inside the parentheses. Now solve for a new $u_{N,4}$ using the Gauss-Seidel method while considering the equation linear. This new value of $u_{N,4}$ may be placed as the $u_{N,4}$ in the parentheses and yet another $u_{N,4}$ found using the Gauss-Seidel method. The procedure is continued until the value of $u_{N,4}$ in the parentheses essentially matches the solution value of $u_{N,4}$. At this point a solution for $u_{N,4}$ has been reached. The same approach is also used for the other unknown variables like temperature and pressure.

The procedure just described is further complicated by the fact that many of the coefficients of the unknowns contain properties such as viscosity and thermal conductivity that are essentially temperature dependent. This problem is also overcome by iteration, and the temperature solution from the previous iteration is used to approximate the property values for the following iteration. When the solution is

reached, the temperature distributions do not change significantly for two successive iterations and this approximation method is then sufficiently accurate.

As mentioned, the equations must be examined for which dependent variable's coefficients dominate the particular governing equation. After some study, it was decided that for the present problem the appropriate choices are the following:

Variable	Governing Equation
Axial Velocity, u	Axial Momentum
Radial Velocity, v	Continuity
Temperature, T	Energy Equation
Pressure, p	Radial Momentum

The density, ρ, is related to pressure and temperature by the equation of state, which in this case is the Perfect Gas Law.

Even after the choice of which equation is to be solved for which variable, several paths are left open as to how the Gauss-Seidel type iteration procedure is to be sequenced. Experience showed that the order in which the equations are solved can have an effect on speed of the solution. For the solution the following sequence has been found to give the best results:

1. Energy equations
2. Continuity equations
3. Axial momentum equations
4. Radial momentum equations

Within this sequence there are two alternatives:

1. Use the modified Gauss-Seidel method to solve each type of equation one complete set at a time for each set's associated variable, e.g., temperature, axial velocity, etc. Then repeat the procedure until a solution is reached.
2. Place all the equations in a large overall iteration loop and solve for all variables sequentially using the modified Gauss-Seidel method.

It was found by program experimentation that the second method yields the results with less computer time.

Note that the order of the Gauss-Seidel iteration is important. For the cylindrical geometry the solution iterative process should always start at the centerline and sweep toward the tube wall. This solution order minimizes the error build up associated with the ratio of the radii r_i and r_o appearing in the equations associated with each control volume. If the iteration proceeds from the centerline, then a ratio of $\frac{r_i}{r_o}$, which is less than one, appears as a multiplier in the equations, and any error introduced is decreased by this factor. However, if the solutions start at the wall, then the ratio becomes $\frac{r_o}{r_i}$, which is greater than one; this progressively multiplies any error in the solution made near the wall until it may cause complete loss of solution stability as the centerline is approached.

Since the Gauss-Seidel method relies on an initial approximation as a starting point for iteration, the quality of this approximation has a direct bearing on the rapidity of solution. For the present problem, the solution found at the previous march step is always used to start the

iteration procedure. This was found to be adequate for everything but pressure, which was approximated by calculating a constant properties pressure drop using the local centerline temperature to evaluate the Reynolds number and modified Grashof number. This approach provided an adequate starting point for subsequent iterations.

3.10 Flow Chart of Computer Solution

The flow chart for the computer solution of the problem is shown in Figure 3-5. The following comments are intended as an aid to understanding the steps shown.

The constants defined in Block 1 of the flow chart are mostly those associated with the integral weighting scheme, that is, the s constants illustrated in the expressions (3.3.8), (3.4.5) and others. These were chosen by experiment, and, for the most part, values of 0.5 to 0.6 were found to work best.

The input data of Block 2 consists of the following:

1. Entrance Reynolds Number
2. Modified Entrance Grashof Number
3. Entrance Prandtl Number
4. Entrance Mach Number
5. Size of Axial Step
6. Number of control volumes in radial direction
7. Locations where grid sizes are to change
8. Length of march

The parameters one through four fix the problem mathematically and

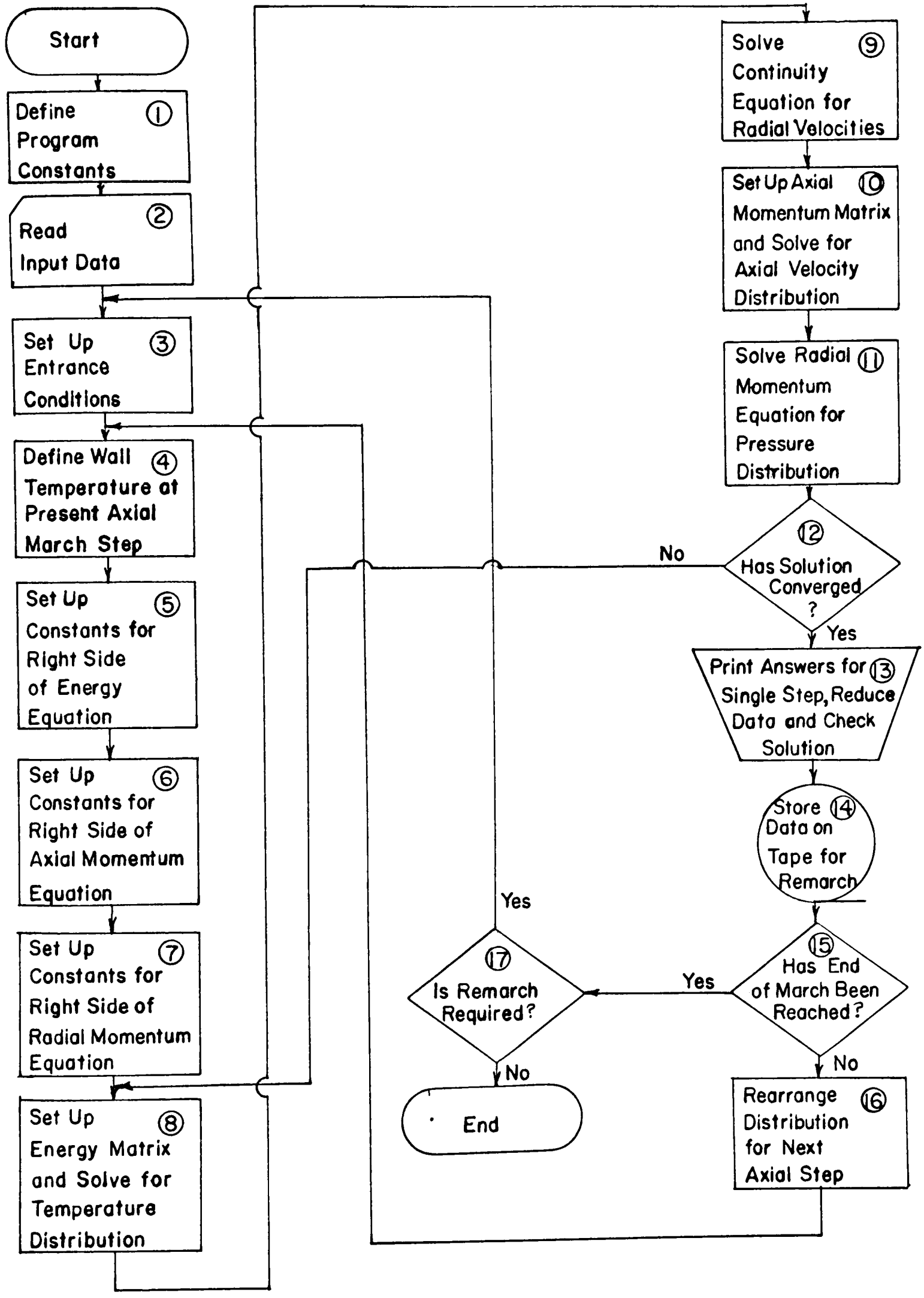

Fig. 3-5.--Computer solution flow chart

physically, while the information conveyed in the data numbered five through eight is necessary only to the computer solution.

In Block 3, the entrance conditions defined in Table 2-1 are generated for use in the computer solution. Following this, a routine which defines the wall temperature associated with the axial location for which the solution is being found is executed as symbolized in Block 4.

In Blocks 5 through 7 the terms which remain constant throughout the solution at each axial step are evaluated. This prevents duplication of effort in the Gauss-Seidel iterative method. Unfortunately for simplicity of programming, as mentioned in the previous section, some terms on the right hand side of the equations must be factored and placed inside the actual iteration loop because they change from iteration to iteration.

In Blocks 8 through 11 the actual Gauss-Seidel type iteration loop is carried out the required number of iterations to achieve a solution for the axial step of interest. Convergence to five places (base 10) was required for temperature and axial velocity, while four place accuracy was imposed on the pressure solution.

After a solution at the specific axial step is achieved, then the resulting data are printed as symbolized in Block 13 of the flow chart. This includes axial and radial velocity profiles, as well as temperature, pressure, and density distributions. Then, before the data are revised for the next axial step, parameters such as friction factor, Nusselt number, and local Reynold's number are reduced from the data and printed.

Equation checks, which will be described later, are also evaluated at this point.

In Block 14, the current solution is recorded on magnetic tape for use as downstream data when remarching is executed.

A decision must then be made as to whether the end of the march in the axial direction has been reached. If the end has not been reached, then another axial march step is to be executed and the internal data must be rearranged to permit the solution. If the end of the march has been reached, the decision must be made whether to go back to the entrance and remarch the length of the tube or to terminate the solution. In practice, only three axial marches were necessary before a complete solution was effected for the input data considered.

3.11 Methods Utilized to Check Validity of Solution

Several precautions were taken to assure, as far as possible, the accuracy and validity of the computer solution. But because of the extreme complexity of the problem no completely rigorous check was available and the checks used are, as the mathematician might state, "necessary, but not sufficient" conditions which must be satisfied.

As the solution progressed, a running check was performed by placing a cylindrical control volume across the entire flow stream. This control volume had its left face at the column labeled "3" in Figure 3-2, and its right face at the column labeled "4." The axial momentum, energy and continuity equations were then evaluated using this control volume. In essence, these checks validated that the whole was consistent

with data obtained from the parts; that is, the solving of individual control volume equations produces a solution that agrees favorably with overall material, momentum, and energy balances on the flow stream. The deviations found were acceptably small and are shown for a typical run in Table 3-4.

As a further check on the energy equation, a computer run was made using the assumption of constant fluid properties. The Nusselt numbers found from this run were compared with Nusselt numbers obtained from a Graetz solution utilizing the same boundary conditions. A description of the Graetz solution is found in Kays [16]. The results of the comparison are shown in Figure 3-6. The discrepancy in Nusselt numbers found near the start of heating may be due more to slow convergence of the Graetz solution near mathematical singularties than to error in the numerical solution. Elsewhere, as illustrated, agreement is good.

As a basic check on the program, a run was made with no heating. In this case all profiles remained unchanged except for pressure which remained constant across the stream and dropped linearly in the axial direction as anticipated. This indicated that, at least near equilibrium, the equations are stable and no error accumulation is encountered.

To check the size of the axial steps used in the numerical march procedure, a technique commonly utilized in numerical analysis was employed. The size of the axial march step was reduced by factors of two until the answers obtained by taking two axial half-steps agreed with values found taking one whole step. The larger step was then taken

TABLE 3-4

FULL STREAM CONTROL VOLUME EQUATION CHECKS FOR RUN 390

A. CONTINUITY EQUATION

Dimensionless axial location $x^+ = \frac{x}{r}$	Mass flow integral[a] $2\int_0^1 \rho^+ u^+ r^+ dr^+$
0.85	0.999970
2.56	0.999397
4.26	0.998182
6.82	0.996701
13.64	0.998329
20.46	0.999643
23.87	1.000275
27.28	1.000783
34.10	1.002069
40.92	1.003149
47.74	1.004076
54.56	1.004896
61.38	1.005636
68.20	1.006330

[a]To completely conserve mass, this integral must exactly equal one at all tube cross sections.

TABLE 3-4--Continued

B. AXIAL MOMENTUM EQUATION TERMS

Dimensionless Axial Location $x^+ = \frac{x}{r}$	Dimensionless Wall Temperature $T_w^+ = \frac{T_w}{T_{b,in}}$	Largest Equation Term	Smallest Equation Term[a]	Summation Error[b]
0.85	1.0029	309.9	3.415	1.516×10^{-3}
2.56	1.059	310.5	3.562	2.13×10^{-2}
4.26	1.197	312.7	4.051	4.25×10^{-2}
6.82	1.439	320.1	5.178	4.06×10^{-2}
13.64	1.541	340.8	12.391	4.21×10^{-2}
20.46	1.541	354.9	25.521	1.12×10^{-1}
23.87	1.541	361.04	25.827	1.11×10^{-1}
27.28	1.541	367.00	26.068	9.37×10^{-2}
34.10	1.541	377.22	52.731	3.02×10^{-1}
40.92	1.541	386.76	53.372	2.69×10^{-1}
47.74	1.541	395.50	53.859	2.37×10^{-1}
54.56	1.541	403.55	54.241	2.12×10^{-1}
61.38	1.541	410.99	54.544	2.00×10^{-1}
68.20	1.541	417.87	54.789	1.73×10^{-1}

[a]Changes in grid size cause sudden changes in size of these terms.

[b]If axial momentum is completely satisfied for the full stream control volume, this sum is zero.

TABLE 3-4--Continued

C. ENERGY EQUATION TERMS

Dimensionless Axial Location $x^+ = \frac{x}{r}$	Dimensionless Wall Temperature $T_w^+ = \frac{T_w}{T_{b,in}}$	Largest Dimensionless Energy Convection Term	Dimensionless Heat Transfer at Wall[a] $\int_{x_1^+}^{x_r^+} k^+ \frac{\partial T^+}{\partial r^+} dx^+$	Summation Error[b]
0.85	1.0029	0.0245	0.0151	7.03×10^{-3}
2.46	1.059	0.6470	0.3608	9.11×10^{-2}
4.26	1.197	2.8962	1.2259	1.40×10^{-1}
6.82	1.439	9.6668	2.5313	7.01×10^{-2}
13.64	1.541	27.0809	3.5911	1.00×10^{-1}
20.46	1.541	38.5384	5.4967	1.81×10^{-1}
23.87	1.541	43.3333	4.9155	1.19×10^{-1}
27.28	1.541	47.7200	4.4804	9.41×10^{-2}
34.10	1.541	55.4720	8.0308	2.78×10^{-1}
40.92	1.541	62.3063	7.0518	2.17×10^{-1}
47.74	1.541	68.4158	6.2776	1.68×10^{-1}
54.56	1.541	73.9277	5.6498	1.37×10^{-1}
61.38	1.541	78.9286	5.1193	1.18×10^{-1}
68.20	1.541	83.4866	4.6570	9.98×10^{-2}

[a]Changes in grid size cause sudden changes in size of these terms.

[b]If the energy equation is completely satisfied for the full stream control volume, this sum is zero.

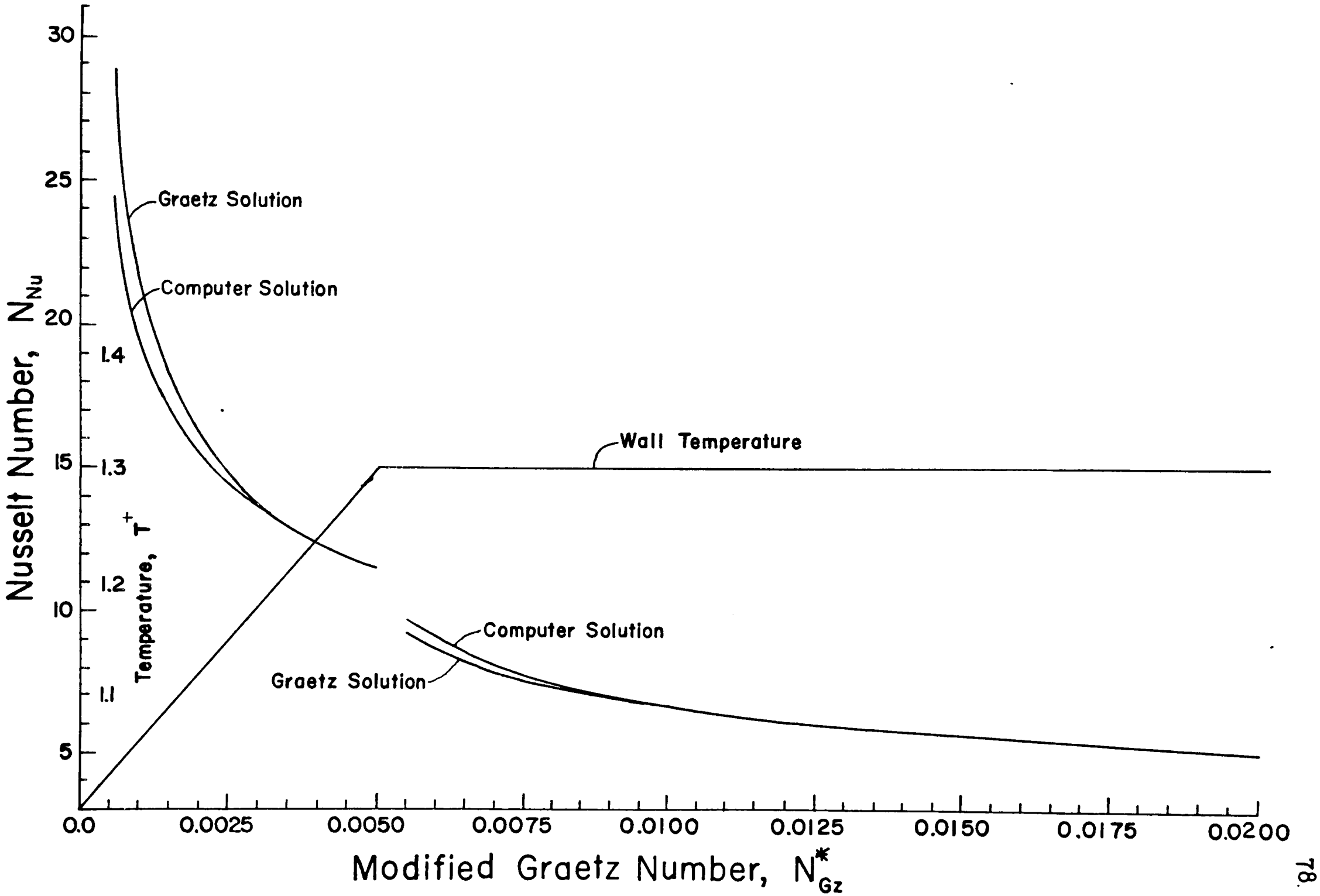

Fig. 3-6.--Comparison of constant properties of computer solution to Graetz solution

to be the largest acceptable step possible in the particular region of interest.

CHAPTER IV

PRESENTATION AND ANALYSIS OF RESULTS

4.1 Restatement of Objectives

In Section 1.6 of Chapter I, a set of investigation objectives is enumerated. The presentation in this chapter is intended to fulfill the major portion of these objectives. The objectives stated in Chapter I include the presentation of solution results in a graphical manner, a direct comparison with experimental results, and the presentation of dimensionless correlations useful in similar engineering analyses. Another objective, the derivation of a computer solvable mathematical model, has been accomplished in the two previous chapters.

4.2 Strategy of Computer Simulation

Because of the lengthy execution time of the complete computer program, a strategy was devised which made maximum use of the data obtained. The runs were designed to overlap and provide data which could be used for both comparison with the experimental work of Kirby [17] and Chance [3] and study of the effect of increasing free convection. How this is accomplished, and how the experimental boundary conditions are simulated will now be discussed.

The experimental apparatus used by Kirby and Chance on which the computer simulations are based is designed to provide an abrupt change

in tube wall temperature. In practice the experimenters found it possible to make a transition from a tube wall temperature of near room temperature to a constant wall temperature of around 1100°F in an axial tube distance equal to about five times the inside tube diameter. In actuality, most of the increase (to 970°F in the 1100°F case) can be accomplished at the first data station 3.41 diameters downstream from start of heating. To simulate this increase to a constant wall temperature in the computer program a fifth degree polynomial in temperature of the form

$$T_w^+ (x^+) = \frac{6(T_2^+ - T_1^+)}{x_1^{+5}} x^{+5} - \frac{15(T_2^+ - T_1^+)}{x_1^{+4}} x^{+4} + \frac{10(T_2^+ - T_1^+)}{x_1^{+3}} x^{+3} \qquad (4.2.1)$$

$$(0 < x^+ < x_1^+)$$

has been selected. Here $T_w^+ (x^+)$ is the dimensionless wall temperature at the axial location x^+, T_1^+ is the initial dimensionless wall temperature at the entrance to heating (equal to one in all cases), T_2^+ is the final desired dimensionless wall temperature, and x_1^+ is the dimensionless axial position where the wall temperature levels off at a constant value of T_2^+. For x^+ greater than x_1^+ the wall temperature is simply

$$T_w^+ (x^+) = T_2^+ \qquad (x^+ > x_1^+) \qquad (4.2.2)$$

For simulation purposes the parameter x_1^+ is adjusted until the wall temperature is fairly well approximated at the experimental station 3.41 tube diameters from the entrance.

A constant tube diameter experimental apparatus like that used by

Kirby and Chance without such extras as gas precoolers inherently has a more or less fixed value of entrance modified Grashof number. Thus this type of apparatus does not allow the study of the effect of this parameter on the flow scheme. Since this dimensionless parameter is closely related to free convection effects, a detailed study of free convection is not possible with such a fixed tube diameter apparatus. The apparatus of Kirby and Chance utilizes a 0.607 inch inside diameter tube which fixes the value of $N^*_{Gr,in}$ at about 116,000 when room temperature air is used as the inlet fluid.

In order to explore the effect of free convection on the flow field and also simulate experimental conditions, a scheme which overlaps the two types of runs has been developed. In this scheme five of the experimental runs have been chosen to be simulated on the computer. These simulations are numerically designated using the experimenters' numbering system. Two of these runs (391 and 392) have been picked as a basis for the study of free convection effects. In these cases the inlet modified Grashof number is varied over the range of zero, four, and eight times its experimental value. For bookkeeping purposes these runs are designated by a hyphen and the Grashof number multiplier following the run number. Thus, Run 392-0 is based on Kirby and Chance experimental Run 392, but the original experimental value of $N^*_{Gr,in}$ has been replaced with zero.

In addition to the experimental comparison and free convection studies, a run has been made utilizing a higher wall temperature than attained in the experimental runs. This run is designated Run 502. A

summary of the computer runs is found in Table 4-1.

4.3 Analysis of the Flow Field

As the fluid flow through the heated section of the tube, the velocity and temperature profiles warp away from their shapes at the entrance. The amount and shape of the warpage is controlled to a great extent by the amount of free convection present in the tube.

A typical development of the axial velocity flow field is illustrated in Figure 4-1. Here, the axial velocity profiles at four different axial locations in the tube are presented for four different values of $N^*_{Gr,in}$ while everything else is held constant to values based on Run 392. Examination of the profiles shows that at each axial location as the amount of free convection increases with increasing $N^*_{Gr,in}$, the centerline velocities tend to decrease while velocities near the tube wall tend to increase. As shown in the profiles at x/D of 30.69, the maximum velocity can occur at a position off the centerline if enough free convection is present. This condition could eventually cause back flow and instability of the fluid flow if the trend were continued. To pursue this edge of stability with the current computer model would raise serious credibility doubts, however.

The radial velocity profiles for six axial locations and two widely differing values of inlet Grashof number are shown in Figure 4-2. The solid line represents the values found for pure forced convection, while the dashed lines show the values for $N^*_{Gr,in} = 927{,}200$. In both cases the trends were the same. A comparatively large negative (toward

TABLE 4-1

SUMMARY OF INPUT DATA FOR COMPUTER SIMULATIONS

Run Number	Final Wall Temperature[a] $T_2^+ = \frac{T_2}{T_{in}}$	Axial Location of Final Wall Temperature[a] $x_1^+ = \frac{x_1}{r_w}$	Entrance Reynold's Number $N_{Re,in}$	Entrance Modified Grashof Number $N^*_{Gr,in}$	Entrance Mach Number M_{in}	Entrance Prandtl Number N_{Pr}
385	1.95	10.0	2090	115,900	.00683	0.69
386	2.103	10.0	1122	107,929	.00348	0.69
390	1.541	10.0	930	112,375	.00340	0.69
391-0	2.361	10.0	1066	0.0	.00348	0.69
391-1	2.361	10.0	1066	115,900	.00348	0.69
391-4	2.361	10.0	1066	463,600	.00348	0.69
391-8	2.361	10.0	1066	927,200	.00348	0.69
392-0	2.81	10.0	2193	0.0	.00683	0.69
392-1	2.81	10.0	2193	115,900	.00683	0.69
392-4	2.81	10.0	2193	463,600	.00683	0.69
392-8	2.81	10.0	2193	927,200	.00683	0.69
502	4.0	10.35	2000	115,900	.00683	0.69

[a]See equations (4.2.1) and (4.2.2) for definition of these variables.

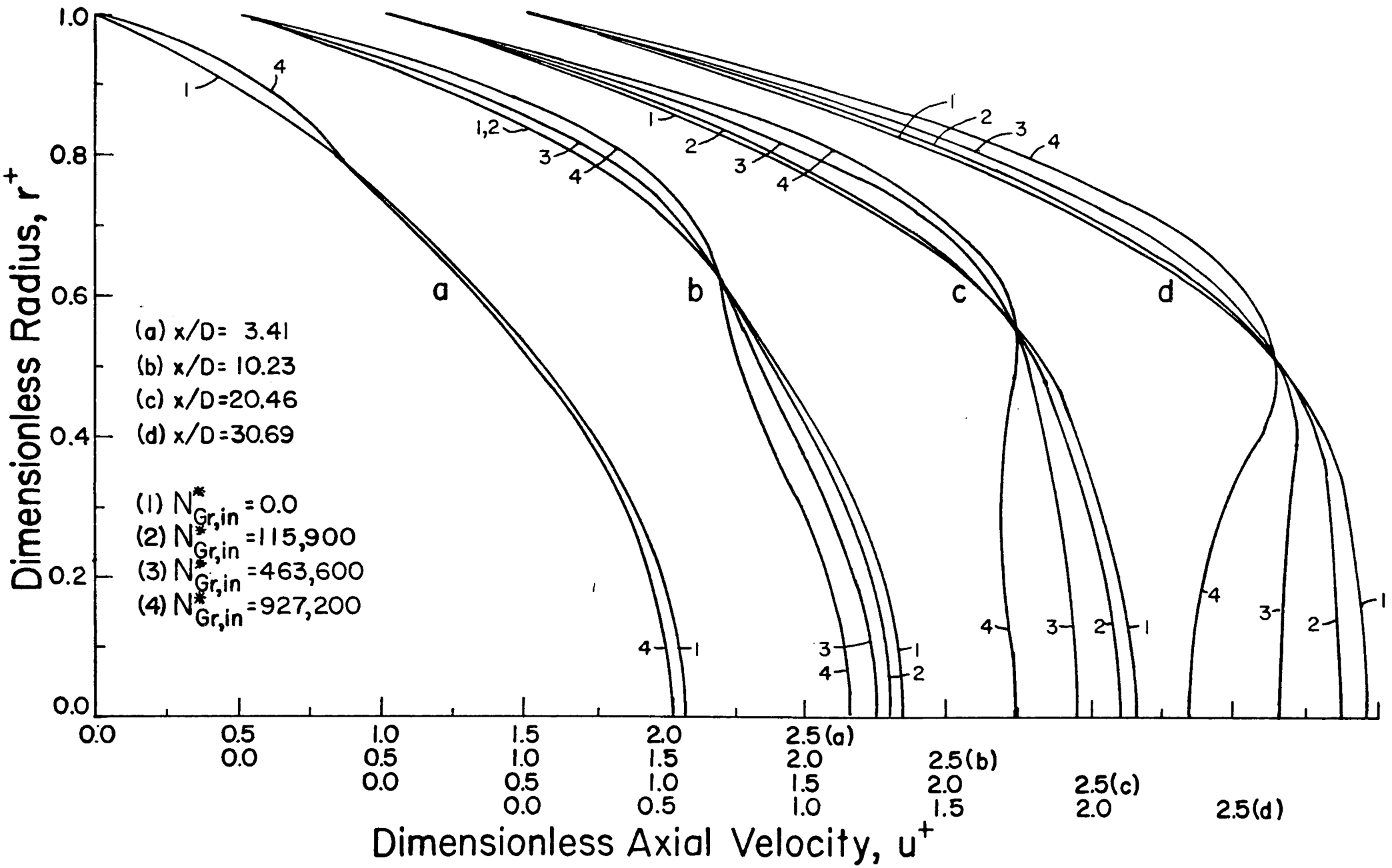

Fig. 4-1.--Variation of axial velocity profiles with free convection (Run 392)

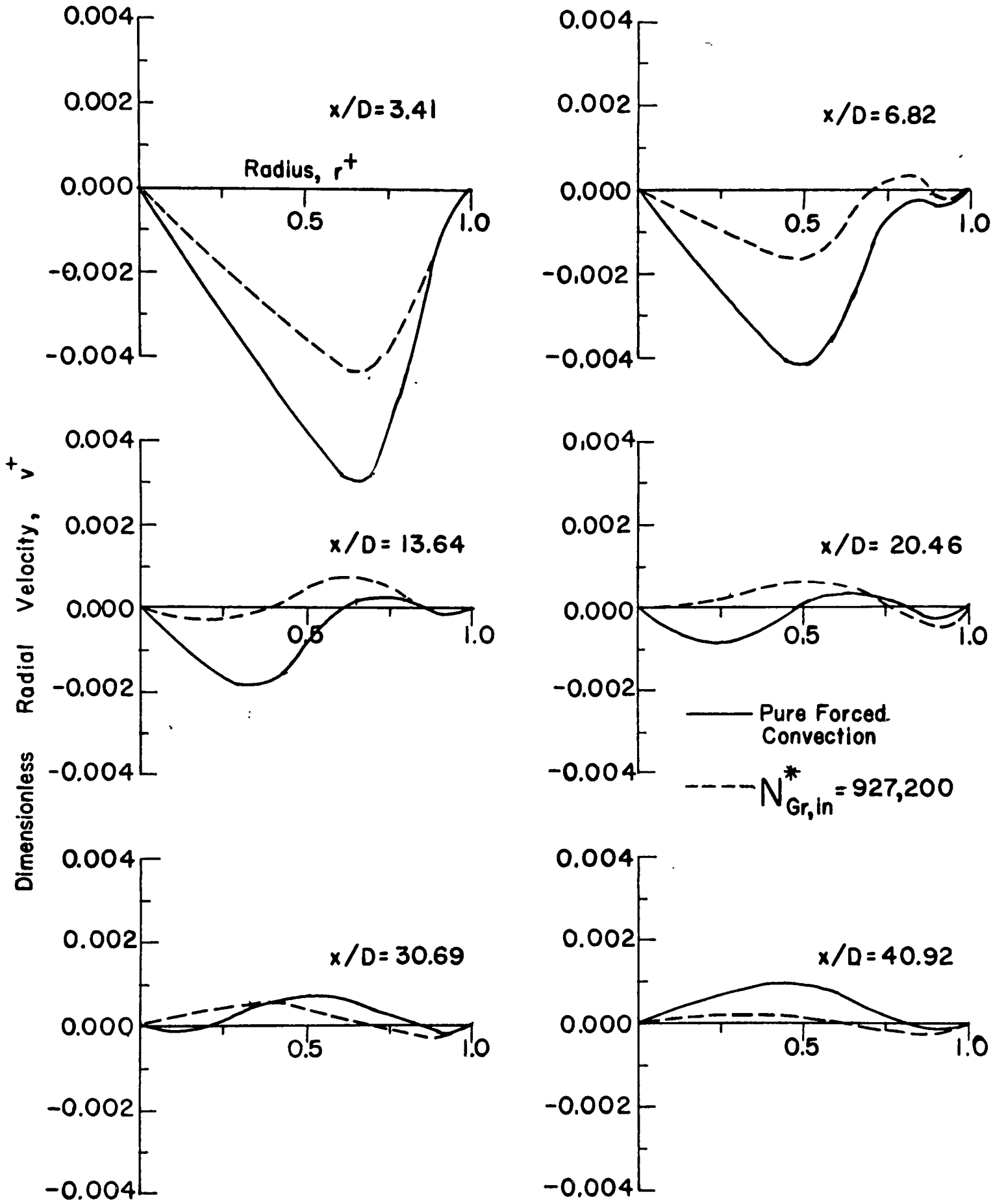

Fig. 4-2--Variation of radial velocity profiles with free convection (Run 392)

the centerline) radial velocity gradually swings positive in a region near the wall as the flow progresses downstream. This trend toward a positive value continues out toward the centerline until the only negative velocity exists in a small region near the wall. The interesting fact is that increased free convection tends to make these radial flow trends appear at stations closer to the entrance and also tends to decrease the magnitudes of the radial velocities where the effects do occur. How this correlates with the fact considered later that friction factors increase with increased free convection is uncertain.

The temperature profiles were little affected by free convection. Typical temperature profiles are shown in Figure 4-3 where the computer simulation values are compared to the experimental profiles of Run 391. Because of the small variations, a meaningful plot showing the variation of temperature with free convection is difficult to develop. On the whole, an increase in free convection tended to cause a slight increase in fluid temperatures across the stream at any axial location.

The variation in pressure across the stream has been found to be small in all cases tested with a very slight decrease in pressure drop occurring in the vicinity of the tube wall. Thus, for the data encountered the assumption of constant pressure across the flow stream is valid.

As for the variation of bulk parameters with free convection, Figures 4-4 and 4-5 illustrate the variation of friction factor and Nusselt number respectively. For these illustrations the definition of

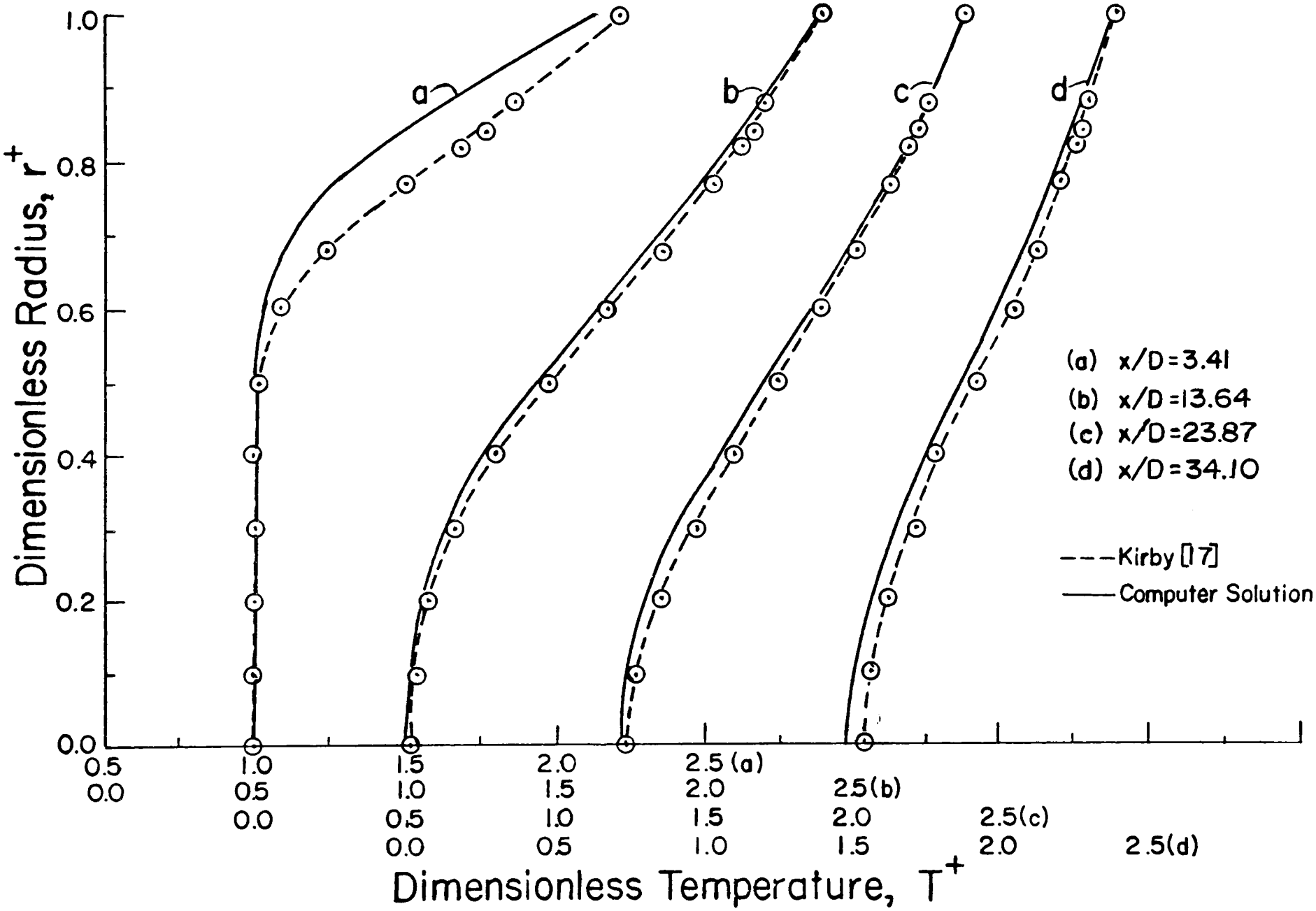

Fig. 4-3--Temperature profile development (Run 391)

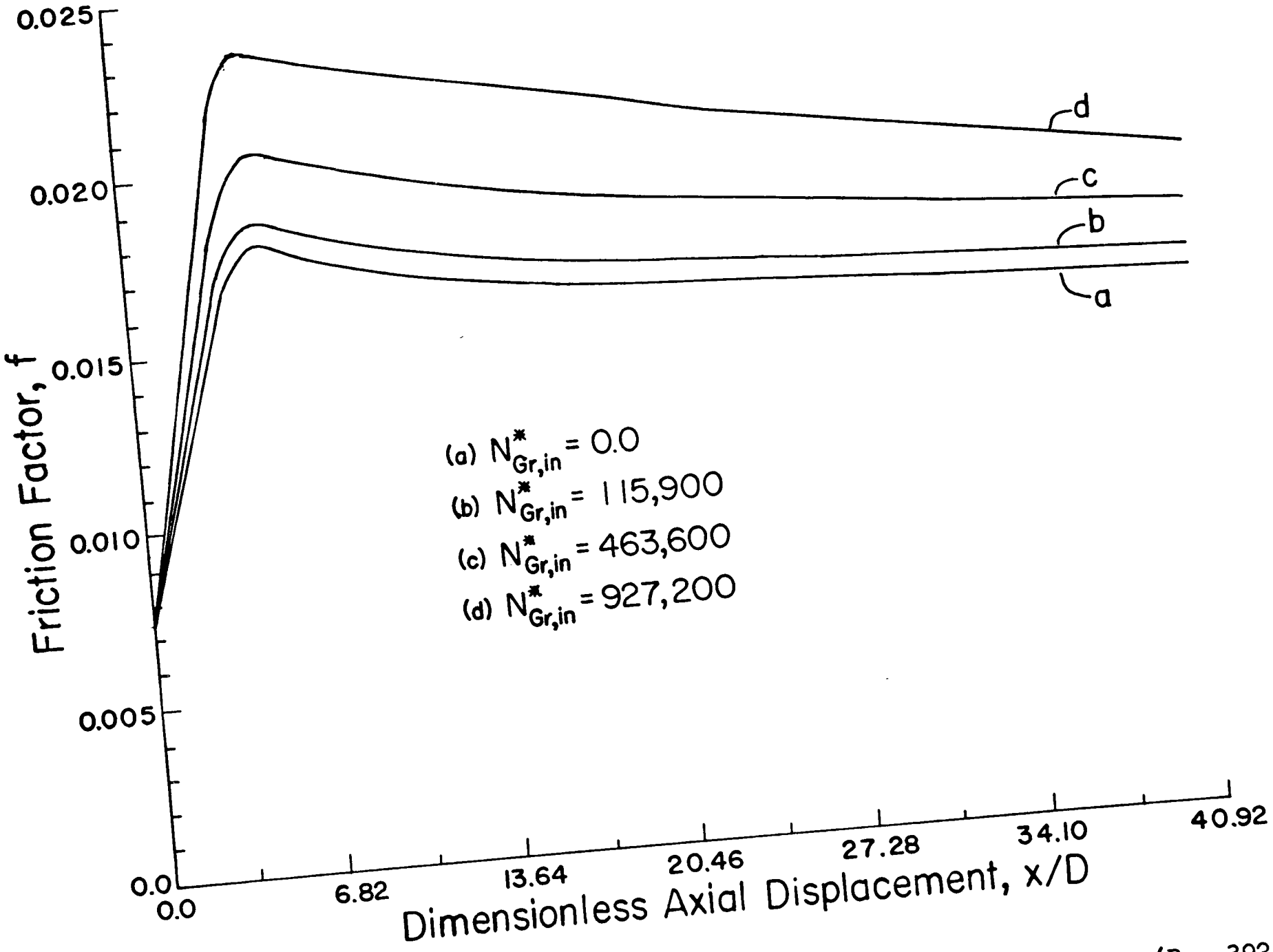

Fig. 4-4.--Variation of friction factor with free convection (Run 392)

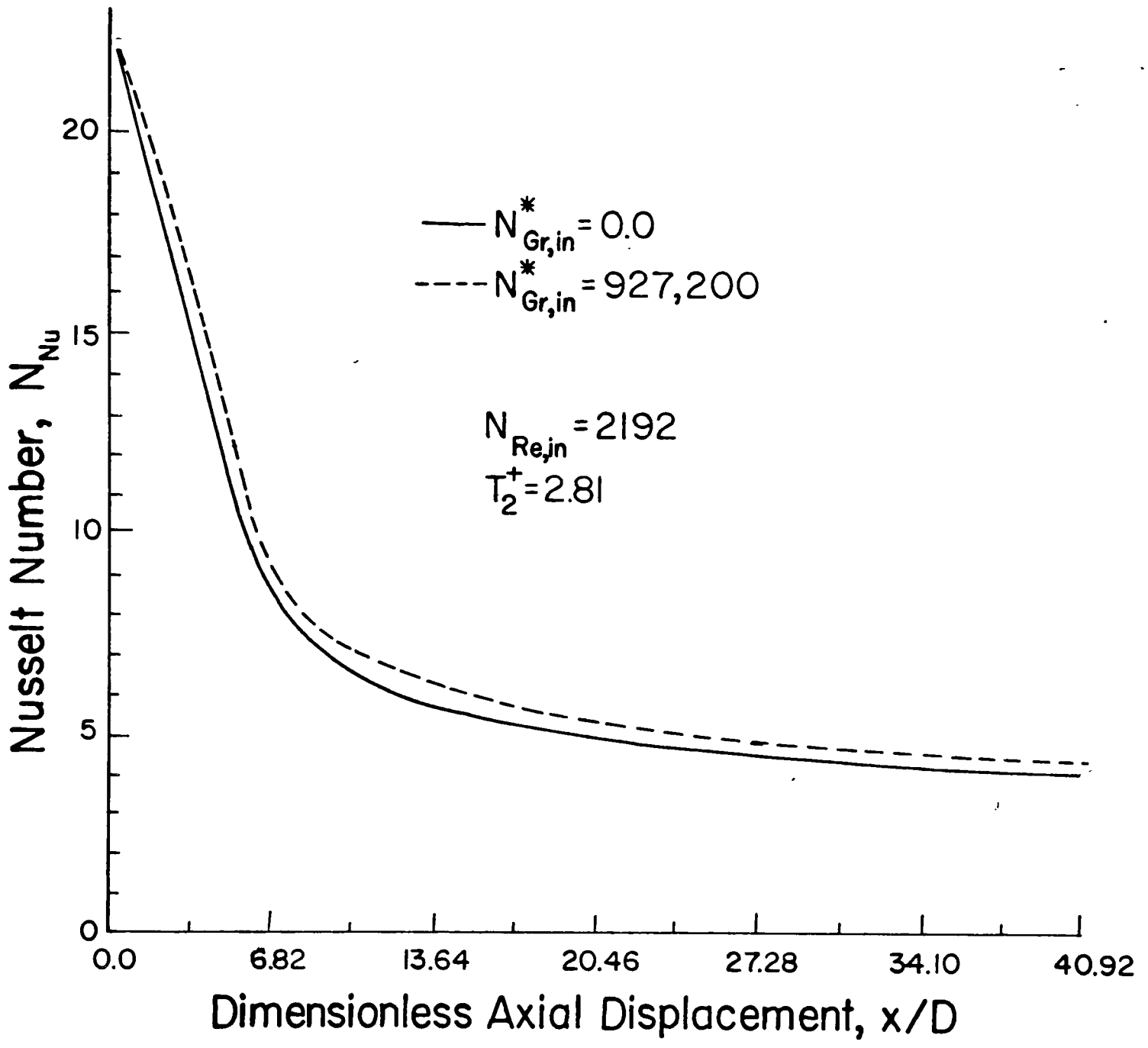

Fig. 4-5--Variation of Nusselt number with free convection (Run 392)

friction factor is taken to be

$$f = \frac{2\,\tau_w \rho_b \pi^2 r_w^4}{\dot{m}^2} \tag{4.3.1}$$

where τ_w is the wall shear stress; r_w is the inside radius of the tube; $\dot{m}$ is the mass flow rate; and ρ_b is the bulk density defined by the relation

$$\rho_b = \frac{2\int_0^{r_w} \rho\, r\, dr}{r_w^2} \tag{4.3.2}$$

The Nusselt number is defined for data reduction purposes as

$$N_{Nu} = \frac{2\, q_w''\, r_w}{(T_w - T_b)k_b} \tag{4.3.3}$$

where q_w'' is the heat flux at the tube wall evaluated using Fourier's Law, T_w is the tube wall temperature, T_b is the bulk fluid temperature defined by the relation

$$T_b = \frac{\int_0^{r_w} \rho\, u\, T\, r\, dr}{\int_0^{r_w} \rho\, u\, r\, dr} \tag{4.3.4}$$

and k_b is the thermal conductivity evaluated at T_b.

The plots reveal that the variation of friction factor with increasing free convection is much stronger than the variation of Nusselt number with free convection. This is because the velocity profiles are much more strongly affected by free convection than the temperature profiles.

4.4 Comparison with Other Analyses

In order to assure the validity of the solution a comparison has been made with the previously mentioned works of Kirby [17] and Chance [3] and with the earlier computer solution of Wilkins [26].

A comparison of some computer solution values of axial velocity to experimental values for Run 391 is shown in Figure 4-6. The cause of the profile irregularity near the wall on experimental profiles in the entrance region has not been successfully explained either by the experimenters or by the program. As seen in the previous section of this chapter, this type of profile irregularity does develop as the free convection effects become more pronounced. One possible explanation of the differences between the experimental and computer values could be the variation between the actual and simulated temperature boundary conditions at the start of heating. If the actual local axial temperature gradients at the wall are much greater than those produced by the fifth degree polynomial used to simulate the increase, then the discrepancy becomes plausible. As shown comparison is good in the middle region with the computed velocities near the centerline tending to exceed the experimental values in the downstream region. One possible explanation of this trend is an accumulation in the numerical solution of effects caused by the difference between the experimental and computed property relations like viscosity and thermal conductivity. In the experimental case these errors would not accumulate in the same manner since at each station data are not completely dependent on all previous stations.

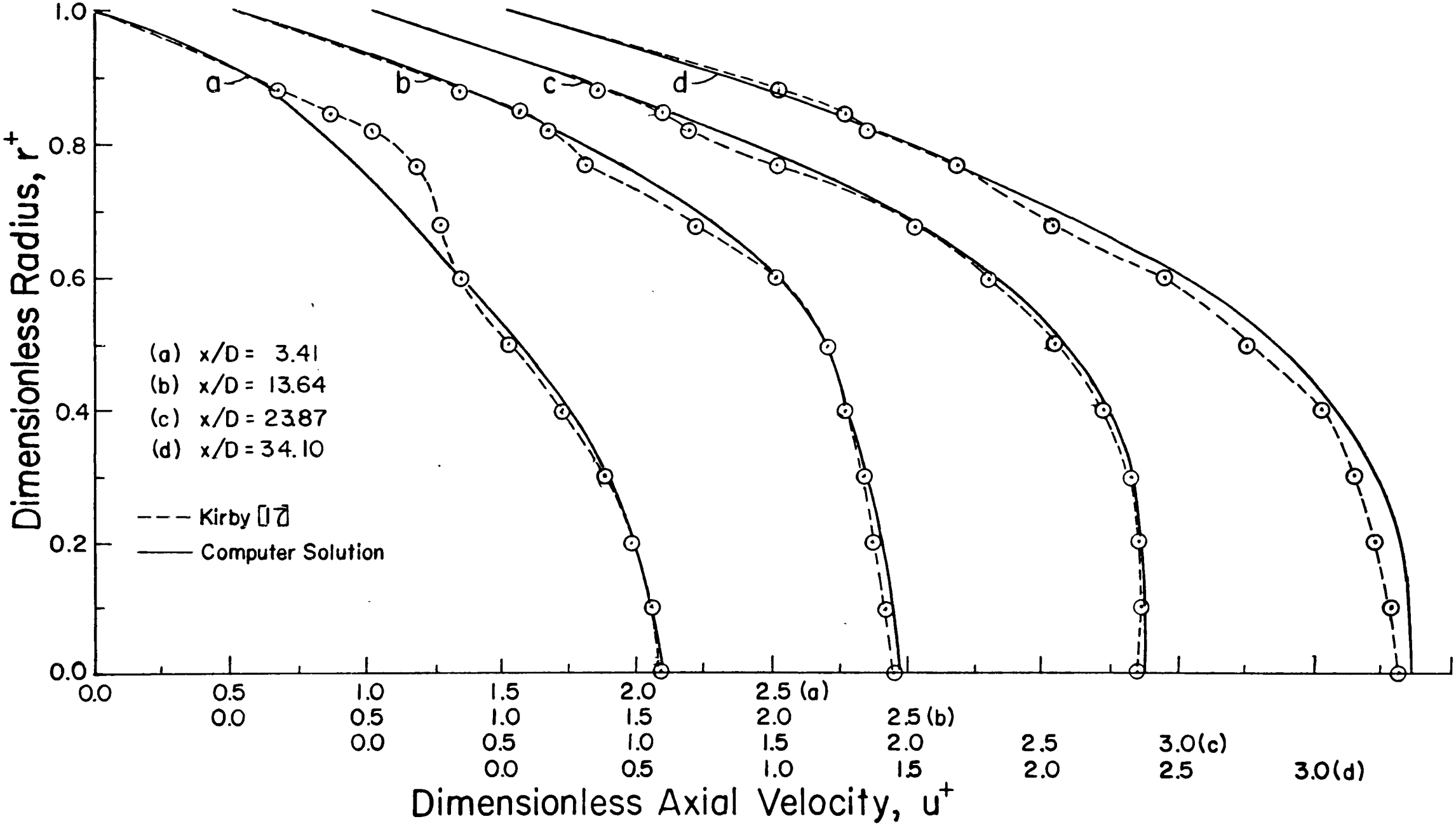

Fig. 4-6--Comparison of computer solution axial velocity profiles to experimental values (Run 391)

Figure 4-7 shows a comparison of the computer values for radial velocity with some profiles deduced from the experimental data for Run 391. To obtain the pseudo-experimental profiles the differential continuity equation in finite difference form was solved for radial velocity using the experimentally obtained axial velocity and temperature profiles to fill in the required unknown quantities. As seen, the agreement is good in spite of the large axial steps (3.41 tube diameters) used in producing the derivative approximations for the pseudo-experimental data.

A comparison of experimental and numerical temperature profiles has already been given in Figure 4-3. Except in the entrance region, the profiles match well. This tends to support the idea that the boundary conditions at the start of heating are not as closely matched as first assumed. The discrepancy in temperature profiles would relate itself through property relations to the axial velocity profiles and the velocity differences discussed earlier in this section.

Experimental values obtained by Kirby and Chance for friction factors and Nusselt numbers are compared with computer values for Run 386 in Figures 4-8 and 4-9. The agreement shown in these figures is typical. Some cases are better, some worse. A summary of the data of this nature for all runs is found in Appendix A.

The comparison to the earlier analysis of Wilkins [26] is complicated by the fact that he has chosen a step change in wall temperature as his temperature boundary condition. This makes an axial station comparison invalid although it is instructional in some respects

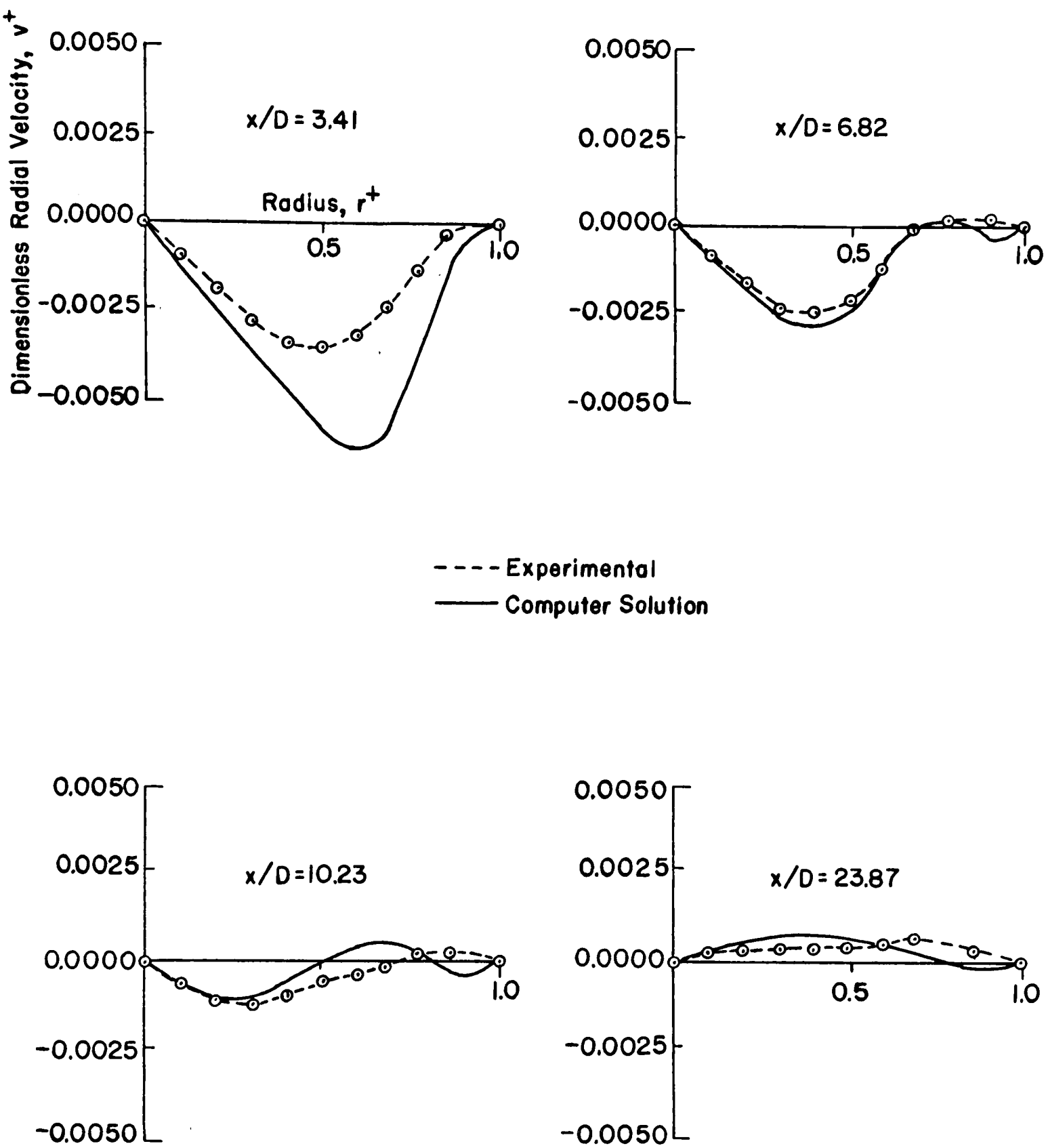

Fig. 4-7.--Comparison of computer solution radial velocity profiles to values deduced from experimental data (Run 391)

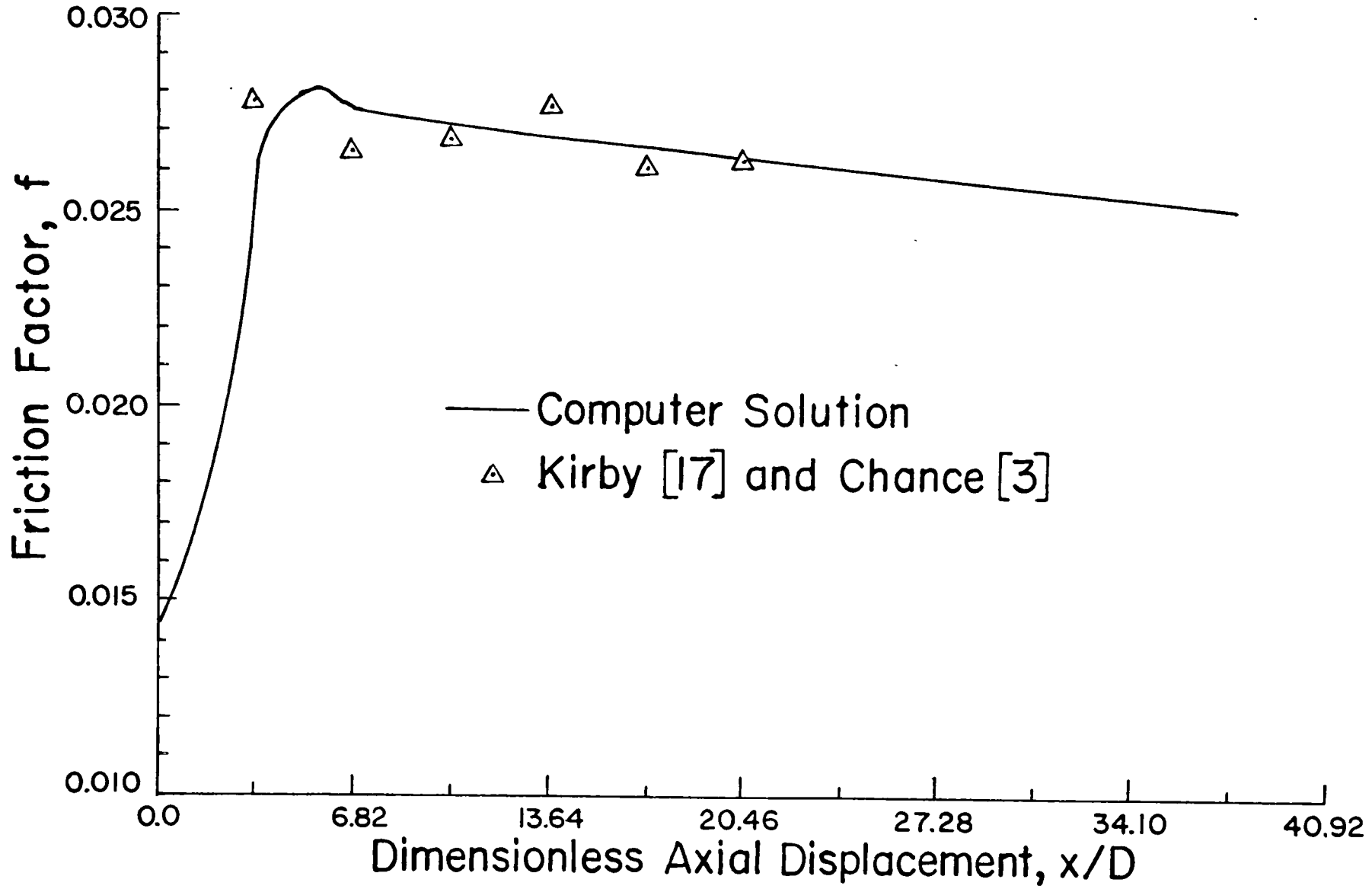

Fig. 4-8.--Comparison of computer solution friction factor values to experimental values (Run 386)

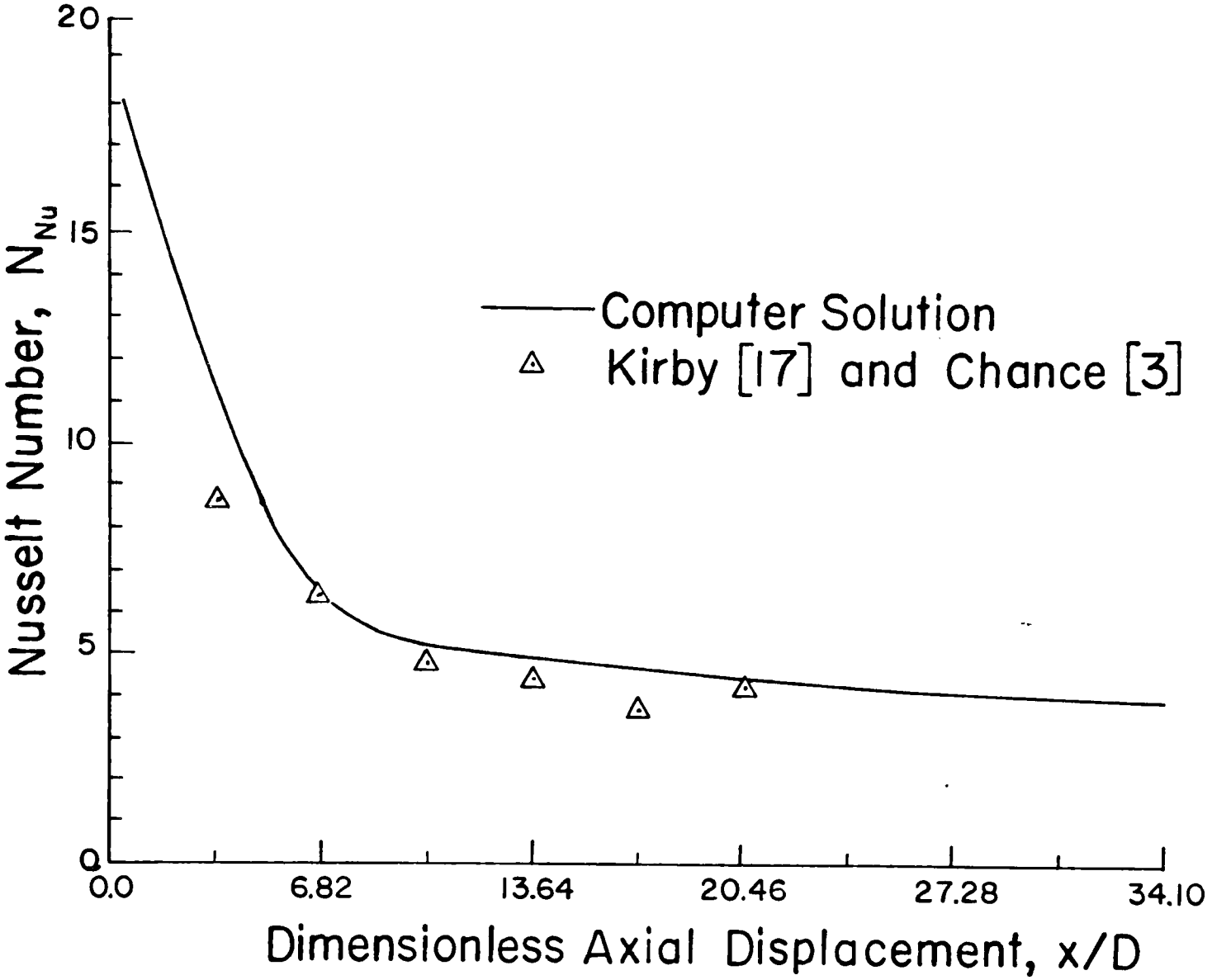

Fig. 4-9.--Comparison of computer solution Nusselt number to experimental values (Run 386)

to attempt this. In Figures 4-10 and 4-11 a plot has been made of three different quantities for several axial locations. The quantities plotted are the following:

1. Wilkins data for a particular axial location
2. The data from Run 392-8 which occurs at approximately the same axial location as Wilkins data
3. The Run 392-8 data from the axial tube location where values most closely match the data of Wilkins

Run 392-8 was chosen because it almost exactly matches Wilkins conditions as shown in his Table 51 with his free convection parameter $F_c = 400.$[1]

As is to be expected, Wilkins' profiles develop faster because a step temperature change is imposed on the fluid at the start of heating. Note, however, that as the flow continues to develop in the downstream direction this effect disappears, and the profiles merge to provide a good match in both velocity and temperature. Also notice that when the velocity profiles of Wilkins are matched, regardless of where they occur, to the velocity profiles found in Run 392-8, a very good match for the temperature profiles occurs at the same axial tube locations. This match can be seen by studying Figures 4-10 and 4-11 simultaneously. This tends to indicate that, at least on a local basis,

---

[1]Wilkins free convection parameter, F_c, is defined in terms of the nomenclature of this report as

$$F_c = 2 \frac{N^*_{Gr,in}}{N_{Re,in}} \frac{\rho_{b,in} - \rho_{w,in}}{\rho_{b,in} + \rho_{w,in}}$$

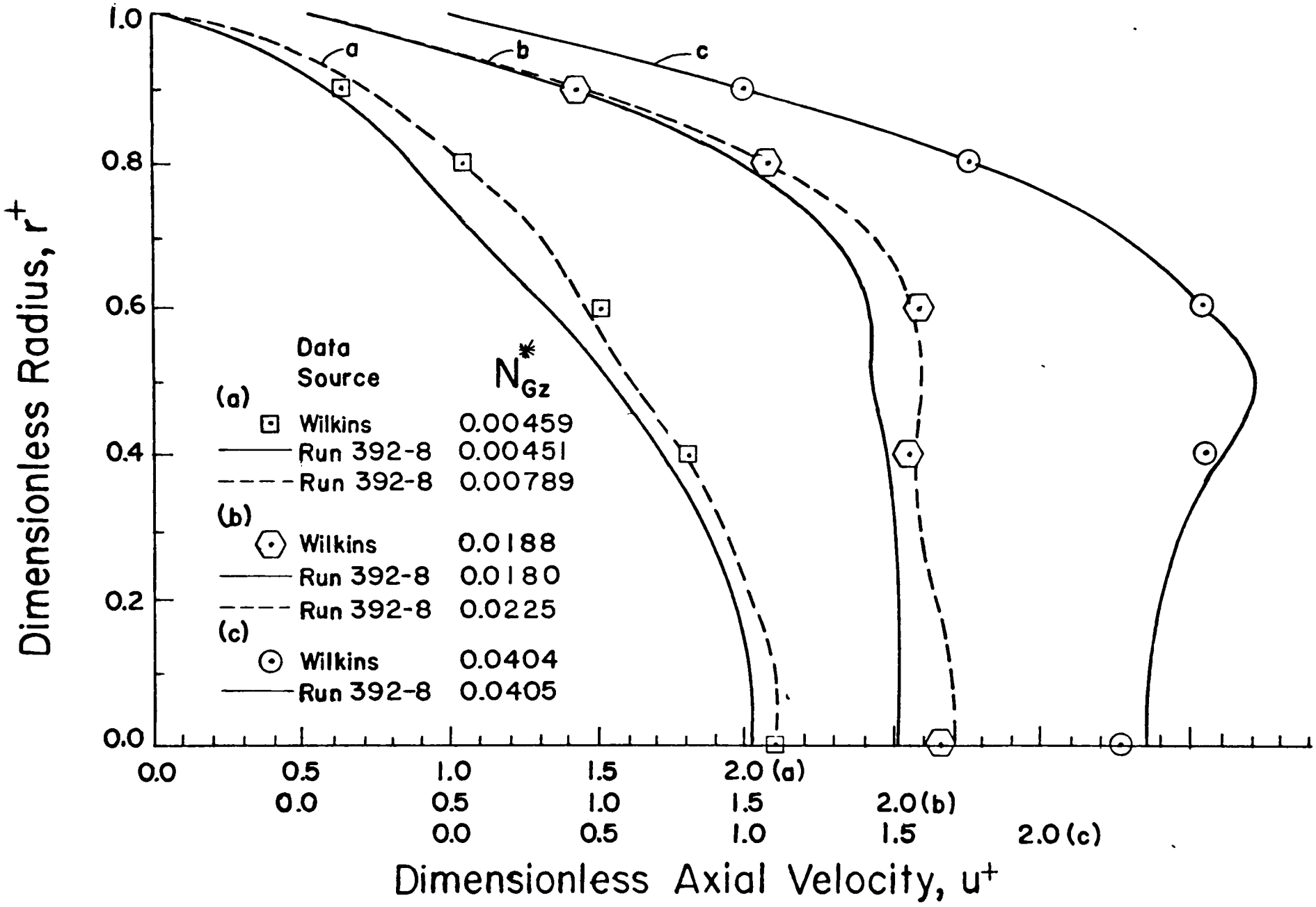

Fig. 4-10.--Axial velocity comparison of Run 392-8 to Table 51 in Wilkins [26]

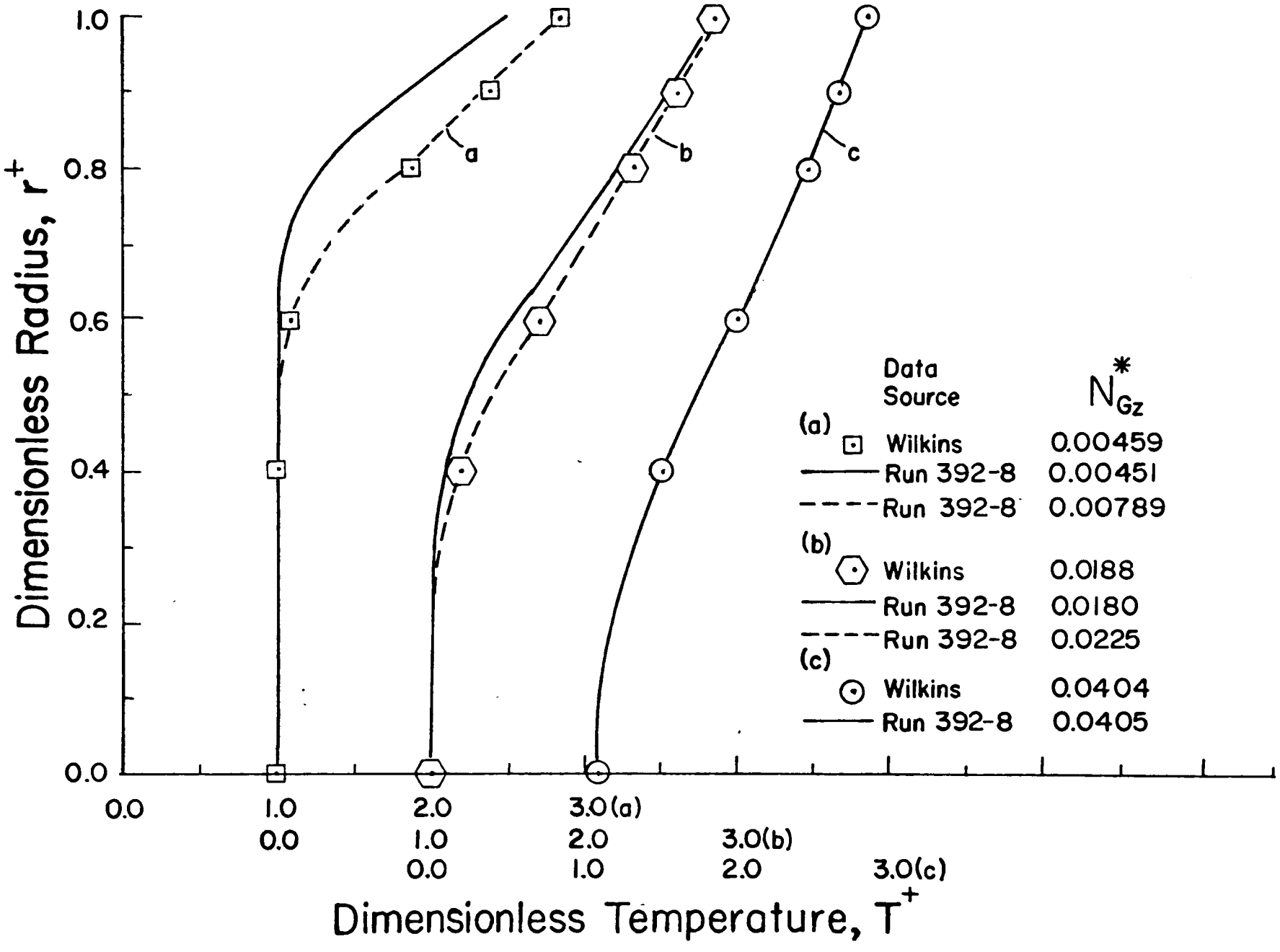

Fig. 4-11.--Temperature comparison of Run 392-8 to Table 51 in Wilkins [26]

the two analyses produce similar results.

4.5 Correlations for Friction Factor and Nusselt Number

By plotting various parameters and examining their trends, two correlations which account for the effect of heating and free convection on the friction factors and Nusselt numbers for air have been developed.

The friction factor correlation is stated as

$$\frac{f}{f_{cp}} = \frac{\rho_b}{\rho_w} + 6.75\text{x}10^{-3} \frac{N_{Re,in}}{N_{Rr,in}} \left(\frac{\rho_b - \rho_w}{\rho_b + \rho_w}\right) \qquad (4.5.1)$$

where f is the desired value of friction factor, based on the definition of equation (4.3.1), f_{cp} is the fully developed laminar flow friction factor evaluated using local heating conditions, ρ_b is the local bulk density, ρ_w is the local density evaluated at the wall, $N_{Re,in}$ is the Reynolds number at the start of heating, and $N_{Fr,in}$ is the entrance Froude number. In this case, the bulk density ρ_b is not the usual $\rho(T_b)$ but rather an integrated average of the form:

$$\rho = \frac{2\int_0^{r_w} \rho \, r\,dr}{r_w^2} \qquad (4.5.2)$$

The maximum deviation of the correlation from the computer values is 11% for all eleven runs. This occurs in the worst case where both a low Reynolds number of about 1000 and a low Froude number of 1.23 indicating large free convection effects are encountered. For the most part, deviation from computer values is 5% or less. The tables of Appendix B show the correlation, computer and experimental values

compared side by side for the various data runs.

The correlation developed from the computer data to relate the Nusselt number to free convection effects is

$$\frac{N_{Nu}}{N_{Nu,pf}} = 1 + 2.25x10^{-4} \frac{N_{Re,in}}{N_{Fr,in}} \qquad (4.5.3)$$

where N_{Nu} is the local Nusselt number, and $N_{Nu,pf}$ is the value of the Nusselt number found for pure forced convection. In general, this correlation is not as accurate as the friction factor correlation, but properly used, it can give an improvement in Nusselt numbers over those found neglecting free convection.

In engineering analyses the correlation could be used in the following manner. Davenport [4], Chance [3] and others established that for cases involving small amounts of free convection, the value of the Nusselt number may be well approximated by the standard constant properties solutions such as the Graetz solution if the properties are evaluated using local bulk conditions such as bulk temperature. If this approach is taken as a basis, then the correlation (4.5.3) may be used to correct the base value of Nusselt number for free convection.

In practice, the data reveals that the maximum Nusselt number correlation error occurs far downstream from the start of heating. This error may be magnified because as the bulk temperature of the fluid approaches the tube wall temperature, the Nusselt number becomes undefined mathematically. This effect may be seen by studying the data presented in Appendix B.

The two correlations have been tried on all the available

computer runs and the experimental data of Kirby [17] and Chance [3]. The results of these comparisons are shown in Appendix B. The rough domain of the source data is as follows:

$$\begin{aligned} 970 &\leqslant N_{Re,in} \leqslant 2190 \\ 1.23 &\leqslant N_{Fr,in} < \infty \\ 0 &\leqslant \frac{\rho_b}{\rho_w} \leqslant 2.6 \end{aligned} \tag{4.5.4}$$

Extrapolation outside of this domain should be done with care especially considering the possibilities of flow instabilities which could occur with large free convection effects.

CHAPTER V

CONCLUSIONS AND RECOMMENDATIONS

5.1 Summary of Results

Perhaps the most unique aspect of this analysis is the point by point comparison of the computer generated flow field to the experimental data of Kirby [17] and Chance [3]. For the problem considered this type of direct simulation has never before been attempted simply because the appropriate data were not available. Agreement between analysis and experiment has been found to be good for most engineering purposes both in the agreement of flow field data and in the agreement of bulk parameters reduced from the local data.

The study of free convection using the computer model also yielded some interesting insights into behavior of the flow field under varying conditions. The results obtained demonstrated the strong influence free convection can have on velocity profiles while at the same time only slightly affecting temperature profiles. This is then reflected in the large variations in friction factor with free convection while Nusselt numbers remain essentially unchanged.

Correlations including free convectional effects have been presented for friction factor and Nusselt numbers which, when properly integrated into one-dimensional flow analyses, can yield more accurate predictions than those which neglect free convection.

The analysis also demonstrated that integral equations are usable for obtaining adequate discrete approximations for computer use. The advantages of the method are somewhat questionable, however, and a further survey of the method will be presented later in this chapter.

For the range of conditions considered, the usual boundary layer assumptions have been found to be valid. This indicates for the temperature ratios and Reynolds numbers encountered in this investigation simpler mathematical models can be used. The upper limit of applicability of these simpler models is still a subject for further study.

5.2 A Critique of Solution Approach

The governing equations for the flow problem considered could have been placed in differential equation form in place of the integral form chosen. No particular advantage was found in the use of the integral equations, but this should not rule out their consideration in future problems.

On the whole, the integral equations seem to produce more bulky and complicated discrete approximations that the differential approach. The trade-off seems to be the replacement of numerous but simple derivative approximations of the differential approach by fewer but more complicated integral approximation terms.

The choice of integral and derivative approximations for use with the integral method is not as open as it may at first appear. As stated in Chapter III, the approximations must be chosen with the idea of producing something akin to diagonal dominance in the linearized

equations. Other considerations can enter in, however. At one time, the computer solution contained the common derivative approximation

$$\frac{\partial f}{\partial r} \simeq \frac{f_{N+1,m} - f_{N-1,m}}{2\Delta r} \tag{5.2.1}$$

in the energy equation. When the solution was found, a zig-zag pattern was noted in the temperature distributions. Since the approximation used for the derivative did not relate f_N to f_{N+1} and f_{N-1} the even numbered grid points had not been adequately tied to the odd-numbered grid points, and, when the solution was reached, it did not represent the physical problem. When the approximation shown above was replaced with the expression

$$\frac{\partial f}{\partial r} \simeq \frac{-2f_{N+2,m} - 3f_{N+1,m} + 6f_{N,m} - f_{N-1,m}}{6\Delta r} \tag{5.2.2}$$

the profiles became smooth and agreed favorably with experimental data.

5.3 Recommendations for Further Study

Study of the results suggests several areas for further explorations. First, although allowance is made in the analysis to exclude from the axial momentum equation the normally employed boundary layer assumptions, this improvement does not significantly improve the quality of the solution for the range of heating considered. This leads to the question of finding exactly where these assumptions do break down. Singh [24] has considered this problem for the energy equation using a constant properties approach, but no detailed variable properties analyses of this nature for either the energy or the momentum equations have been attempted. One possible approach would be to compare a

simplified mathematical model to a more sophisticated model noting the conditions at which the solutions diverge. This type of analysis would preferably be backed by experimental data substantiating the results.

A second area for further study is the investigation of the point at which heating and free convection destroy the stability of the laminar flow regime. In this area experimental data would probably be the easiest to obtain for several reasons. For example, there seems to be no turbulence triggering mechanism inherent in the governing equations of the type used in this investigation. One possible method of including this type of mechanism would be to seek a variational equation based on the Second Law of Thermodynamics, which for the most part has been excluded from the analysis. The magnitude of the problem can be seen in the fact that no successful analytical explanation of the transition from laminar flow to turbulence at high Reynolds numbers has been presented for simple cold flow of a fluid. Furthermore, if a discrete numerical model were used to explore the edge of flow stability, there would be some doubt as to which actually became unstable: the mathematical model or the flow itself.

With only minor modifications the computer program developed here for analysis of upflow of air with heating could be utilized for additional studies such as upflow with cooling, downflow with heating, and downflow with cooling. For gases, the cases of upflow with cooling and downflow with heating are inherently unstable and care should be taken to assure the program is not extended beyond its limits of credibility. With other minor changes the program could be utilized to

simulate the flow of substances other than air. Helium, carbon dioxide, and steam are logical choices although the selection is not limited to gases.

For the same geometry utilized in this investigation, the analysis of transients provides an additional area of further study. The study of the hydrodynamic transient induced by time dependent temperature boundary conditions has been presented by Kliewer [18] for the tubular geometry. Kliewer's numerical model includes radial velocity and temperature dependent fluid property values.

LIST OF REFERENCES

1. Abramowitz, Milton and Irene A. Stegun (Editors). Handbook of Mathematical Functions with Formulas, Graphs, and Mathematical Tables. National Bureau of Standards AMS 55. Washington: U. S. Government Printing Office, 1964.

2. Brown, George M. "Heat or Mass Transfer in Laminar Flow in a Circular or Flat Conduit." A.I. Ch. E. Journal, Vol. 6, June, 1960, pp. 179-183.

3. Chance, James L. "An Experimental Investigation of Heat Transfer and Friction in a Circular Tube for Laminar Flow of Air under Conditions of Large Transverse Temperature Gradients." Unpublished Doctoral Dissertation, Texas Tech University, 1969.

4. Davenport, M. E. "The Effect of Transverse Temperature Gradients on the Heat, Transfer and Friction Factor for Laminar Flow of Gases." Unpublished Ph. D Thesis, Department of Mechanical Engineering, Stanford University, July, 1962.

5. Dalle Donne, M., and F. H. Bowditch. "High Temperature Heat Transfer--Local Heat Transfer and Average Friction Coefficients for Laminar, Transitional and Turbulent Flow of Air in a Tube at High Temperature." Nuclear Engineering, Vol. 8, 1963, pp. 20-29.

6. Deissler, R. G. "Analytical Investigation of Fully Developed Laminar Flow in Tubes with Heat Transfer with Properties Variable Along the Radius." NACA Technical Note 2410, July, 1951.

7. _____, and Alden F. Presler. "Analysis of Developing Laminar Flow and Heat Transfer in a Tube for a Gas with Variable Properties," Proceedings of the Third International Heat Transfer Conference, Chicago, Illinois, August 8, 1966.

8. Fadeeva, V. N. Computational Methods of Linear Algebra. Dover Publications, Inc., 1959.

9. Graetz L. "Uber die Warmeleitungsfahigkeit von Flussigkeiten." Annalen der Physik, Vol. 25, 1885, pp. 337-357.

10. Hallman, T. M. "Combined Forced and Free-Laminar Heat Transfer in Vertical Tubes with Uniform Internal Heat Generation." Trans. ASME, Vol. 28, 1956, pp. 1831-1841.

11. Hancock, Dain M. "A Review of Analyses for Laminar Flow Heat Transfer with Variable Physical Properties." Unpublished Master's Thesis, Texas Tech University, 1965.

12. Henrici, Peter. Elements of Numerical Analysis. New York: John Wiley and Sons, Inc., 1964.

13. Hornbeck, Robert W. "An All-Numerical Method for Heat Transfer in the Inlet of a Tube," ASME Paper 65-WA/HT-36, 1065.

14. Hughes, William F., and Eber W. Gaylord. Basic Equations of Engineering Science. New York: Schaum Publishing Company, 1964.

15. Kays, W. M., and W. B. Nicoll. "Laminar Flow Heat Transfer to a Gas with Large Temperature Differences." Journal of Heat Transfer, Trans. ASME, Vol. 85, 1963, pp. 322-338.

16. Kays, W. M., Convective Heat and Mass Transfer. New York: McGraw-Hill Book Company, 1966.

17. Kirby, Gerald S. "The Effect of Transverse Temperature Gradients on the Velocity and Temperature Profiles for Laminar Flow of Air." Unpublished Doctoral Dissertation, Texas Tech University, 1969.

18. Kliewer, Raymond. "A Finite Difference Study of Transient Heat Transfer Involving Hydrodynamic Variation in the Thermal Entrance Region of a Circular Tube." Unpublished Doctoral Dissertation, Texas Tech University, 1970.

19. Koppel, L. B., and J. M. Smith. "Laminar Flow Heat Transfer Variable Physical Properties," ASME Paper No. 61-SA-32, 1961.

20. McMordie, R. K., and A. F. Emery. "A Numerical Solution for Laminar-Flow Heat Transfer in Circular Tubes with Axial Conduction and Developing Thermal and Velocity Fields," ASME Paper 66-WA/HT-7, 1966.

21. Schlichting, Hermann. Boundary Layer Theory. New York: McGraw-Hill Book Company, 1960.

22. Sellars, J. R., Myron Tribus, and J. S. Kline. "Heat Transfer to Laminar Flow in a Round Tube or Flat Conduit--The Graetz Problem Extended," Trans. ASME, Vol. 78, 1956, pp. 441-448.

23. Siegel, R., E. M. Sparrow, and T. M. Hallman. "Steady Laminar Heat Transfer in a Circular Tube with Prescribed Wall Heat Flux," Appl. Sci. Res., Sec. A, Vol. 7, 1958, pp. 386-392.

24. Singh, S. R. "Heat Transfer by Laminar Flow in a Cylindrical Tube," Appl. Sci. Res., Sec. A, Vol. 7, 1958, pp. 325-340.

25. Varga, Richard S. Matrix Iterative Analysis. New Jersey: Prentice Hall, Inc., 1962.

26. Wilkins, Bert Jr. "Nonisothermal Laminar Flow and Heat Transfer with Temperature Dependent Physical Properties." Unpublished Ph. D. Thesis, School of Chemical Engineering, Georgia Institute of Technology, April, 1965.

27. Worsøe-Schmidt, Peder M. Finite Difference Solution for Laminar Flow of Gas in a Tube at a High Heating Rate. Technical Report No. 247-8, Nuclear Technology Laboratory, Stanford, California, November, 1964.

APPENDIX A: DATA SUMMARY

RUN 385

$N_{Re,in} = 2089.5$, $N^{*}_{Gr,in} = 115{,}900$, $N_{Pr,in} = 0.69$, $M_{in} = 0.00683$

Numerical Solution						Experimental Values of Kirby [17] and Chance [3]				
x/D	N_{Re}	f	N_{Nu}	T_b^+	T_w^+/T_b^+	N_{Re}	f	N_{Nu}	T_b^+	T_w^+/T_b^+
1.71	2082	0.00901	18.23	1.006	1.205	---	---	---	---	---
3.41	2034	0.01279	14.26	1.041	1.703	2000	0.01345	9.55	1.051	1.696
6.82	1929	0.01382	7.92	1.126	1.732	1897	0.01449	7.90	1.128	1.721
10.23	1866	0.01358	6.34	1.184	1.648	1883	0.01351	6.43	1.181	1.645
13.64	1818	0.01342	5.61	1.231	1.582	1778	0.01289	5.63	1.251	1.578
17.05	1779	0.01329	5.14	1.272	1.531	1742	0.01407	4.83	1.270	1.532
20.46	1745	0.01321	4.85	1.308	1.491	1708	0.01402	4.28	1.306	1.489
23.87	1716	0.01312	4.63	1.342	1.451	1684	0.01246	5.34	1.335	1.456
27.28	1689	0.01304	4.46	1.373	1.418	1646	0.01156	5.41	1.381	1.404
30.69	1666	0.01298	4.32	1.403	1.388	1628	0.01423	4.10	1.405	1.380
34.10	1644	0.01291	4.22	1.430	1.362	1593	0.01433	4.43	1.440	1.353
37.51	1625	0.01286	4.14	1.455	1.340	1572	0.01180	3.60	1.465	1.330
40.92	1607	0.01281	4.08	1.479	1.320					
44.33	1591	0.01276	4.03	1.502	1.299					
47.74	1575	0.01271	3.99	1.524	1.280					
51.15	1561	0.01267	3.97	1.555	1.255					
54.56	1548	0.01264	3.94	1.564	1.246					

RUN 386

$N_{Re,in} = 1121.5$, $N^{*}_{GR,in} = 107{,}929$, $N_{Pr,in} = 0.69$, $M_{in} = 0.00348$

Numerical Solution						Experimental Values of Kirby [17] and Chance [3]				
x/D	N_{Re}	f	N_{Nu}	T_b^+	T_w^+/T_b^+	N_{Re}	f	N_{Nu}	T_b^+	T_w^+/T_b^+
1.71	1114	0.01743	14.84	1.010	1.232	---	---	---	---	---
3.41	1071	0.02578	11.67	1.072	1.767	1042	0.02780	8.53	1.092	1.681
6.82	982	0.02776	6.45	1.219	1.728	954	0.02650	6.32	1.231	1.703
10.23	933	0.02717	5.26	1.317	1.599	913	0.02589	4.82	1.318	1.597
13.64	897	0.02669	4.69	1.396	1.508	876	0.0]766	4.46	1.398	1.506
17.05	869	0.02634	4.40	1.463	1.438	849	0.02613	3.62	1.460	1.441
20.46	846	0.02602	4.20	1.522	1.391	832	0.02637	4.10	1.520	1.396
23.87	827	0.02575	4.08	1.575	1.337					
27.28	811	0.02551	4.00	1.623	1.296					
30.69	796	0.02530	3.96	1.667	1.262					
34.10	784	0.02511	3.94	1.707	1.232					

RUN 390

$N_{Re,in} = 929.9$, $N^{*}_{Gr,in} = 112{,}375$, $N_{Pr,in} = 0.69$, $M_{in} = 0.00340$

Numerical Solution						Experimental Values of Kirby [17] and Chance [3]				
x/D	N_{Re}	f	N_{Nu}	T_b^+	T_w^+/T_b^+	N_{Re}	f	N_{Nu}	T_b^+	T_w^+/T_b^+
1.71	927	0.01919	13.69	1.005	1.113	---	---	---	---	---
3.41	907	0.02457	10.46	1.038	1.389	884	0.02231	6.88	1.065	1.387
6.82	865	0.02623	5.96	1.113	1.382	852	0.02497	5.89	1.120	1.376
10.23	840	0.02604	4.96	1.163	1.322	822	0.02608	5.03	1.176	1.311
13.64	822	0.02581	4.50	1.202	1.281	807	0.02614	3.85	1.210	1.276
17.05	807	0.02562	4.28	1.237	1.248	788	0.02445	3.76	1.241	1.242
20.46	794	0.02543	4.13	1.266	1.218	779	0.02513	3.02	1.260	1.222
23.87	783	0.02524	4.04	1.293	1.191	766	0.02579	4.09	1.286	1.198
27.28	773	0.02506	3.98	1.317	1.170	753	0.02557	4.31	1.316	1.171
30.69	765	0.02489	3.96	1.339	1.151					
34.10	757	0.02473	3.96	1.358	1.135					

RUN 391-0

$N_{Re,in} = 1066.1$, $N^{*}_{Gr,in} = 0.0$, $N_{Pr,in} = 0.69$, $M_{in} = 0.00348$

x/D	N_{Re}	f	N_{Nu}	T_b^+	T_w^+/T_b^+
1.71	1057	0.01840	14.61	1.012	1.285
3.41	1005	0.02762	11.47	1.091	1.928
6.82	904	0.02951	6.25	1.279	1.848
10.23	849	0.02871	5.04	1.404	1.681
13.64	811	0.02820	4.49	1.505	1.570
17.05	781	0.02787	4.21	1.590	1.485
20.46	758	0.02762	4.02	1.665	1.419
23.87	738	0.02744	3.91	1.732	1.361
27.28	721	0.02729	3.84	1.792	1.318
30.69	707	0.02717	3.81	1.847	1.279
34.10	694	0.02708	3.79	1.879	1.258
37.51	683	0.02701	3.80	1.943	1.215
40.92	673	0.02696	3.82	1.985	1.190

Note: No experimental comparison is available for this run.

RUN 391-1

$N_{Re,in} = 1066.1$, $N^{*}_{Gr,in} = 115{,}900$, $N_{Pr,in} = 0.69$, $M_{in} = 0.00348$

Numerical Solution						Experimental Values of Kirby [17] and Chance [3]				
x/D	N_{Re}	f	N_{Nu}	T_b^+	T_w^+/T_b^+	N_{Re}	f	N_{Nu}	T_b^+	T_w^+/T_b^+
1.71	1057	0.01919	14.71	1.013	1.285	---	---	---	---	---
3.41	1004	0.03000	11.68	1.093	1.925	943	0.03467	7.68	1.170	1.884
6.82	901	0.03232	6.37	1.285	1.840	859	0.03433	5.78	1.321	1.791
10.23	846	0.03139	5.16	1.412	1.672	807	0.03095	4.71	1.441	1.638
13.64	807	0.03069	4.61	1.515	1.560	772	0.03181	4.42	1.531	1.545
17.05	777	0.03017	4.33	1.603	1.475	742	0.03000	4.36	1.631	1.448
20.46	753	0.02972	4.14	1.679	1.409	720	0.02767	3.39	1.702	1.387
23.87	733	0.02933	4.03	1.748	1.352	706	0.02973	3.51	1.755	1.346
27.28	716	0.02900	3.97	1.809	1.308	686	0.03057	4.06	1.831	1.293
30.69	702	0.02873	3.93	1.865	1.268	673	0.02971	3.78	1.885	1.256
34.10	690	0.02847	3.95	1.916	1.232	660	0.02927	3.88	1.939	1.223
37.51	679	0.02827	3.95	1.962	1.202					
40.92	669	0.02809	4.00	2.005	1.079					

RUN 391-4

$N_{Re,in} = 1066.1$, $N^{*}_{Gr,in} = 463{,}000$, $N_{Pr,in} = 0.69$, $M_{in} = 0.00348$

x/D	N_{Re}	f	N_{Nu}	T_b^+	T_w^+/T_b^+
1.71	1057	0.02157	15.00	1.013	1.282
3.41	1001	0.03724	12.29	1.098	1.920
6.82	894	0.04114	6.76	1.301	1.815
10.23	836	0.03994	5.55	1.436	1.646
13.64	796	0.03861	4.96	1.546	1.529
17.05	765	0.03732	4.72	1.640	1.441
20.46	741	0.03606	4.53	1.722	1.371
23.87	720	0.03492	4.43	1.795	1.318
27.28	704	0.03390	4.38	1.860	1.271
30.69	689	0.03302	4.37	1.918	1.232
34.10	677	0.03226	4.40	1.970	1.200
37.51	666	0.03161	4.47	2.017	1.171
40.92	657	0.03106	4.56	2.060	1.148

Note: No experimental comparison is available for this run.

RUN 391-8

$N_{Re,in}$ = 1066.1, $N^{*}_{Gr,in}$ = 927,200, $N_{Pr,in}$ = 0.69, M_{in} = 0.00348

x/D	N_{Re}	f	N_{Nu}	T_b^+	T_w^+/T_b^+
1.71	1057	0.02475	15.39	1.013	1.285
3.41	998	0.04705	13.05	1.104	1.906
6.82	885	0.05393	7.29	1.320	1.790
10.23	825	0.05267	6.08	1.465	1.613
13.64	783	0.05050	5.51	1.584	1.491
17.05	750	0.04746	5.36	1.689	1.400
20.46	724	0.04438	5.14	1.780	1.329
23.87	704	0.04164	5.07	1.859	1.271
27.28	687	0.03943	5.01	1.927	1.228
30.69	673	0.03765	5.05	1.987	1.190
34.10	661	0.03620	5.13	2.040	1.159
37.51	651	0.03502	5.29	2.086	1.131
40.92	643	0.03404	5.52	2.128	1.111

Note: No experimental comparison is available for this run.

RUN 392-0

$N_{Re,in} = 2192.5$, $N^{*}_{Gr,in} = 0.0$, $N_{Pr,in} = 0.69$, $M_{in} = 0.00683$

x/D	N_{Re}	f	N_{Nu}	T_b^+	T_w^+/T_b^+
1.71	2177	0.00956	19.03	1.011	1.383
3.41	2082	0.01602	15.35	1.080	2.285
6.28	1888	0.01748	8.25	1.250	2.244
10.23	1781	0.01688	6.50	1.364	2.061
13.64	1704	0.01648	5.63	1.457	1.930
17.05	1642	0.01626	5.16	1.540	1.825
20.46	1592	0.01604	4.82	1.613	1.740
23.87	1549	0.01587	4.56	1.680	1.672
27.28	1511	0.01573	4.37	1.743	1.611
30.69	1479	0.01561	4.23	1.800	1.561
34.10	1449	0.01551	4.12	1.855	1.515
37.51	1423	0.01542	4.04	1.906	1.474
40.92	1400	0.01534	3.98	1.954	1.439

Note: No experimental comparison is available for this run.

RUN 392-1

$N_{Re,in} = 2192.5$, $N^{*}_{Gr,in} = 115{,}900$, $N_{Pr,in} = 0.69$, $M_{in} = 0.00683$

Numerical Solution						Experimental Values of Kirby [17] and Chance [3]				
x/D	N_{Re}	f	N_{Nu}	T_b^+	T_w^+/T_b^+	N_{Re}	f	N_{Nu}	T_b^+	T_w^+/T_b^+
1.71	2177	0.00975	19.09	1.011	1.384	---	---	---	---	---
3.41	2081	0.01658	15.46	1.081	2.282	1963	0.01347	12.52	1.145	2.266
6.28	1886	0.01816	8.32	1.252	2.241	1773	0.01638	8.07	1.320	2.143
10.23	1778	0.01757	6.56	1.367	2.057	1725	0.01933	5.32	1.400	2.019
13.64	1701	0.01715	5.69	1.461	1.921	1646	0.01848	5.23	1.500	1.888
17.05	1639	0.01690	5.21	1.544	1.819	1597	0.01776	4.67	1.565	1.806
20.46	1588	0.01665	4.87	1.618	1.738	1546	0.01669	4.46	1.644	1.720
23.87	1545	0.01645	4.61	1.686	1.666	1512	0.01714	4.00	1.700	1.665
27.28	1508	0.01627	4.42	1.749	1.606	1470	0.01654	3.69	1.763	1.607
30.69	1475	0.01613	4.27	1.807	1.556	1450	0.01658	4.03	1.803	1.566
34.10	1446	0.01600	4.17	1.862	1.509	1415	0.01658	4.54	1.880	1.508
37.51	1419	0.01588	4.08	1.914	1.468	1384	0.01578	3.94	1.932	1.466
40.92	1396	0.01578	4.02	1.962	1.431	1362	0.01660	3.67	1.980	1.431

RUN 392-4

$N_{Re,in}$ = 2192.5, $N^{*}_{Gr,in}$ = 463,600, $N_{Pr,in}$ = 0.69, M_{in} = 0.00683

x/D	N_{Re}	f	N_{Nu}	T_b^+	T_w^+/T_b^+
1.71	2177	0.01031	19.24	1.010	1.386
3.41	2080	0.01827	15.80	1.082	2.280
6.28	1881	0.02025	8.50	1.257	2.236
10.23	1771	0.01967	6.74	1.375	2.041
13.64	1692	0.01920	5.85	1.472	1.909
17.05	1630	0.01887	5.37	1.557	1.805
20.46	1578	0.01853	5.02	1.634	1.720
23.87	1534	0.01823	4.75	1.704	1.648
27.28	1497	0.01796	4.56	1.768	1.589
30.69	1464	0.01771	4.41	1.828	1.539
34.10	1434	0.01749	4.30	1884	1.490
37.51	1408	0.01728	4.22	1.937	1.450
40.92	1384	0.01709	4.16	1.986	1.415

Note: No experimental comparison is available for this run.

RUN 392-8

$N_{Re,in} = 2192.5$, $N^{*}_{Gr,in} = 927{,}200$, $N_{Pr,in} = 0.69$, $M_{in} = 0.00683$

x/D	N_{Re}	f	N_{Nu}	T_b^+	T_w^+/T_b^+
1.71	2178	0.01106	19.44	1.010	1.385
3.41	2077	0.02054	16.23	1.084	2.280
6.28	1874	0.02313	8.77	1.264	2.221
10.23	1762	0.02261	6.98	1.386	2.025
13.64	1682	0.02210	6.07	1.486	1.890
17.05	1617	0.02166	5.59	1.575	1.782
20.46	1565	0.02118	5.23	1.654	1.699
23.87	1520	0.02073	4.96	1.727	1.628
27.28	1482	0.02031	4.76	1.794	1.565
30.69	1449	0.01990	4.62	1.856	1.513
34.10	1419	0.01952	4.50	1.913	1.468
37.51	1393	0.01916	4.42	1.967	1.428
40.92	1370	0.01882	4.35	2.018	1.392

Note: No experimental comparison is available for this run.

RUN 502

$N_{Re,in}$ = 2000.0, $N^{*}_{Gr,in}$ = 115,900, $N_{Pr,in}$ = 0.69, M_{in} = 0.00683

x/D	N_{Re}	f	N_{Nu}	T_b^+	T_w^+/T_b^+
2.07	1957	0.01446	18.33	1.033	1.889
4.14	1749	0.02705	13.84	1.221	3.130
8.28	1480	0.02626	7.11	1.567	2.555
12.42	1347	0.02499	5.65	1.805	2.216
16.56	1256	0.02411	4.93	2.002	1.999
20.70	1189	0.02349	4.53	2.172	1.843
24.84	1137	0.02299	4.26	2.324	1.720
28.98	1094	0.02259	4.09	2.462	1.622
33.12	1058	0.02226	3.97	2.588	1.545
37.26	1027	0.02199	3.90	2.705	1.480
41.40	1000	0.02176	3.87	2.813	1.422
45.54	977	0.02156	3.85	2.914	1.372
49.68	956	0.02140	3.85	3.008	1.330
53.82	938	0.02126	3.88	3.095	1.292
57.96	922	0.02115	3.92	3.176	1.261
62.10	908	0.02105	3.97	3.252	1.230
66.24	895	0.02098	4.03	3.322	1.205
70.38	883	0.02092	4.10	3.388	1.181
74.52	873	0.02087	4.19	3.448	1.148
78.66	863	0.02083	4.28	3.505	1.141
82.80	855	0.02080	4.40	3.557	1.125

Note: No experimental comparison is available for this run.

APPENDIX B: COMPARISON OF CORRELATIONS TO NUMERICAL AND EXPERIMENTAL RESULTS

RUN 385

$N_{Re,in} = 2089.5$, $N_{Fr,in} = 37.6$

x/D	ρ_b^+	ρ_w^+	f/f_{cp}		
			Correlation	Computer	Experimental
1.71	0.7919	0.8262	1.20	1.18	---
3.41	0.8860	0.5644	1.65	1.62	1.68
6.28	0.7966	0.5128	1.63	1.67	1.716
10.23	0.7581	0.5128	1.55	1.58	1.55
13.64	0.7319	0.5128	1.50	1.52	1.43
17.05	0.7114	0.5128	1.45	1.48	1.53
20.46	0.6952	0.5128	1.42	1.44	1.50
23.87	0.6811	0.5128	1.38	1.41	1.31
27.28	0.6688	0.5128	1.35	1.38	1.19
30.69	0.6579	0.5127	1.33	1.35	1.45
34.10	0.6483	0.5127	1.30	1.33	1.43
37.51	0.6395	0.5127	1.28	1.31	1.16
40.92	0.6317	0.5127	1.27	1.29	---
44.33	0.6243	0.5127	1.25	1.27	---
47.74	0.6178	0.5127	1.24	1.25	---
51.15	0.6116	0.5127	1.22	1.24	---
54.56	0.6060	0.5127	1.21	1.23	---

RUN 386

$N_{Re,in} = 1121.5$, $N_{Fr,in} = 11.65$

x/D	ρ_b^+	ρ_w^+	f/f_{cp}		
			Correlation	Computer	Experimental
1.71	0.9069	0.8038	1.26	1.21	---
3.41	0.8452	0.5274	1.75	1.73	1.81
6.28	0.7300	0.4755	1.67	1.70	1.58
10.23	0.6830	0.4755	1.55	1.58	1.48
13.64	0.6511	0.4755	1.47	1.50	1.52
17.05	0.6267	0.4755	1.41	1.43	1.39
20.46	0.6082	0.4755	1.36	1.38	1.37
23.87	0.5918	0.4755	1.31	1.33	---
27.28	0.5792	0.4755	1.29	1.29	---
30.69	0.5672	0.4755	1.25	1.26	---
34.10	0.5580	0.4755	1.23	1.24	---

RUN 390

$N_{Re,in} = 929.9$, $N_{Fr,in} = 7.69$

x/D	ρ_b^+	ρ_w^+	f/f_{cp}		
			Correlation	Computer	Experimental
1.71	0.9787	0.8931	1.14	1.11	---
3.41	0.9083	0.6947	1.42	1.39	1.23
6.82	0.8344	0.6489	1.38	1.42	1.33
10.23	0.8033	0.6489	1.33	1.37	1.34
13.64	0.7817	0.6489	1.29	1.32	1.42
17.05	0.7650	0.6489	1.25	1.29	1.20
20.46	0.7516	0.6489	1.22	1.26	1.23
23.87	0.7400	0.6489	1.19	1.23	1.23
27.28	0.7303	0.6489	1.18	1.21	1.21
30.69	0.7216	0.6489	1.15	1.19	---
34.10	0.7143	0.6489	1.14	1.17	---

RUN 391-0

$N_{Re,in} = 1066.1$, $N_{Fr,in} \longrightarrow \infty$ (pure forced convection)

x/D	ρ_b^+	ρ_w^+	f/f_{cp}	
			Correlation	Computer
1.71	0.9511	0.7685	1.24	1.22
3.41	0.8154	0.4749	1.72	1.73
6.82	0.6847	0.4235	1.62	1.63
10.23	0.6309	0.4235	1.49	1.48
13.64	0.5956	0.4235	1.41	1.38
17.05	0.5700	0.4235	1.34	1.30
20.46	0.5492	0.4235	1.29	1.25
23.87	0.5329	0.4235	1.26	1.21
27.28	0.5188	0.4235	1.23	1.17
30.69	0.5075	0.4235	1.20	1.14
34.10	0.4973	0.4235	1.17	1.12
37.51	0.4891	0.4235	1.15	1.10
40.92	0.4814	0.4235	1.13	1.08

RUN 391-1

$N_{Re,in} = 1066.1$, $N_{Fr,in} = 9.82$

x/D	ρ_b^+	ρ_w^+	f/f_{cp}			$N_{Nu}/N_{Nu,pf}$	
			Correlation	Computer	Experimental	Correlation	Computer
1.71	0.9511	0.7685	1.31	1.27	---	1.024	1.01
3.41	0.8154	0.4749	1.88	1.87	2.04	1.024	1.02
6.82	0.6847	0.4234	1.77	1.79	2.02	1.024	1.02
10.23	0.6309	0.4235	1.63	1.62	1.52	1.024	1.02
13.64	0.5956	0.4235	1.53	1.51	1.54	1.024	1.03
17.05	0.5700	0.4235	1.45	1.41	1.39	1.024	1.03
20.46	0.5492	0.4235	1.39	1.34	1.25	1.024	1.03
23.87	0.5392	0.4235	1.34	1.28	1.31	1.024	1.03
27.28	0.5188	0.4235	1.30	1.24	1.31	1.024	1.03
30.69	0.5075	0.4235	1.26	1.20	1.25	1.024	1.04
34.10	0.4973	0.4235	1.23	1.18	1.21	1.024	1.04
37.51	0.4891	0.4235	1.21	1.15	---	1.024	1.04
40.92	0.4814	0.4235	1.18	1.13	---	1.024	1.05

RUN 391-4

$N_{Re,in} = 1066.1$, $N_{Fr,in} = 2.46$

x/D	ρ_b^+	ρ_w^+	f/f_{cp}		$N_{Nu}/N_{Nu,pf}$	
			Correlation	Computer	Correlation	Computer
1.71	0.9511	0.7685	1.54	1.42	1.097	1.03
3.41	0.8154	0.4749	2.51	2.33	1.097	1.07
6.82	0.6847	0.4235	2.29	2.28	1.097	1.08
10.23	0.6309	0.4235	2.05	2.06	1.097	1.10
13.64	0.5956	0.4235	1.88	1.89	1.097	1.10
17.05	0.5700	0.4235	1.76	1.74	1.097	1.12
20.46	0.5492	0.4235	1.66	1.63	1.097	1.12
23.87	0.5329	0.4235	1.58	1.53	1.097	1.13
27.28	0.5188	0.4235	1.51	1.45	1.097	1.14
30.69	0.5075	0.4235	1.45	1.39	1.097	1.15
34.10	0.4973	0.4235	1.40	1.33	1.097	1.16
37.51	0.4981	0.4235	1.36	1.28	1.097	1.18
40.92	0.4814	0.4235	1.31	1.25	1.097	1.19

RUN 391-8

$N_{Re,in}$ = 1066.1, $N_{Fr,in}$ = 1.23

x/D	ρ_b^+	ρ_w^+	f/f_{cp}		$N_{Nu}/N_{Nu,pf}$	
			Correlation	Computer	Correlation	Computer
1.71	0.9511	0.7685	1.64	1.64	1.195	1.05
3.41	0.8154	0.4749	3.09	2.93	1.195	1.14
6.82	0.6847	0.4235	2.96	2.98	1.195	1.17
10.23	0.6309	0.4235	2.60	2.71	1.195	1.21
13.64	0.5956	0.4235	2.36	2.47	1.195	1.22
17.05	0.5700	0.4235	2.18	2.22	1.195	1.27
20.46	0.5492	0.4235	2.02	2.05	1.195	1.27
23.87	0.5329	0.4235	1.91	1.83	1.195	1.29
27.28	0.5188	0.4235	1.80	1.69	1.195	1.30
30.69	0.5075	0.4235	1.71	1.58	1.195	1.32
34.10	0.4973	0.4235	1.63	1.50	1.195	1.35
37.51	0.4981	0.4235	1.56	1.42	1.195	1.39
40.92	0.4814	0.4235	1.50	1.36	1.195	1.44

RUN 392-0

$N_{Re,in} = 2192.5$, $N_{Fr,in} \longrightarrow \infty$ (pure forced convection)

x/D	ρ_b^+	ρ_w^+	f/f_{cp}	
			Correlation	Computer
1.71	0.9504	0.7139	1.33	1.30
3.41	0.8175	0.4048	2.02	2.09
6.82	0.6881	0.3559	1.94	2.06
10.23	0.6337	0.3559	1.78	1.88
13.64	0.5972	0.3553	1.68	1.75
17.05	0.5699	0.3558	1.60	1.67
20.46	0.5480	0.3558	1.54	1.60
23.87	0.5298	0.3558	1.49	1.54
27.28	0.5143	0.3558	1.44	1.49
30.69	0.5009	0.3558	1.41	1.45
34.10	0.4892	0.3558	1.37	1.40
37.51	0.4784	0.3558	1.34	1.38
40.92	0.4654	0.3558	1.31	1.34

RUN 392-1

$N_{Re,in} = 2192.5$, $N_{Fr,in} = 41.5$

x/D	ρ_b^+	ρ_w^+	f/f_{cp}			$N_{Nu}/N_{Nu,pf}$	
			Correlation	Numerical	Computer	Correlation	Computer
1.71	0.9504	0.7139	1.38	1.33	---	1.012	1.00
3.41	0.8175	0.4048	2.14	2.16	1.67	1.012	1.01
6.82	0.6881	0.3559	2.05	2.14	1.82	1.012	1.01
10.23	0.6337	0.3559	1.88	1.96	2.08	1.012	1.01
13.64	0.5972	0.3558	1.77	1.83	1.90	1.012	1.01
17.05	0.5699	0.3558	1.68	1.74	1.77	1.012	1.01
20.46	0.5480	0.3558	1.62	1.67	1.61	1.012	1.01
23.87	0.5298	0.3558	1.56	1.59	1.62	1.012	1.01
27.28	0.5143	0.3558	1.50	1.54	1.52	1.012	1.01
30.69	0.5009	0.3558	1.47	1.49	1.50	1.012	1.01
34.10	0.4892	0.3558	1.43	1.45	1.47	1.012	1.01
37.51	0.4784	0.3558	1.39	1.41	1.37	1.012	1.01
40.92	0.4654	0.3558	1.36	1.38	1.41	1.012	1.01

RUN 392-4

$N_{Re,in} = 2192.5$, $N_{Fr,in} = 10.4$

x/D	ρ_b^+	ρ_w^+	f/f_{cp}		$N_{Nu}/N_{Nu,pf}$	
			Correlation	Computer	Correlation	Computer
1.71	0.9507	0.7139	1.54	1.41	1.047	1.01
3.41	0.8195	0.4048	2.49	2.38	1.047	1.03
6.82	0.6918	0.3559	2.49	2.39	1.047	1.03
10.23	0.6375	0.3559	2.16	2.19	1.047	1.04
13.64	0.6009	0.3558	2.04	2.04	1.047	1.04
17.05	0.5735	0.3558	1.93	1.94	1.047	1.04
20.46	0.5509	0.3558	1.84	1.85	1.047	1.04
23.87	0.5323	0.3558	1.77	1.77	1.047	1.04
27.28	0.5161	0.3558	1.70	1.70	1.047	1.04
30.69	0.5021	0.3558	1.64	1.64	1.047	1.04
34.10	0.4902	0.3558	1.59	1.58	1.047	1.04
37.51	0.4790	0.3558	1.54	1.54	1.047	1.04
40.92	0.4697	0.3558	1.50	1.50	1.047	1.05

RUN 392-8

$N_{Re,in} = 2192.5$, $N_{Fr,in} = 5.19$

x/D	ρ_b^+	ρ_w^+	f/f_{cp}		$N_{Nu}/N_{Nu,pf}$	
			Correlation	Computer	Correlation	Computer
1.71	0.9512	0.7139	1.73	1.58	1.095	1.02
3.41	0.8221	0.4048	2.97	2.67	1.095	1.06
6.82	0.6966	0.3559	2.84	2.72	1.095	1.06
10.23	0.6430	0.3559	2.55	2.52	1.095	1.07
13.64	0.6064	0.3558	2.40	2.35	1.095	1.08
17.05	0.5784	0.3558	2.25	2.23	1.095	1.08
20.46	0.5552	0.3558	2.14	2.12	1.095	1.09
23.87	0.5358	0.3558	2.04	2.01	1.095	1.09
27.28	0.5189	0.3558	1.96	1.92	1.095	1.09
30.69	0.5043	0.3558	1.89	1.84	1.095	1.09
34.10	0.4911	0.3558	1.82	1.77	1.095	1.09
37.51	0.4797	0.3558	1.75	1.71	1.095	1.09
40.92	0.4692	0.3558	1.69	1.65	1.095	1.09

RUN 502

$N_{Re,in} = 2000$, $N_{Fr,in} = 34.5$

x/D	ρ_b^+	ρ_w^+	f/f_{cp}	
			Correlation	Computer
2.07	0.8875	0.6715	1.84	1.77
4.14	0.6855	0.2613	2.81	2.96
8.28	0.5400	0.2500	2.30	2.43
12.42	0.4765	0.2500	2.12	2.10
16.56	0.4356	0.2500	1.85	1.89
20.70	0.4064	0.2499	1.71	1.75
24.84	0.3837	0.2499	1.61	1.64
28.98	0.3657	0.2499	1.54	1.54
33.12	0.3509	0.2499	1.47	1.47
37.28	0.3387	0.2499	1.42	1.42
41.40	0.3283	0.2499	1.36	1.36
45.54	0.3196	0.2499	1.33	1.32
49.68	0.3120	0.2499	1.29	1.28
53.82	0.3056	0.2499	1.26	1.25
57.96	0.2998	0.2498	1.24	1.22
62.10	0.2949	0.2498	1.20	1.19
66.24	0.2904	0.2498	1.19	1.17
70.38	0.2865	0.2498	1.18	1.15
74.52	0.2829	0.2498	1.15	1.14
78.66	0.2799	0.2498	1.13	1.12
82.80	0.2769	0.2498	1.13	1.11

APPENDIX C: DEFINITION OF BULK PARAMETERS

The bulk parameters used in this investigation are the following:

Bulk Density

$$\rho_b \triangleq \frac{2\int_0^{r_w} \rho\, r\, dr}{r_w^2}$$

Bulk Velocity

$$u_b \triangleq \frac{\int_0^{r_w} \rho\, u\, r\, dr}{\int_0^{r_w} \rho\, r\, dr}$$

Bulk Temperature

$$T_b \triangleq \frac{\int_0^{r_w} \rho\, u\, T\, r\, dr}{\int_0^{r_w} \rho\, u\, r\, dr}$$

Bulk Viscosity

$$\mu_b \triangleq \mu\,(T_b)$$

Bulk Thermal Conductivity

$$k_b \triangleq k\,(T_b)$$